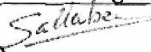
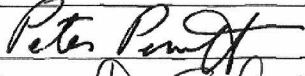


		Model Error Resolution Document <small>Complete only applicable items.</small>		QA: QA Page 1 of 73
1. Document Number: ANL-WIS-PA-000001		2. Revision/Addendum: REV 03	3. ERD: 03	
4. Title: EBS Radionuclide Transport Abstraction		5. No. of Pages Attached: 72		
6. Description of and Justification for Change (Identify affected pages, applicable CRs and TBVs): This Error Resolution Document (ERD) is provided to update the <i>EBS Radionuclide Transport Abstraction</i> (EBS RTA) in order to resolve issues identified in the condition reports (CRs) summarized below. The revisions identified are necessary to add clarity and strengthen the discussion within the EBS RTA. However, there are no impacts on the results or conclusions of the EBS RTA due to the clarifications and text revisions provided in this ERD. An impact evaluation was performed for EBS RTA REV 03 [DIRS 177407] in which 23 controlled documents were found to reference the EBS RTA. Only five of these 23 controlled documents use the EBS RTA REV 03 as a direct input: <ul style="list-style-type: none"> • <i>Total System Performance Assessment Model/Analysis for the License Application</i> (MDL-WIS-PA-000005 REV 00 AD 01, SNL 2008 [DIRS 183478]) • <i>Engineered Barrier System: Physical and Chemical Environment</i> (ANL-EBS-MD-000033 REV 06, SNL 2007 [DIRS 177412]) • <i>In-Package Chemistry Abstraction</i> (ANL-EBS-MD-000037 REV 04 AD 01, SNL2007 [DIRS 180506]) • <i>Postclosure Nuclear Safety Design Bases</i> (ANL-WIS-MD-000024 REV 01, SNL 2008 [DIRS 177464]) • <i>Features, Events, and Processes for the Total System Performance Assessment: Analyses</i> (ANL-WIS-MD-000027 REV 00, SNL 2008 [DIRS 183041]) However, only the <i>Total System Performance Assessment</i> (TSPA) model is affected by the changes contained in this ERD. Although no direct inputs were impacted, minor text modifications are recommended in <i>Waste Form and In-Drift Colloids-Associated Radionuclide Concentrations: Abstraction and Summary</i> (MDL-EBS-PA-000004 REV 03, SNL 2007 [DIRS 177423]) and in <i>Features, Events, and Processes for the Total System Performance Assessment: Analyses</i> (ANL-WIS-MD-000027 REV 00, SNL 2008 [DIRS 183041]) in order to make them consistent with the EBS RTA definition of kinetic sorption of plutonium and americium on iron oxyhydroxide colloids in the EBS. In addition, the modifications to the EBS transport model identified in CR 13644 will need to be incorporated in a future update of the TSPA-LA model.				
	Printed Name	Signature	Date	
7. Checker	Cédric Sallaberry		03/29/2010	
8. QCS/QA Reviewer	Peter Persoff		03/26/2010	
9. Originator	James D. Schreiber		03/29/2010	
10. Responsible Manager	Robert J. MacKinnon		03/29/2010	

(Block 6, Continued)

An impact analysis was also performed for the three DTNs modified as part of the resolution of the CRs discussed below. DTN: SN0703PAEBSRTA.002 [DIRS 186557] is a direct input to *Dissolved Concentration Limits of Elements with Radioactive Isotopes* (ANL-WIS-MD-000010 REV 06, SNL 2007 [DIRS 177418]), but the spreadsheet modified in the DTN is not used in that report. The revised DTN: MO0812TSPAOSIA.000 [DIRS 186579] is not used as direct input to any controlled documents. DTN: SN0703PAEBSRTA.001 [DIRS 185343] is used as direct input to the TSPA model (SNL 2008 [DIRS 183478]), but none of the revisions impacts the TSPA model.

The *Safety Analysis Report (SAR)*, *Final Environmental Impact Statement (FEIS)*, and *Supplemental Environmental Impact Statement (SEIS)* have also been evaluated for impact from changes in this ERD. Minor modifications of SAR Sections 2.3.7 and 2.4 from CR 13644 have been identified. These changes, however, will have no effect on the results or conclusions of the SAR. None of the changes documented in this ERD has any impact upon the FEIS or the SEIS.

The four CRs addressed in the ERD are summarized as follows:

1) CR 13644 – GoldSim stoichiometric coefficients.

This CR concerns an issue that occurs when converting aqueous plutonium and americium to irreversibly sorbed plutonium and americium on iron oxyhydroxide colloids, where the conversion rate is sometimes capped in order to assure a well-conditioned coefficient matrix in the GoldSim cell network solver in TSPA calculations. Resolution of CR 13644 is addressed in Section I.

2) CR 13957 – Surface complexation model K_d parameters.

This CR concerns errors in an Excel spreadsheet “Colloid_Stat_CP_ZPC_output.xls” in DTN: SN0703PAEBSRTA.002 [DIRS 186557], an output DTN from the EBS RTA, used to calculate K_d values for radionuclides and nickel from PHREEQC surface complexation model simulations. Resolution of CR 13957 is addressed in Section II.

3) CR 13966 – Error in spreadsheet formula in DTN: SN0307PAEBSRTA.001.

This CR identifies an error in Excel spreadsheet “Corrosion Products Isotherm 7-19-2007.xls” in DTN: SN0703PAEBSRTA.001 [DIRS 185343], an output DTN from the EBS RTA, used to calculate the water vapor adsorption isotherm for steel corrosion products. Resolution of CR 13966 is addressed in Section III.

4) CR 14260 – Two errors in DTN: MO0812TSPAOSIA.000.

This CR identifies an error in Excel spreadsheet “Final_Surf_Complx_Regression.xls” in DTN: MO0812TSPAOSIA.000 [DIRS 186579], a DTN containing the analysis used to evaluate the impact of over-sorption on corrosion products in Cell 2 of the EBS transport model. This analysis was documented in ERD 02 of the EBS RTA. Resolution of CR 14260 is addressed in Section IV.

References used in this ERD are listed in Section V.

I. CR 13644 Resolution

CR 13644 identifies an issue that occurs when converting aqueous Pu to irreversibly sorbed Pu on iron oxyhydroxide colloids, where the conversion rate is sometimes capped in order to assure a well-conditioned coefficient matrix in the GoldSim cell network solver in TSPA calculations. The stoichiometric coefficients for determining the amount converted were incorrectly implemented when the maximum conversion rate is invoked, leading to small errors in the calculated values of the stoichiometric coefficients.

This condition has negligible impacts on dose to the reasonably maximally exposed individual (RMEI) calculated in the TSPA. The cumulative effect on dose of the changes listed below are included in an impact assessment documented in ERD 07 of the *Total System Performance Assessment Model/Analysis for the License Application* (MDL-WIS-PA-000005 REV 00 AD 01, SNL 2008 [DIRS 183478]). Because the impacts on dose are negligible, it is determined that CR 13644 does not impact the conclusions in the SAR. However, SAR Sections 2.3.7 and 2.4 will be modified to indicate that plutonium and americium undergo kinetic sorption (instead of irreversible sorption) onto iron oxyhydroxide colloids in the EBS, but undergo irreversible sorption in the lower natural barrier. Similar changes are necessary in FEP 2.1.09.02.0A and FEP 2.1.09.17.0A of *Features, Events, and Processes for the Total System Performance Assessment: Analyses* (ANL-WIS-MD-000027 REV 00, SNL 2008 [DIRS 183041]), and in *Waste Form and In-Drift Colloids-Associated Radionuclide Concentrations: Abstraction and Summary* (MDL-EBS-PA-000004 REV 03, SNL 2007 [DIRS 177423]).

The following summarizes the changes made to the EBS transport model to resolve CR 13644. It is recommended that these changes be incorporated in a future version of the TSPA-LA model. Additional changes to the text of the EBS RTA Section 6 to resolve CR 13644 are shown in Attachment 1.

1. The implementation error related to the calculation of conversion rate for performing kinetic sorption of plutonium and americium on the stationary corrosion products and iron oxyhydroxide colloids is corrected. Because of this error, both dissolved mass and precipitated mass in Cell 2 (corrosion product domain) were being used in the forward rate calculations instead of just the dissolved mass, leading to over-sorption on the stationary corrosion products and iron oxyhydroxide colloids. In order to correct the error, the ratio of dissolved to total mass in the Cell pathway is calculated for plutonium and americium separately at the end of each time step. This ratio is then applied in the next time step to adjust the conversion rate so that only the dissolved mass is considered in the forward rate calculations.
2. The calculations feed for determining stoichiometry in the forward and backward reactions is no longer taken from the conversion rate calculations. Instead, the stoichiometry is calculated separately as a function of bulk surface area and therefore defined more rigorously and in a transparent manner.
3. The maximum conversion rate (transfer rate) limit for kinetic sorption calculations is increased to the point where the calculated conversion rate is not restricted by the limits imposed by the GoldSim code (in the base case, the conversion rate limit was set at 10^4

per year). This is achieved by making the first time step much smaller than the base case within the EBS_Submodel and Aleatory_Submodel. The global time steps remain unchanged. The GoldSim code V. 9.60.300 (STN: 10344-9.60-03. [DIRS 184387]) limits the transfer rate to 10^7 divided by the nominal time step, where the nominal time step is the larger of the first time step or the simulation duration divided by 10^8 . In the base case, the first time step was set at 10 years for the 10,000-year simulation and 250 years for the 1,000,000-year simulation; therefore, the maximum transfer rate that could be applied was 10^6 for the 10,000-year simulation and 4×10^4 for the 1,000,000-year simulation. But by reducing the first time step length (in the EBS_Submodel and Aleatory_Submodel) to a value less than one year, the transfer rate limit has been effectively increased so that the theoretical transfer rates, based on bulk surface areas, can be applied without being limited by the code. The first time step length is reduced to 0.001 years for the 10,000-year simulation and 0.01 years for the 1,000,000-year simulation.

4. Kinetic desorption of plutonium and americium from the iron oxyhydroxide colloids is applied in the corrosion products domain to enforce consistent treatment of sorption of plutonium and americium among the stationary corrosion products and iron oxyhydroxide colloids. This update allows sorption of plutonium and americium on iron oxyhydroxide colloids in amounts predicted by the competitive sorption-based surface complexation model and allows desorption of plutonium and americium on iron oxyhydroxide colloids only in the corrosion products domain. Once the iron oxyhydroxide colloids leaves the corrosion products domain, the kinetically sorbed mass of plutonium and americium mass is treated as irreversibly attached to the iron oxyhydroxide colloids for transport in the downstream domains of the EBS and in the far-field.

A backward conversion rate is calculated for plutonium and americium on iron oxyhydroxide colloids separately, similar to that used for the stationary corrosion products. As a result, changes to the “Species” element are made to account for mass transfer from the “*I_f*” species to the corresponding dissolved species. The calculation to determine the stoichiometry to account for the relative proportion of the mass allotted to desorption and radioactive decay is incorporated.

5. The minimum dissolved concentration value that is used in the regression equation to determine the K_d value for sorption on corrosion products is increased to 10^{-9} mol/L (from 10^{-15} mol/L) to match the lower bound considered in the surface complexation-based modeling from which the regression equations are derived. As a result, the K_d value applied at the threshold concentration (such as at the start of the time step in which waste form degradation and mobilization occurs) is more defensible.
6. An adjustment factor is applied to the stoichiometry calculation performed for the iron oxyhydroxide colloids. The default value for the factor is 1 but is adjusted for the time step when the iron oxyhydroxide colloid suspension becomes unstable after having been stable in the previous time step. The adjustment factor is calculated by taking the ratio of the iron oxyhydroxide colloid concentration under unstable conditions to the concentration in the previous time step. This adjustment is only made for one time step

when the transition from stable to unstable conditions occurs. This is done to overcome the one-time-step lag imposed by the GoldSim code in solving the kinetic sorption-desorption equations. Forcing this adjustment allows the stoichiometry to use the bulk surface area of the iron oxyhydroxide colloids for the unstable conditions rather than the previous value, when the iron oxyhydroxide colloids were stable.

7. A workaround to accommodate the weakness in the looping decay chain logic for the Pipe Pathway elements in GoldSim is implemented. The looping decay chain implementation became necessary when desorption was added to $I_f^{241}Am$, the desorption of ^{241}Am mass that is kinetically sorbed to iron oxyhydroxide colloids in the corrosion products domain. Although the looping decay chain logic implemented in the EBS Transport Model using the Cell Pathways worked fine, it could not be applied to the Pipe Pathways elsewhere in the TSPA-LA model. The workaround that is implemented involves logic to decay ^{245}Cm and ^{241}Pu to ^{241}Am in the EBS Cell pathways, outside of the Cell-net calculations performed internally in GoldSim.
8. A new regression equation is implemented for calculating the K_d value of uranium based on the surface complexation modeling when the dissolved concentration of uranium is greater than 10^{-4} mol/L and the sorption sites are less than 4 mol-sites/L. This equation is described in ANL-WIS-PA-000001 REV 03 ERD 02. Also, a regression equation is developed for converting sorbed moles of uranium to the mole-sites occupied by uranium due to the presence of polynuclear uranium species. This equation is used for the purpose of displaying the results and is not used in the EBS transport calculations.

None of these changes impacts the conclusions of the EBS RTA.

II. CR 13957 Resolution

CR 13957 identifies an error found in a spreadsheet used to calculate K_d values for radionuclides and nickel. The spreadsheet (“Colloid_Stat_CP_ZPC_output.xls” from DTN: SN0703PAEBSRTA.002, Revision 000 [DIRS 186557], an output DTN from ANL-WIS-PA-000001 REV 03) uses outputs from PHREEQC surface complexation model simulations. K_d values are calculated as a function of these outputs and additional parameter values for corrosion product and colloid properties. The latter values are not always correctly lined up with the PHREEQC outputs (e.g., see rows 158-166 in worksheet Total_out), which causes many of the K_d calculations to be wrong. These calculations are not used in figures or abstractions used in the TSPA-LA Model; instead, calculations in spreadsheet “Final_Calc_Results_Surf_Complx_Data_1.xls” from the same DTN, which do not have this error, are used as input to TSPA-LA Model. In addition, the PHREEQC input files for runs 21-50 documented in the same DTN are incorrect. They all appear to be equivalent to run 1. However, the spreadsheet outputs for these runs are not equivalent and may be correct. The resolution of this CR includes a recheck of all calculations and files in the DTN.

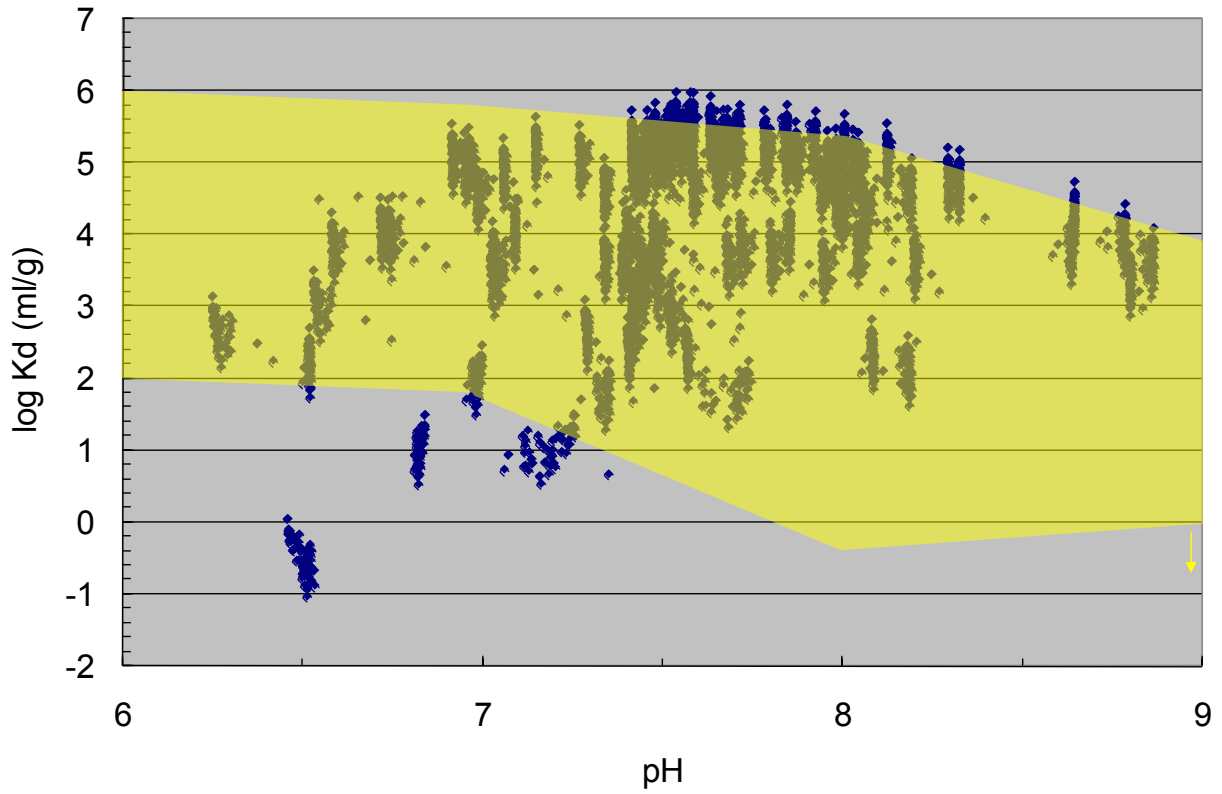
To resolve CR 13957, the following actions are completed:

1. Output DTN: SN0703PAEBSRTA.002 is revised (Revision 001, [DIRS186557]) to include the input files for all runs in the DTN. PHREEQC runs are repeated using

qualified PHREEQC V. 2.11.01 (STN: 10068-2.11-01 [DIRS 185868]). All “.out” files are included in the revised DTN.

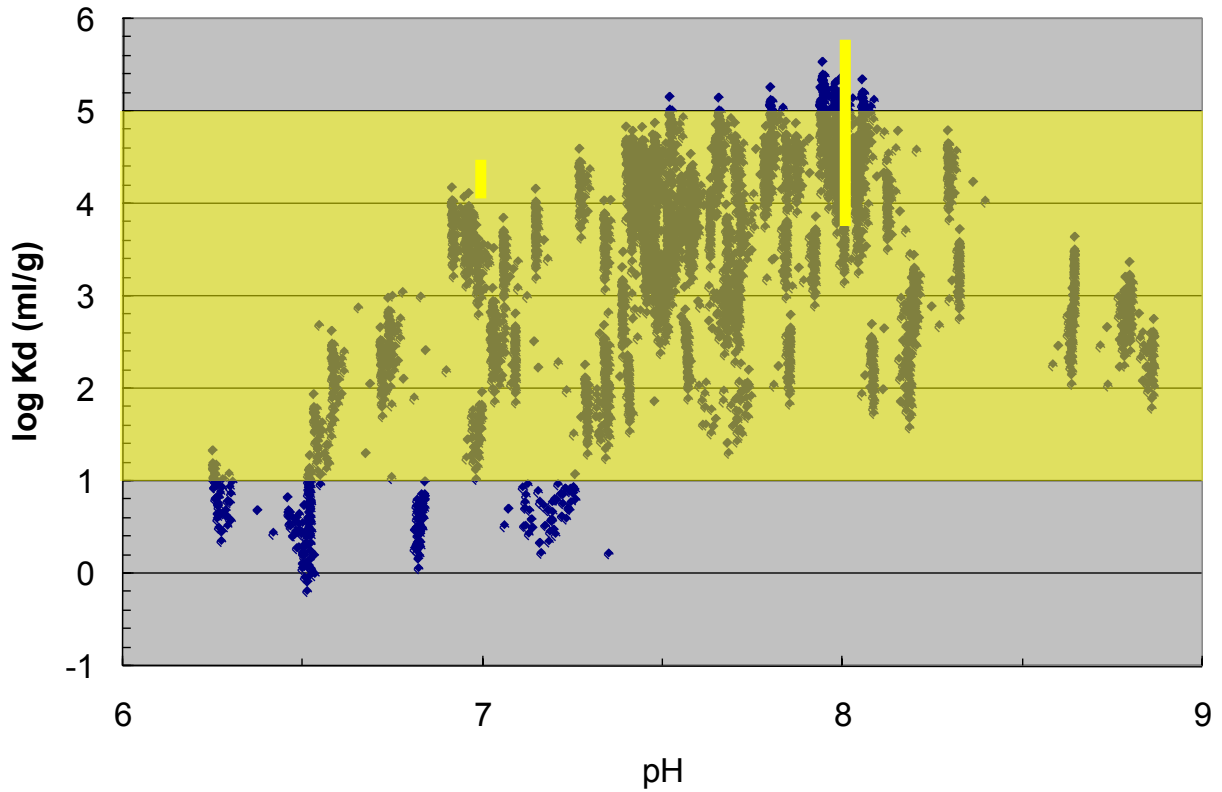
2. Output DTN: SN0703PAEBSRTA.002 is revised again (Revision 002, [DIRS 186557]) to add an evaluation of the impacts of revising the PHREEQC runs (Revision 001) on the coefficients in Table 6.5-14, which is a direct input to the TSPA-LA Model. The evaluation is documented in spreadsheet “Final_Surf_Complx_Regression_coeff.xls” and indicates a negligible relative percent difference of less than 0.090%. Table 6.5-14 is not updated with the new coefficients shown in Appendix A of this ERD (ERD 03), and thus the change is not propagated to downstream documents, nor the TSPA-LA Model, because the impact determined from this analysis is negligible.
3. The following changes are made in ANL-WIS-PA-000001 REV 03:
 - a. Figures in Section 7.2.3 are updated to be consistent with Revision 001 of SN0703PAEBSRTA.002 ([DIRS 186557]). Although the new data are not propagated to the TSPA-LA Model the figures in Section 7.2.3 are revised to verify that, with the small changes in the updated competitive surface complexation model (C-SCM), the model is still valid when compared to current literature. See Figures 7.2-11[a] to 7.2-15[a].
 - b. CR 13957 indicates that the last value in Table 6.3-6, p. 6-59, should be 0.05263. This change is not made. This value is the probability in a discrete distribution that the sorption site density for HFO will be 5.65 sites nm⁻². For several other site density values, a probability of 0.05263, to five decimal places, is listed in Table 6.3-6, and that is also the probability of a site density of 5.65 sites nm⁻². However, the sum of probabilities for all discrete site density values must equal 1.0. Due to rounding to five decimal places, the sum would be 0.99998 if a probability of 0.05263 were used for all site density values where it is warranted. In order to bring the sum to 1.0, the probability of the last site density value in the table (5.65 sites nm⁻²) is increased by a negligible amount, 0.00002, to a value of 0.05265.
 - c. p. 6-199, 2nd full paragraph, 9th line: Change “sorbed actinide concentrations” to “sorbed actinide moles”
 - d. p. 7-39, 10th line of paragraph: Change “4,900 to 170,000” to “4,900 to 700,000”

None of these changes impacts the conclusions of the EBS RTA, and no downstream usage—neither the LA nor other project documents—is impacted.



Sources: Yellow shaded area, EPA 1999 [DIRS 170376]; Blue diamonds, DTN: SN0703PAEBSRTA.002 [DIRS 186557], Excel spreadsheet, *Surf_Compplx_Validation_figs_REV01.xlsx*, worksheet "Kd-U_pH"

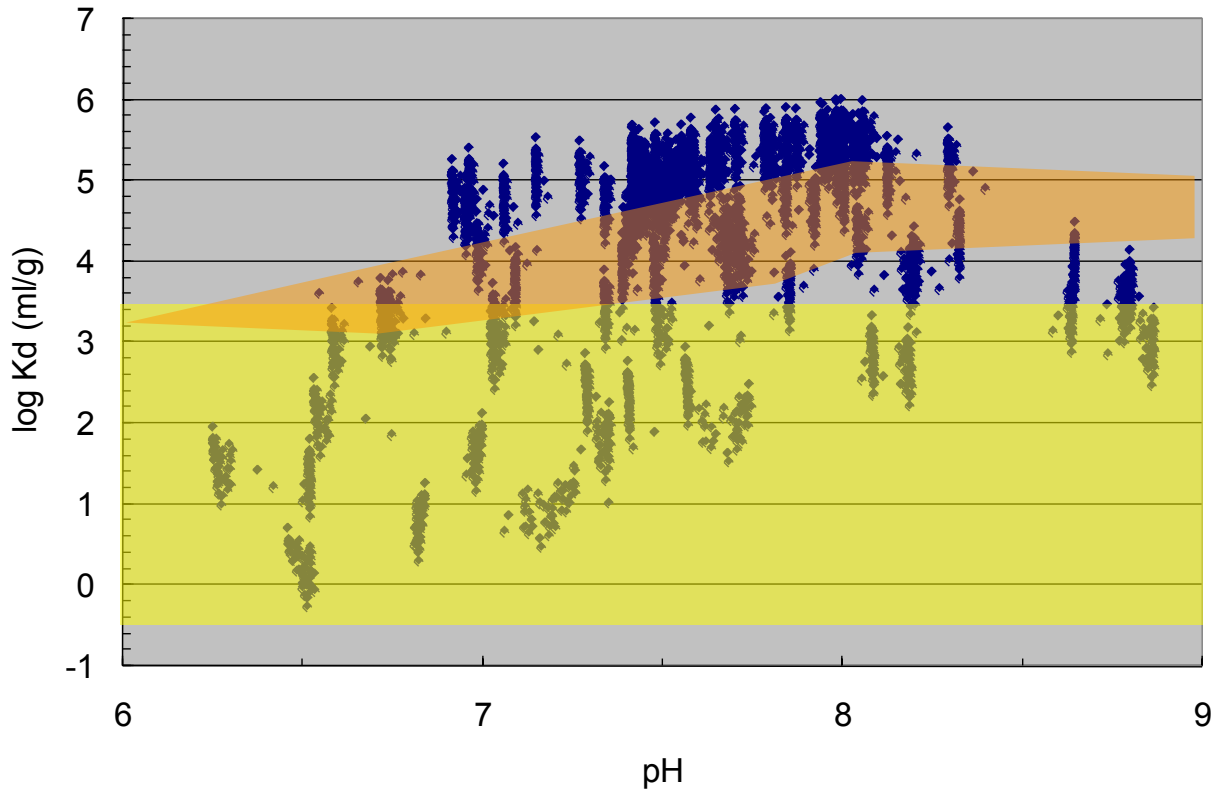
Figure 7.2-11[a]. EPA U Soil K_d s and C-SCM Iron Oxide K_d s



Sources: Yellow shaded area, EPA 1999 [DIRS 170376]; Yellow bars, Lu et al. 2000 [DIRS 166315] and Sanchez et al. [DIRS 107213]; Blue diamonds, DTN: SN0703PAEBSRTA.002 [DIRS 186557], Excel spreadsheet *Surf_Complx_Validation_figs_REV01.xlsx*, worksheet "Kd-Pu_pH"

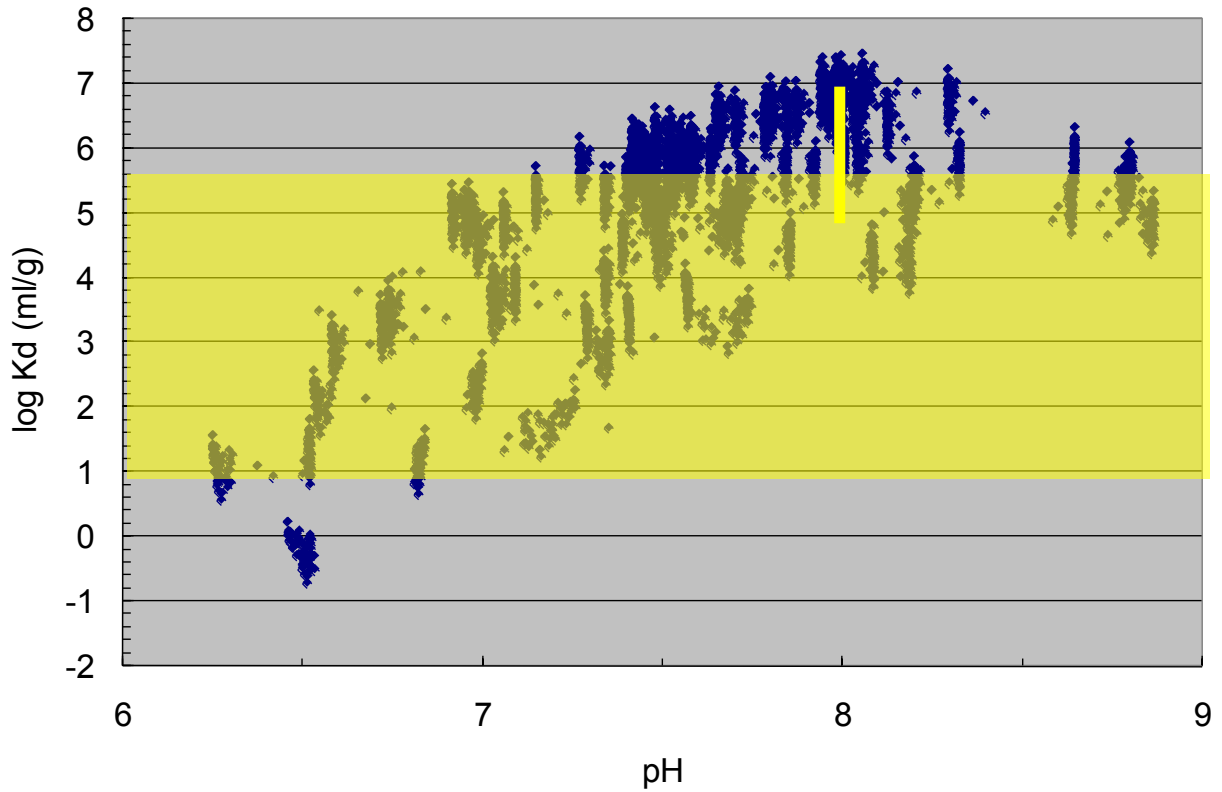
NOTE: The yellow bar at pH 8 is the range of Pu K_d s measured on hematite colloids by Lu et al. (2000 [DIRS 166315]); the yellow bar at pH 7 shows estimated Pu K_d s from Sanchez et al. (1985 [DIRS 107213]).

Figure 7.2-12[a]. EPA Pu Soil K_d s and C-SCM Iron Oxide K_d s



Sources: Yellow shaded area, EPA 1999 [DIRS 170376]; Orange shaded area, Jerden and Kropf 2007 [DIRS 181295]; Blue diamonds, DTN: SN0703PAEBSRTA.002 [DIRS 186557], Excel spreadsheet, *Surf_Complx_Validation_figs_REV01.xlsx*, worksheet "Kd-Np_pH"

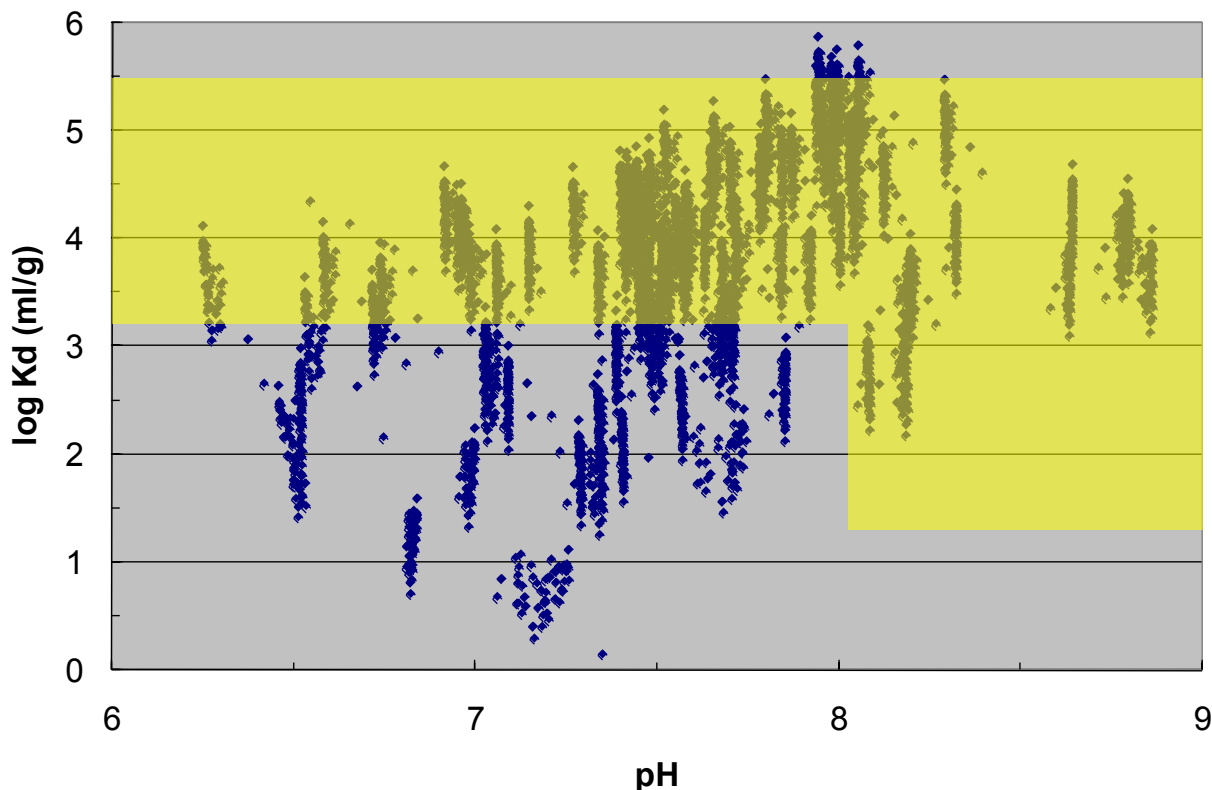
Figure 7.2-13[a]. EPA Np Soil K_d s and C-SCM Iron Oxide K_d s



Sources: Yellow shaded area, EPA 1999 [DIRS 170376]; Yellow bar, Lu et al. 2000 [DIRS 166315]; Blue diamonds, DTN: SN0703PAEBSRTA.002 [DIRS 186557], Excel spreadsheet, *Surf_Complx_Validation_figs_REV01.xlsx*, worksheet "Kd-Am_pH"

NOTE: The yellow bar at pH 8 is the range of Am K_d s measured on hematite colloids by Lu et al. (2000 [DIRS 166315])

Figure 7.2-14[a]. EPA Am Soil K_d s and C-SCM Iron Oxide K_d s



Sources: Yellow shaded area, EPA 1999 [DIRS 170376]; Blue diamonds, DTN: SN0703PAEBSRTA.002 [DIRS 186557], Excel spreadsheet, *Surf_Complx_Validation_figs_REV01.xlsx*, worksheet "Kd-Th_pH"

Figure 7.2-15[a]. EPA Th Soil K_d s and C-SCM Iron Oxide K_d s

III. CR 13966 Resolution

CR 13966 points out an error in Excel spreadsheet "Corrosion Products Isotherm 7-19-2007.xls" in DTN: SN0703PAEBSRTA.001 [DIRS 185343], which is an output DTN from the EBS RTA. In worksheet "Composite Isotherm," cell D527 contains a formula that is in error. The formula reads "`=SUM(D5,D522);`" it should read "`SUM(D5:D522).`" This error has no effect on nuclear safety or waste isolation, because if the error is corrected, the results of the spreadsheet that are used in the TSPA, namely, the parameters s and k used in the composite Frenkel-Halsey-Hill water vapor adsorption isotherm for corrosion products, change only very slightly (about 1 part in 1000). These parameters are actually the bounds on uniform distributions of s and k , which are sampled parameters in the TSPA. The old and new ranges are compared in Table 1. (The values changed here were changed once before to address CR 11755 in the EBS RTA ERD 01.)

Since these parameters are sampled in the TSPA, this slight change in their values would have no discernible impact on the results of the TSPA calculation. None of these changes impacts the conclusions of the EBS RTA, and no downstream usage—neither the LA nor other project documents—is impacted.

Table 1. Comparison of FHH Parameter Ranges Before and After Correction in Excel Spreadsheet “Corrosion Products Isotherm 7-19-2007.xls” in DTN: SN0703PAEBSRTA.001 [DIRS 185343]

Range	s	k
Before correction	1.493 – 1.799	1.030 – 1.326
After correction	1.493 – 1.800	1.030 – 1.327

In addition to the error described in CR 13966, an error occurs in another worksheet (“Composite – Fewer Outliers”) of the same spreadsheet. In this worksheet, cell D514 contains a formula that reads “=SUM(E5,E509);” it should read “=SUM(D5:D509).” This worksheet explores the effect of excluding certain outlying data. Since the effect is not significant, and since the exclusion of the data is not justifiable, the results of this worksheet are not documented in the EBS RTA and are not used in the TSPA. Therefore, this error has no impact on the conclusions of the EBS RTA, and no downstream usage—neither the LA nor other project documents—is impacted.

IV. CR 14260 Resolution

CR 14260 documents two errors detected in DTN: MO0812TSPAOSIA.000 [DIRS 186579]. This DTN was originally presented in the EBS RTA ERD 02, Section II, to resolve CR 12998. DTN: MO0812TSPAOSIA.000 contains a supplemental sorption model that is more accurate under certain sorption site and uranium concentration conditions. The two errors described in CR 14260 include:

1. Cell C15 of worksheet, “README” in Excel file, “Final_Surf_Complx_Regression.xls”, says “This GoldSim model uses an alternative Uranium Kd when Uranium concentrations are greater than 1e-4 mole/L, and the number of sorption sites per liter of water is less than 2 mole-sites/L...”. The correct number of sorption sites per liter of water is “less than 4 mole-sites/L.”
2. DTN: MO0812TSPAOSIA.000 does not contain the regression equation spreadsheet that converts the log of sorbed Uranium in moles per kg of corrosion products to the log of mole sites occupied by U per kg of CP mass.

To resolve CR 14260, the following actions are completed:

1. DTN: MO0812TSPAOSIA.000 is revised (Revision 001) to include the Excel spreadsheet, “Final_Surf_Complx_Regression_Rev02.xls”. This spreadsheet replaces “Final_Surf_Complx_Regression.xls” from the original DTN, corrects the error in the README file, and includes the worksheet of the regression equation that is used in the impact analysis identified in resolution of CR 12998 documented in the EBS RTA ERD 02, to convert the log of sorbed Uranium in moles per kg of corrosion products to the log of mole sites occupied by U per kg of CP mass.
2. In Section II.3 of EBS RTA ERD 02, change:

“water is typically less than 2 mol-sites/L (a value below the 10th percentile of the range”

to:

“water is typically less than 4 mol-sites/L (a value below the 30th percentile of the range”

3. Replace Section 9.4 of the parent document (p. 9-38), with the following text:

SN0703PAEBSRTA.001. Inputs Used in the Engineered Barrier System (EBS) Radionuclide Transport Abstraction. Submittal date: 04/10/2008.

SN0703PAEBSRTA.002. Surface Complexation Modeling Results, Actinide Kd Abstractions and pH Abstraction. Submittal date: 02/04/2010.

MO0812TSPAOSIA.000. Over Sorption Impact Assessment. Submittal date: 02/08/2010.

The corrections identified above have no impact on the conclusions in the EBS RTA, nor do they have any impact on downstream documents.

V. References

This section lists references that are used to resolve the CRs in this ERD.

V.1. Documents Cited

- 177418 SNL (Sandia National Laboratories) 2007. *Dissolved Concentration Limits of Elements with Radioactive Isotopes*. ANL-WIS-MD-000010 REV 06. Las Vegas, Nevada: Sandia National Laboratory. ACC: DOC.20070918.0010; DOC.20100125.0001.
- 177412 SNL (Sandia National Laboratories) 2007. *Engineered Barrier System: Physical and Chemical Environment*. ANL-EBS-MD-000033 REV 06. Las Vegas, Nevada: Sandia National Laboratories. ACC: DOC.20070907.0003; LLR.20080328.0031; DOC.20090204.0002; DOC.20090929.0022.
- 180506 SNL (Sandia National Laboratories) 2007. *In-Package Chemistry Abstraction*. ANL-EBS-MD-000037 REV 04 AD 01. Las Vegas, Nevada: Sandia National Laboratories. ACC: DOC.20070816.0004; DOC.20051130.0007; LLR.20080325.0276; DOC.20081120.0004.
- 177423 SNL (Sandia National Laboratories) 2007. *Waste Form and In-Drift Colloids-Associated Radionuclide Concentrations: Abstraction and Summary*. MDL-EBS-PA-000004 REV 03. Las Vegas, Nevada: Sandia National Laboratories. ACC: DOC.20071018.0019; LLR.20080325.0281.
- 183041 SNL (Sandia National Laboratories) 2008. *Features, Events, and Processes for the Total System Performance Assessment: Analyses*. ANL-WIS-MD-000027 REV 00. Las Vegas, Nevada: Sandia National Laboratories. ACC: DOC.20080307.0003; DOC.20080407.0009; LLR.20080522.0166; DOC.20080722.0002;

DOC.20090130.0001; DOC.20090312.0002; DOC.20090414.0002;
DOC.20091221.0001.

177464 SNL (Sandia National Laboratories) 2008. *Postclosure Nuclear Safety Design Bases*. ANL-WIS-MD-000024 REV 01. Las Vegas, Nevada: Sandia National Laboratories. ACC: DOC.20080226.0002; DOC.20080314.0004; LLR.20080507.0018; DOC.20080610.0007; DOC.20090310.0001.

183478 SNL (Sandia National Laboratories) 2008. *Total System Performance Assessment Model /Analysis for the License Application*. MDL-WIS-PA-000005 REV 00 AD 01. Las Vegas, Nevada: Sandia National Laboratories. ACC: DOC.20080312.0001; LLR.20080414.0037; LLR.20080507.0002; LLR.20080522.0113; DOC.20080724.0005; DOC.20090106.0001.

V.2. Software Codes

185868 PHREEQC V. 2.11.01. 2008. WIN 2000. STN: 10068-2.11-01.

184387 GoldSim V. 9.60.300. 2008. WIN 2000, WINXP, WIN2003. STN: 10344-9.60-03.

V.3. Source Data, Listed by Data Tracking Number

185343 SN0703PAEBSRTA.001. Inputs Used in the Engineered Barrier System (EBS) Radionuclide Transport Abstraction. Submittal date: 04/10/2008.

186557 SN0703PAEBSRTA.002. Surface Complexation Modeling Results, Actinide Kd Abstractions and pH Abstraction. Submittal date: 02/04/2010.

186579 MO0812TSPAOSIA.000. Over Sorption Impact Assessment. Submittal date: 02/08/2010.

Attachment 1. Revisions to the EBS RTA Section 6 to Resolve CR 13644

Changes made to the EBS RTA Section 6 (Model Discussion) to resolve CR 13644 are shown by change tracking. Changes made to the EBS RTA Section 6 in ERD 01 and ERD 02 are not included here. Text deletions are indicated by colored strikethrough and colored text, and text insertions are indicated by colored underlined text; equation changes are indicated by colored strikethrough or colored underline, but no change in font color. Black change bars appear in the margin wherever changes occur.

The following sections contain revisions (Sections 6.5.2.4.1, 6.5.2.4.4, and 6.5.4.2.5 are included without change for completeness, since all of Section 6.5.2.4 pertains to CR 13644 resolution):

6.5.1.2 EBS Transport Model

6.5.2 Summary of Computational Model

6.5.2.4 Sorption onto Iron Oxyhydroxide Colloids and Stationary Corrosion Products

6.5.2.4.1 Sampling Methodology

6.5.2.4.2 Surface Complexation Modeling

6.5.2.4.3 Abstraction and Multiple Linear Regression

6.5.2.4.4 Analysis

6.5.2.4.5 Results

6.5.2.4.6 Model Implementation

6.5.2.5 Discretization and Development of Computational Model for the TSPA

6.5.2.7 Stoichiometry for Conversion of Radionuclide Mass to Kinetically Sorbed Mass onto Iron Oxyhydroxide Colloids, Stationary Corrosion Products, and Waste Form Colloids

6.5.2.7.1 Conceptual Model

6.5.2.7.2 Stoichiometry Calculations

6. MODEL DISCUSSION

6.5.1.2 EBS Transport Model

The EBS transport model consists of a system of coupled mass balance equations for each radionuclide species. Some species occur as embedded mass on the waste form colloids and kinetically sorbed mass on iron oxyhydroxide colloids and corrosion products. The waste form embedded mass and kinetic sorption mass on the iron products are treated as distinct species with their own mass balance equations. Coupling of mass balance equations occurs in the spatial sense due to advective/diffusive transport. Coupling occurs between parent and daughter species due to radioactive decay and coupling of mass balance equations occur due to the processes which generate the embedded and kinetic sorption masses. The transport model is more complex than the flow model for several reasons. The transport model is necessarily transient because the mass of each radionuclide at any particular location is dependent on its history (i.e., how far it has traveled, the quantity remaining at the source, and the extent of radioactive decay or ingrowth). Further, several complex interacting processes occur in transport, including dissolution and precipitation, sorption, advective transport, diffusion, and colloid-facilitated transport. The term “colloid-facilitated transport” includes numerous phenomena, including adsorption and desorption of radionuclides onto mobile and immobile colloids, capture of colloids by solid surfaces and the air-water interface, filtering, dispersion, and diffusion. Transport can take place at any degree of water saturation greater than zero, so the model has to account for water saturation. Dissolution and precipitation may occur at finite rates or sufficiently fast to reach equilibrium. Solubility limits that determine whether, or to what extent, these processes occur are dependent on the chemical environment of the EBS. The EBS transport model applies to the waste package, the invert, and the invert/UZ interface.

Transport of rind mass and corrosion products out of the waste package is not explicitly accounted as the depletion inside the waste package is likely to be insignificant compared to the available mass. For example, the CSNF rind mass that is predominantly made up of schoepite would not be depleted even though uranium transport is modeled. Assuming uranium solubility of 10^{-5} mol L⁻¹ (a constant high value) and multiplying it by the constant advective flux through the waste package of 100 L yr⁻¹ over a time period of one million years results in the transport of 1000 mol of uranium, which is about 3 percent of the ²³⁸U mass per CSNF waste package. The relative mass of corrosion products that would get depleted would be even less because the solubility of ferrihydrite is smaller than that of the uranium, and there is much more corrosion products mass than the rind mass.

Mass Balance for Dissolved and Reversibly Sorbed Radionuclides

As with the flow model, the details of pore structure within the EBS are not important, and macroscopic mass balances using phenomenological rate expressions are appropriate. The starting point is the equation of continuity, or mass balance equation, for each dissolved radionuclide species i (Bird et al. 1960 [DIRS 103524], p. 561):

$$\frac{\partial \rho_i}{\partial t} = -\nabla \cdot \mathbf{J}_i + Q_i^m + \Lambda_i. \quad (\text{Eq. 6.5.1.2-1})$$

Here, ρ_i is the mass concentration of dissolved radionuclide species i ($\text{kg } i \text{ m}^{-3}$ bulk volume), \mathbf{J}_i is the mass flux vector (or mass specific discharge) ($\text{kg m}^{-2} \text{ s}^{-1}$) of dissolved radionuclide species i in the mobile water phase and accounts for advection, hydrodynamic dispersion, and diffusion of the dissolved radionuclide species i . The term Q_i^m is the net rate on a bulk volume basis ($\text{kg m}^{-3} \text{ s}^{-1}$) of the various mass transfer processes, including reversible and kinetic sorption onto solid stationary materials in the EBS, dissolution and precipitation, and the various colloid-facilitated transport processes. The reaction term, Λ_i , accounts for radioactive decay and ingrowth on a bulk volume basis (i.e., production by decay of the parent of i) ($\text{kg m}^{-3} \text{ s}^{-1}$). Each of these terms is expanded and described in more detail below, then simplified as appropriate for application in the TSPA Model.

It is convenient to develop the transport model following the approach normally taken in the literature (Corapcioglu and Jiang 1993 [DIRS 105761], pp. 2217 to 2219; Choi and Corapcioglu 1997 [DIRS 161621], p. 306), with particular attention to colloid-facilitated transport, since the complexity of those processes tends to dominate the mathematical formulation. First, Equation 6.5.1.2-1 is rewritten in terms of concentrations of radionuclides in an unsaturated porous medium. The density, or mass concentration, of dissolved radionuclide species i is given by:

$$\begin{aligned}\rho_i &= \phi S_w C_i \\ &= \theta_w C_i,\end{aligned}\tag{Eq. 6.5.1.2-2}$$

where C_i is the concentration on a water volume basis of radionuclide species i (kg m^{-3}), ϕ is the porosity (m^3 void m^{-3} bulk volume) of a representative elemental volume of EBS, and S_w is the water saturation (m^3 water m^{-3} void), and θ_w is the water content (m^3 water m^{-3} bulk volume), expressed as a fraction, as distinguished from θ , which is expressed as a percentage. The expression for ρ_i is inserted into Equation 6.5.1.2-1, resulting in:

$$\frac{\partial(\theta_w C_i)}{\partial t} = -\nabla \cdot \mathbf{J}_i + Q_i^m + \Lambda_i.\tag{Eq. 6.5.1.2-3}$$

The concentration C_i may be constrained by the solubility limit, C_{si} , which is evaluated in *Dissolved Concentration Limits of Elements with Radioactive Isotopes* (SNL 2007 [DIRS 177418], Section 6.1) for each of 17 elements (actinium, americium, carbon, cesium, chlorine, iodine, neptunium, protactinium, lead, plutonium, radium, selenium, strontium, technetium, thorium, tin, and uranium). Dissolved concentration limits for plutonium, neptunium, uranium, thorium, americium, protactinium, and tin are presented as tabulated functions of environmental conditions (namely, pH and CO_2 fugacity) with one or more uncertainty terms or distributions. Fixed solubility limits are given for the other elements in the list (SNL 2007 [DIRS 177418], Table 8-1), except for actinium and lead, for which transport is not modeled in the TSPA because of their short half-life (about 22 years). To account for actinium dose, secular equilibrium with ^{231}Pa is assumed (SNL 2007 [DIRS 177418], Section 6.1). Lead dose effects are calculated in the TSPA by assuming secular equilibrium with ^{226}Ra (SNL 2007 [DIRS 177418], Section 6.1).

The mass flux vector is expressed as

$$\mathbf{J}_i = -\theta_w \mathbf{D}_i \cdot \nabla C_i + \mathbf{q}_w C_i, \quad (\text{Eq. 6.5.1.2-4})$$

where \mathbf{D}_i is the hydrodynamic dispersion tensor of species i ($\text{m}^2 \text{s}^{-1}$), and \mathbf{q}_w is the specific discharge vector, or Darcy velocity, of water (m s^{-1}). The specific discharge vector is related to the water flow rates F_j ($\text{m}^3 \text{s}^{-1}$) in each pathway j of the EBS flow model (Section 6.5.1.1) by:

$$\mathbf{q}_w = \frac{F_j}{A} \mathbf{n}, \quad (\text{Eq. 6.5.1.2-5})$$

where A is the spatially dependent cross sectional flow area within the pathway j (m^2), and \mathbf{n} is a unit vector in the direction of the flow path. Because of the complex flow geometry in the EBS, assigning a value to A is not always straightforward; for example, for pathway 4 (Section 6.5.1.1), flow through the waste package, A can be the cross sectional area of corrosion patches or some fraction of the cross sectional area of a waste package.

The hydrodynamic dispersion, \mathbf{D}_i , can be expressed in terms of two components:

$$\mathbf{D}_i = \mathbf{D}_{di} + D_{mi} \mathbf{I}, \quad (\text{Eq. 6.5.1.2-6})$$

where \mathbf{D}_{di} is the mechanical dispersivity associated with the interstitial water velocity, D_{mi} is the effective molecular diffusion coefficient ($\text{m}^2 \text{s}^{-1}$), which implicitly includes the effects of tortuosity, and \mathbf{I} is the identity tensor. The dispersivity can be broken down into lateral and longitudinal dispersivities. However, the dispersivity in the EBS is ignored (see Section 6.3.1.2). Consequently, the hydrodynamic dispersion is accounted for solely by molecular diffusion. The free water diffusion coefficients for all radionuclides in the EBS are given in Table 4.1-7. Modifications to the diffusion coefficient for the porosity, saturation, and temperature within the waste package are described in Section 6.3.4.3. The effects of concentrated solutions are ignored. Throughout the mathematical description of the radionuclide transport, $D_i = D_{mi}$ represents the effective diffusion coefficient for species i . Since $D_{mi} \mathbf{I} \cdot \nabla C_i = D_i \nabla C_i$, the mass flux vector in Equation 6.5.1.2-4 is:

$$\mathbf{J}_i = -\theta_w D_i \nabla C_i + \mathbf{q}_w C_i. \quad (\text{Eq. 6.5.1.2-7})$$

The term Q_i^m ($\text{kg m}^{-3} \text{s}^{-1}$) in Equation 6.5.1.2-3 is expanded to account for individual contributions of different processes to radionuclide transport:

$$Q_i^m = Q_{idp} - Q_{is}^{rev} - Q_{is}^{kinetic} + Q_{iaq}^{kinetic} - Q_{icm}^{rev} - Q_{icm}^{kinetic} - Q_{icc} - Q_{icc}^{int} \pm Q_{imt} - Q_{icm}^{embed}. \quad (\text{Eq. 6.5.1.2-8})$$

The first term is the source term, Q_{idp} , accounting for the rate of dissolution or precipitation of species i . If the mass balance equation calculates a concentration below the solubility limit, then dissolution occurs, and mass is moved from precipitate to solution ($Q_{idp} > 0$). If a concentration above the solubility limit is calculated, then precipitation occurs, and mass is moved from solution to precipitate ($Q_{idp} < 0$).

The next seven terms in Equation 6.5.1.2-8 account for sorption-related processes. Q_{is}^{rev} is the net rate of reversible sorption of radionuclide species i onto the stationary solid matrix (internal waste package corrosion products and invert matrix). Q_{icm}^{rev} is the net rate of reversible sorption of radionuclide species i onto mobile colloid surfaces. Development of this term requires assumptions regarding the reversibility of radionuclide sorption onto colloids and is discussed below. $Q_{is}^{kinetic}$ is the rate of kinetic sorption of radionuclide species i onto the stationary solid matrix (internal waste package corrosion products), and $Q_{icm}^{kinetic}$ is the rate of kinetic sorption of radionuclide species i onto mobile colloid surfaces. $Q_{iaq}^{kinetic}$ is the combined rate of kinetic desorption of radionuclide species i from the stationary iron oxyhydroxide corrosion products material and iron oxyhydroxide colloids to solution (in the corrosion product domain), which can be separated into the kinetic desorption rate from stationary corrosion products ($Q_{is_aq}^{kinetic}$) and the kinetic desorption rate from iron oxyhydroxide colloids ($Q_{icm_aq}^{kinetic}$). ~~No~~ desorption is modeled for the stationary corrosion products and iron oxyhydroxide mobile colloids in order to apply a site constraint for sorption of Plutonium and Americium in the corrosion products domain and is not inconsistent with the limited desorption data that is available. Q_{icm}^{rev} is the net rate of reversible sorption of radionuclide species i onto mobile colloid surfaces. Development of this term requires assumptions regarding the reversibility of radionuclide sorption onto colloids and is discussed below. $Q_{icm}^{kinetic}$ is the rate of kinetic sorption of radionuclide species i onto mobile colloid surfaces.

The terms Q_{icc} and Q_{icc}^{int} are the net rates of sorption of radionuclide species i onto immobile colloid surfaces captured by the stationary solid matrix and by the air-water interface, respectively. Wan and Wilson (1994 [DIRS 124994]) found that “particle transport was tremendously retarded by the air-water interface acting as a strong sorption phase” (Choi and Corapcioglu 1997 [DIRS 161621], p. 301). However, as a bounding assumption (BSC 2005 [DIRS 177423], Assumption 5.4), sorption by the air-water interface is assumed not to occur ($Q_{icc}^{int} = 0$). Distribution coefficients for sorption onto the stationary solid matrix and onto immobile colloid surfaces will generally be different. However, it is difficult to distinguish among various types of matrixes and immobile colloids. Therefore, no distinction is made, and the term Q_{icc} (sorption onto immobile colloids) is lumped in with Q_{is}^{rev} or $Q_{is}^{kinetic}$ (sorption onto the stationary solid matrix). Sorption and retardation in the waste package are discussed in more detail in Section 6.3.4.2.

The term Q_{imt} is the net rate of interface transfer of dissolved mass between the continua in a dual continuum. The sign of this transfer term is determined by the sign of the concentration difference between the media and which medium is associated with the mass balance equation. This term is included even though it is zero in the single-continuum domains that represent the EBS in the RTA radionuclide transport abstraction in order to keep the mass balance equations as generally applicable as possible. In particular, the equations apply in the dual-continuum invert model presented as an ACM in Section 6.6.3.

The term Q_{icm}^{embed} is the rate of mass conversion from dissolved state to embedded state onto waste form colloids for radionuclide species i . Radionuclides become embedded only in waste form colloids, not in iron oxyhydroxide or groundwater colloids. The conversion rate to embedded species is represented by a first order conversion of the species in solution:

$$Q_{icm}^{embed} = \theta_w \lambda_i^{embed} C_i, \quad (\text{Eq. 6.5.1.2-9})$$

where λ_i^{embed} is the first order rate constant (s^{-1}) for mass conversion from the dissolved state to the embedded state onto waste form colloids for radionuclide species i .

Ingrowth and decay are expressed as:

$$\Lambda_i = \lambda_i^p r_{Mi}^p \theta_w C_i^p - \lambda_i \theta_w C_i. \quad (\text{Eq. 6.5.1.2-10})$$

Ingrowth is the production of radionuclide species i mass by the decay of its parent species and occurs at a rate proportional to the concentration of the parent, C_i^p ($kg\ m^{-3}$), and the parent species decay constant, λ_i^p (s^{-1}). The decay constant is related to the half-life, $t_{1/2,i}^p$ (s), of the radionuclide by:

$$\lambda_i^p = \frac{\ln(2)}{t_{1/2,i}^p}. \quad (\text{Eq. 6.5.1.2-11})$$

The term r_{Mi}^p in the production rate is the dimensionless ratio of the mass (kg) of species i produced by decay of the parent species to the mass (kg) of the parent species lost by decay. This is equal to the ratio of the atomic weight of species i to that of its parent. Similarly, mass of species i is lost by decay at a rate $\lambda_i \theta_w C_i$ ($kg\ m^{-3}\ s^{-1}$), where λ_i is the decay constant for species i (s^{-1}), defined analogously to λ_i^p .

Mass transport of dissolved and reversibly sorbed radionuclide species i in the aqueous phase is then given by:

$$\begin{aligned} \frac{\partial(\theta_w C_i)}{\partial t} &= \nabla \cdot (\theta_w D_i \nabla C_i) - \nabla \cdot \mathbf{q}_w C_i \\ &\quad + Q_{idp} - Q_{is}^{rev} - Q_{is}^{irrev} - Q_{icm}^{rev} - Q_{icm}^{irrev} \\ &\quad \pm Q_{imt} - Q_{icm}^{embed} + \theta_w (\lambda_i^p r_{Mi}^p C_i^p - \lambda_i C_i), \\ \frac{\partial(\theta_w C_i)}{\partial t} &= \nabla \cdot (\theta_w D_i \nabla C_i) - \nabla \cdot \mathbf{q}_w C_i \\ &\quad + Q_{idp} - Q_{is}^{rev} - Q_{is}^{kinetic} - Q_{icm}^{rev} - Q_{icm}^{kinetic} \\ &\quad \pm Q_{imt} - Q_{icm}^{embed} + \theta_w (\lambda_i^p r_{Mi}^p C_i^p - \lambda_i C_i) \end{aligned} \quad (\text{Eq. 6.5.1.2-12})$$

which is essentially identical to Equations 19 and 20 by Choi and Corapcioglu (1997 [DIRS 161621], p. 306), with the addition of decay and ingrowth terms and a dissolution/precipitation source term, Q_{idp} . A further modification of the equations by Choi and

Corapcioglu involves the diffusive term, $\nabla \cdot (\theta_w D_i \nabla C_i)$, which Choi and Corapcioglu write as $\nabla \cdot [D_i \nabla (\theta_w C_i)]$. This form of the term incorrectly models diffusive flux based on the species concentration gradient with respect to bulk volume. Instead, the diffusive flux is determined by the concentration gradient with respect to the water volume. The incorrect form allows diffusion to occur in the absence of a concentration gradient as long as the water content, θ_w , varies.

The source term for radionuclide species i reversibly sorbed onto the stationary solid matrix (corrosion products or invert matrix) is given by:

$$Q_{is}^{rev} = \frac{\partial(\rho_b K_{dis} C_i)}{\partial t} - \rho_b (\lambda_i^p r_{Mi}^p K_{dis}^p C_i^p - \lambda_i K_{dis} C_i), \quad (\text{Eq. 6.5.1.2-13})$$

where ρ_b is the dry bulk density of the stationary solid matrix (kg m^{-3} bulk volume). A linear sorption isotherm is used for the relationship between the aqueous and solid phase equilibrium concentration, expressed in terms of a sorption distribution coefficient of the dissolved species i , K_{dis} (m^3 water kg^{-1} solid [customary units of mL g^{-1}]). K_{dis} depends both on the radionuclide species i being sorbed and on the solid substrate, either stationary iron oxyhydroxide corrosion products or invert material or both, in this case.

The source term for radionuclide species i kinetically sorbed onto the stationary solid iron oxyhydroxide corrosion products is given by:

$$Q_{is}^{kinetic} = \rho_b \bar{s}_{CP} k_{if} C_i \quad (\text{Eq. 6.5.1.2-14})$$

where \bar{s}_{CP} is the specific surface area of iron oxyhydroxide corrosion products [$\text{m}^2 \text{CP kg}^{-1} \text{CP}$], and k_{if} is the kinetic forward rate constant for species i (m^3 water $\text{m}^{-2} \text{CP s}^{-1}$). The reaction is modeled as first order in the solution concentration. The kinetic sorption to the iron oxyhydroxide corrosion products is modeled as experiencing a slow desorption. This is a mass transfer from the [stationary corrosion product material](#) to solution. The source term representing the [is-kinetic desorption process from stationary corrosion products](#) is:

$$Q_{iaq}^{kinetic} = \rho_b \bar{s}_{CP} k_{ir} \hat{C}_{iCP} - Q_{is-aq}^{kinetic} = \rho_b \bar{s}_{CP} k_{irs} \hat{C}_{iCP} - \quad (\text{Eq. 6.5.1.2-15})$$

where k_{irs} is the reverse sorption (or desorption) rate [from the iron oxyhydroxide stationary corrosion products](#), ~~and~~ \hat{C}_{iCP} is the concentration of species i on the iron oxyhydroxide [stationary corrosion products](#) on a water volume basis.

The source term for radionuclide species i reversibly sorbed onto the mobile colloids is given by:

$$Q_{icm}^{rev} = \frac{\partial[\theta_w (K_{dicWF} C_{cWF} + K_{dicFeO} C_{cFeO} + K_{dicGW} C_{cGW}) C_i]}{\partial t} + \nabla \cdot (\mathbf{J}_{icWF} + \mathbf{J}_{icFeO} + \mathbf{J}_{icGW}) - \theta_w [\lambda_i^p r_{Mi}^p (C_{icWF}^p + C_{icFeO}^p + C_{icGW}^p) - \lambda_i (C_{icWF} + C_{icFeO} + C_{icGW})], \quad (\text{Eq. 6.5.1.2-16})$$

where C_{icWF} , C_{icFeO} , and C_{icGW} are the concentrations on a water volume basis of radionuclide species i reversibly sorbed onto the mobile waste form (WF) colloids, iron oxyhydroxide (FeO)

colloids originating from corrosion products, and groundwater (GW) colloids, respectively ($\text{kg } i \text{ m}^{-3} \text{ water}$). The superscript p refers to the parent of radionuclide species i . The terms C_{cWF} , C_{cFeO} , and C_{cGW} are the concentrations on a water volume basis of mobile waste form, iron oxyhydroxide, and groundwater colloids, respectively ($\text{kg colloid m}^{-3} \text{ water}$). The K_d values of radionuclide species i for the respective colloids are K_{dicWF} , K_{dicFeO} , and K_{dicGW} (customary units: mL g^{-1}). The first term on the right side of Equation 6.5.1.2-16 accounts for the accumulation of mass of radionuclide species i reversibly sorbed to colloids. The second term on the right hand side of Equation 6.5.1.2-16 accounts for mass transport by advection and diffusion of radionuclide species i reversibly sorbed to colloids. The third line of Equation 6.5.1.2-16 accounts for production or loss of mass of radionuclide species i reversibly sorbed to colloids by ingrowth and decay.

The vectors for mass fluxes of mobile colloids, \mathbf{J}_{icWF} , \mathbf{J}_{icFeO} , and \mathbf{J}_{icGW} , are:

$$\mathbf{J}_{icWF} = -\theta_w D_c \nabla (K_{dicWF} C_{cWF} C_i) + \mathbf{q}_w K_{dicWF} C_{cWF} C_i \quad (\text{Eq. 6.5.1.2-17})$$

$$\mathbf{J}_{icFeO} = -\theta_w D_c \nabla (K_{dicFeO} C_{cFeO} C_i) + \mathbf{q}_w K_{dicFeO} C_{cFeO} C_i \quad (\text{Eq. 6.5.1.2-18})$$

$$\mathbf{J}_{icGW} = -\theta_w D_c \nabla (K_{dicGW} C_{cGW} C_i) + \mathbf{q}_w K_{dicGW} C_{cGW} C_i \quad (\text{Eq. 6.5.1.2-19})$$

The source term for radionuclide species i kinetically sorbed onto the mobile iron oxyhydroxide colloids ([forward reaction](#)) is given by:

$$Q_{icm}^{kinetic} = \theta_w C_{cFeO} \bar{s}_{cFeO} k_{if} C_i, \quad (\text{Eq. 6.5.1.2-20})$$

where \bar{s}_{cFeO} is the specific surface area of mobile iron oxyhydroxide colloids ($\text{m}^2 \text{ colloids kg}^{-1} \text{ colloids}$), and k_{if} is the forward rate constant for kinetic sorption ($\text{m}^3 \text{ water m}^{-2} \text{ FeO colloids s}^{-1}$). The rate constant k_{if} for mobile iron oxyhydroxide colloids is the same as for stationary iron oxyhydroxide corrosion products. The reaction is modeled as first order in the solution concentration. Kinetic sorption onto mobile colloids occurs only onto mobile iron oxyhydroxide colloids, not onto mobile waste form or mobile groundwater colloids. As discussed earlier, radionuclides may become embedded in waste form colloids, which has a similar net effect as kinetic sorption but is modeled as a distinctly separate process.

[A kinetic desorption model is implemented for the iron oxyhydroxide colloids similar to the stationary corrosion products \(Equation 6.5.1.2-15\). The source term representing the kinetic desorption process from the iron oxyhydroxide colloids is:](#)

$$Q_{icm_aq}^{kinetic} = \theta_w C_{cFeO} \bar{s}_{cFeO} k_{ircm} \hat{C}_{icFeO} \quad (\text{Eq. 6.5.1.2-20a})$$

[where \$k_{ircm}\$ is the reverse sorption \(or desorption\) rate from the iron oxyhydroxide colloids to the solution, and \$\hat{C}_{icFeO}\$ is the concentration of species \$i\$ on the iron oxyhydroxide colloids on a water volume basis \(\$\text{kg } i \text{ m}^{-3} \text{ water}\$ \).](#)

The term Q_{imt} is the net rate of interface transfer of dissolved and reversibly sorbed mass between the continua in a dual continuum material (as in the dual continuum invert ACM; see Section 6.6.3) on a bulk volume basis ($\text{kg m}^{-3} \text{s}^{-1}$). The dual-continuum invert model conceptualizes the invert as crushed in-situ material with inter-pore space as the pore space between solid particles. The intra-pore space is the pore space within the solid particles. Q_{imt} is given by Corapcioglu and Wang (1999 [DIRS 167464], p. 3265); Gerke and van Genuchten (1996 [DIRS 167466], p. 345):

$$Q_{imt} = \gamma_d [(C_i)_{intra} - (C_i)_{inter}] + \gamma_c [(C_{icWF})_{intra} - (C_{icWF})_{inter} + (C_{icFeO})_{intra} - (C_{icFeO})_{inter} + (C_{icGW})_{intra} - (C_{icGW})_{inter}] \quad (\text{Eq. 6.5.1.2-21})$$

In a single-continuum material, $Q_{imt} = 0$. The dissolved and colloid mass transfer coefficients, γ_d and γ_c , respectively, depend on which continuum the mass balance represents. For the dissolved mass transfer term applied to the intragranular mass balance:

$$\gamma_d = \alpha \phi_{intra} S_{w_intra}, \quad (\text{Eq. 6.5.1.2-22})$$

and applied to the intergranular mass balance:

$$\gamma_d = \alpha \phi_{intra} S_{w_intra} \left(\frac{1 - w_{inter}}{w_{inter}} \right), \quad (\text{Eq. 6.5.1.2-23})$$

where w_{inter} is the ratio of the intergranular continua volume to the total bulk volume, and α is the first-order mass transfer coefficient (s^{-1}) of the form:

$$\alpha = \frac{\beta}{d^2} D_{ie}, \quad (\text{Eq. 6.5.1.2-24})$$

β is a dimensionless geometry-dependent coefficient, d is a characteristic length (m) of the matrix structure (e.g., half the aggregate width or half the fracture spacing), and D_{ie} is an effective diffusion coefficient ($\text{m}^2 \text{s}^{-1}$) that represents the diffusion properties of the interface between the two continua for radionuclide species i . Because the intergranular continuum is open pore space, diffusion is expected to be controlled by the diffusive properties of the intragranular continuum. Thus, D_{ie} is taken to be the effective diffusion coefficient in the intragranular continuum. The colloid coefficient γ_c is evaluated similarly to the dissolved coefficient, but uses an effective colloid diffusion coefficient to evaluate α in Equation 6.5.1.2-24. The mass transfer function between the two invert continua is described in Section 6.6.3.1 in connection with a dual-continuum invert ACM. Since the EBS is modeled as a single continuum in the EBS transport model, the interface transfer term Q_{imt} is zero and is not included in the mass balance equations that follow.

In a dual-continuum material, the intergranular porosity ϕ_{inter} and intragranular porosity ϕ_{intra} are defined as follows. Let V_p be the total volume of pore space in the bulk material, which has a

total volume of V_t . The intergranular pore space has a total volume designated by V_{t_inter} and a pore volume of V_{p_inter} . Similarly, the intragranular pore space has a total volume designated by V_{t_intra} and a pore volume of V_{p_intra} . $V_p = V_{p_intra} + V_{p_inter}$ and $V_t = V_{t_intra} + V_{t_inter}$. The porosities are defined as:

$$\phi_{inter} = \frac{V_{p_inter}}{V_t} \quad (\text{Eq. 6.5.1.2-25})$$

and

$$\phi_{intra} = \frac{V_{p_intra}}{V_t}. \quad (\text{Eq. 6.5.1.2-26})$$

The total bulk porosity of the material is:

$$\phi_t = \frac{V_p}{V_t} = \phi_{inter} + \phi_{intra}. \quad (\text{Eq. 6.5.1.2-27})$$

The parameter w_{inter} is the ratio of the intergranular continuum volume to the total bulk volume:

$$w_{inter} = \frac{V_{t_inter}}{V_t}. \quad (\text{Eq. 6.5.1.2-28})$$

Then $\left(\frac{1 - w_{inter}}{w_{inter}} \right)$ is the ratio of intragranular continuum volume to intergranular continuum volume:

$$\frac{1 - w_{inter}}{w_{inter}} = \frac{1 - \frac{V_{t_inter}}{V_t}}{\frac{V_{t_inter}}{V_t}} = \frac{V_t - V_{t_inter}}{V_{t_inter}} = \frac{V_{t_intra}}{V_{t_inter}}. \quad (\text{Eq. 6.5.1.2-29})$$

Mass Balance for Radionuclides Kinetically Sorbed onto Iron Oxyhydroxide Mobile Colloids and Stationary Corrosion Products

The mass balance for kinetically sorbed radionuclides on mobile iron oxyhydroxide colloids, which originate in the corrosion products, accounts for advection, diffusion, and decay and is given by:

$$\frac{\partial(\theta_w \hat{C}_{icFeO})}{\partial t} = -\nabla \cdot (\mathbf{J}_{icFeO}^{kinetic}) + Q_{icm}^{kinetic} - Q_{icm_aq}^{kinetic} + \theta_w (\lambda_i^p r_{Mi}^p \hat{C}_{icFeO}^p - \lambda_i \hat{C}_{icFeO})$$
~~$$\frac{\partial(\theta_w \hat{C}_{icFeO})}{\partial t} = -\nabla \cdot (\mathbf{J}_{icFeO}^{kinetic}) + Q_{icm}^{kinetic} + \theta_w (\lambda_i^p r_{Mi}^p \hat{C}_{icFeO}^p - \lambda_i \hat{C}_{icFeO}), \quad (\text{Eq. 6.5.1.2-30})$$~~

where

$$\mathbf{J}_{icFeO}^{kinetic} = -\theta_w D_c \nabla (\hat{C}_{icFeO}) + \mathbf{q}_w \hat{C}_{icFeO}. \quad (\text{Eq. 6.5.1.2-31})$$

The quantity \hat{C}_{icFeO} is the concentration of radionuclide species i kinetically sorbed onto mobile iron oxyhydroxide colloids on a water volume basis ($\text{kg } i \text{ m}^{-3} \text{ water}$). The source term for radionuclide species i kinetically sorbed onto the mobile corrosion products colloids, $Q_{icm}^{kinetic}$, is given by Equation 6.5.1.2-20. [The source term for the radionuclide species \$i\$ kinetically desorbing from the iron oxyhydroxide colloids, \$Q_{icm_aq}^{kinetic}\$, is given by Equation 6.5.1.2-20a.](#)

The mass balance for kinetically adsorbed radionuclides onto stationary iron oxyhydroxide corrosion products accounts for decay and is given by:

~~$$\frac{\partial(\theta_w \hat{C}_{iCP})}{\partial t} = Q_{is}^{kinetic} - Q_{is_aq}^{kinetic} + \theta_w (\lambda_i^p r_{Mi}^p \hat{C}_{iCP}^p - \lambda_i \hat{C}_{iCP})$$~~

$$\frac{\partial(\theta_w \hat{C}_{iCP})}{\partial t} = Q_{is}^{kinetic} - Q_{is_aq}^{kinetic} + \theta_w (\lambda_i^p r_{Mi}^p \hat{C}_{iCP}^p - \lambda_i \hat{C}_{iCP}), \quad (\text{Eq. 6.5.1.2-32})$$

where \hat{C}_{iCP} is the concentration of radionuclide species i kinetically adsorbed onto stationary iron oxyhydroxide corrosion products on a water volume basis ($\text{kg } i \text{ m}^{-3}$). The source term for radionuclide species i kinetically sorbed onto the solid stationary iron oxyhydroxide corrosion products, $Q_{is}^{kinetic}$, is given by Equation 6.5.1.2-14. The source term for the radionuclide species i kinetically desorbing from the solid stationary iron oxyhydroxide corrosion products, $Q_{is_aq}^{kinetic}$, is given by Equation 6.5.1.2-15.

Mass Balance for Waste Form Colloid Particles

The waste form colloids are generated in the waste form domain and are transported in accordance with an advective/diffusive mass balance. The waste form colloid concentration is subject to stability constraints based on the local domain chemistry. The iron oxyhydroxide and groundwater colloids both exist in the corrosion products and invert domains; their stability and concentrations are dependent on the local domain chemistry (BSC 2005 [DIRS 177423]). Because seepage brings the groundwater colloids into the EBS, the groundwater colloids are

modeled as having the same concentration in both the waste package and invert. Similarly, due to the presence of steel in both waste package and invert, it is reasonable for iron oxyhydroxide colloids to have the same concentrations in both domains as well, if the colloids are stable under the local conditions. Hence, no transport mass balance equations are required for iron oxyhydroxide and groundwater colloids. Since waste form colloids can only be generated in the waste form domain, it is necessary to know how much of the waste form colloid mass has moved by advection and diffusion into the corrosion product and invert domains. Thus, an advective/diffusive mass balance must be applied to compute the waste form colloid mass in each of the downstream domains. The stability for waste form colloids is checked in each domain, since they may be stable in the corrosion product domain but precipitate in the invert domain.

The mass balance for waste form colloidal particles suspended in the aqueous phase can be expressed as (Choi and Corapcioglu 1997 [DIRS 161621], p. 302):

$$\frac{\partial(\theta_w C_{cWF})}{\partial t} = -\nabla \cdot \mathbf{J}_{cWF} - Q_{cWF} - Q_{cWF}^{int} - Q_{cWFfg} + Q_{cWFs} \pm Q_{cWFmt} \quad (\text{Eq. 6.5.1.2-33})$$

The quantity C_{cWF} is the concentration of suspended waste form colloids in the aqueous phase ($\text{kg waste form colloids m}^{-3}$ water), and \mathbf{J}_{cWF} is the mass flux vector of waste form colloids ($\text{kg m}^{-2} \text{s}^{-1}$). The term Q_{cWFfg} is the net rate of waste form colloid removal from suspension ($\text{kg m}^{-3} \text{s}^{-1}$) by means of physical filtering (pore clogging, sieving, and straining) and by gravitational settling. Physical filtering and gravitational settling are assumed not to occur (Assumption 5.7). Thus, the term Q_{cWFfg} is neglected. The term Q_{cWF} ($\text{kg m}^{-3} \text{s}^{-1}$) is the net rate of waste form colloid capture on the solid surface. Although colloid capture on the solid surface is akin to sorption and a different process from physical filtration, the net effect is indistinguishable from physical filtration, and it is also neglected ($Q_{cWF} = 0$). The term Q_{cWF}^{int} ($\text{kg m}^{-3} \text{s}^{-1}$) represents capture at the air-water interface; as mentioned earlier, this term is neglected as a bounding assumption (BSC 2005 [DIRS 177423], Assumption 5.4).

With these assumptions, Equation 6.5.1.2-33 simplifies to:

$$\frac{\partial(\phi S_w C_{cWF})}{\partial t} = -\nabla \cdot \mathbf{J}_{cWF} + Q_{cWFs} \pm Q_{cWFmt} \quad (\text{Eq. 6.5.1.2-34})$$

The source term, Q_{cWFs} ($\text{kg m}^{-3} \text{s}^{-1}$), in Equation 6.5.1.2-34 represents the formation or degradation of waste form colloids. Colloid formation may be rate limited, or it may be instantaneous, with equilibrium between the colloids and their dissolved components. In either case, colloid stability is strongly dependent on the chemical environment, specifically on the pH and ionic strength of the aqueous phase. The colloid source term is the subject of *Waste Form and In-Drift Colloids-Associated Radionuclide Concentrations: Abstraction and Summary* (BSC 2005 [DIRS 177423]), and is discussed further below.

The term Q_{cWFmt} is the net rate of interface transfer of waste form colloidal mass between the intergranular and intragranular continua in a dual continuum model, such as the dual continuum invert ACM (Section 6.6.3). For a single continuum, $Q_{cWFmt} = 0$. The sign of this transfer term

is determined by the sign of the waste form colloid concentration difference between the media and which medium is associated with the mass balance equation. This is analogous to the colloid transfer term in Equation 6.5.1.2-21:

$$Q_{cWFmt} = \gamma_c [(C_{cWF})_{intra} - (C_{cWF})_{inter}]. \quad (\text{Eq. 6.5.1.2-35})$$

Since Equation 6.5.1.2-34 is for the waste form colloid particles themselves, as opposed to radionuclides sorbed onto the particles, there are no decay or ingrowth terms.

The mass flux vector for waste form colloids is expressed as (Choi and Corapcioglu 1997 [DIRS 161621], p. 303, Equation 4):

$$\begin{aligned} \mathbf{J}_{cWF} &= \mathbf{J}_{cB} + \mathbf{J}_{cMD} + \mathbf{q}_w C_{cWF} \\ &= -\theta_w D_B \nabla C_{cWF} - \theta_w D_{MD} \nabla C_{cWF} + \mathbf{q}_w C_{cWF} \\ &= -\theta_w D_c \nabla C_{cWF} + \mathbf{q}_w C_{cWF}, \end{aligned} \quad (\text{Eq. 6.5.1.2-36})$$

where subscript *B* refers to Brownian diffusion, and *MD* refers to mechanical dispersion. The mechanical dispersion and Brownian diffusion terms can be lumped together in a colloid hydrodynamic dispersion term with a colloid dispersion or diffusion coefficient D_c ($\text{m}^2 \text{s}^{-1}$). The colloid diffusion coefficient is given by the Stokes-Einstein equation (Equation 6.3.4.4-1). The mass balance on waste form colloid particles, Equation 6.5.1.2-34, then becomes (with the term Q_{cWFmt} , Equation 6.5.1.2-35, no longer included, since it is zero for the EBS as currently modeled):

$$\frac{\partial(\theta_w C_{cWF})}{\partial t} = \nabla \cdot (\theta_w D_c \nabla C_{cWF}) - \nabla \cdot (\mathbf{q}_w C_{cWF}) + Q_{cWFs} \quad (\text{Eq. 6.5.1.2-37})$$

Mass Balance for Embedded Mass on Waste Form Colloids

The mass balance for the radionuclide species *i* embedded on waste form colloids is:

$$\begin{aligned} \frac{\partial(\theta_w C_i^{embed})}{\partial t} &= \nabla \cdot (\theta_w D_c \nabla C_i^{embed}) - \nabla \cdot (\mathbf{q}_w C_i^{embed}) \\ &\quad + \theta_w (\lambda_i^p r_{Mi}^p C_i^{p,embed} - \lambda_i C_i^{embed}) + Q_{icm}^{embed}, \end{aligned} \quad (\text{Eq. 6.5.1.2-38})$$

where C_i^{embed} and $C_i^{p,embed}$ are the concentrations of species *i* and the parent of species *i*, respectively, embedded on waste form colloids.

Summary of Mass Balances

Inserting the source terms into Equation 6.5.1.2-12, and neglecting the dual continuum interface transport, gives the equation for the transport of radionuclides dissolved in the aqueous phase and reversibly sorbed:

$$\begin{aligned}
 \frac{\partial}{\partial t} [\theta_w R_{fi} C_i] &= \nabla \cdot (\theta_w D_i \nabla C_i) \\
 &+ \nabla \cdot \{ \theta_w D_c \nabla [(K_{dicWF} C_{cWF} + K_{dicFeO} C_{cFeO} + K_{dicGW} C_{cGW}) C_i] \} \\
 &- \nabla \cdot [\mathbf{q}_w (1 + K_{dicWF} C_{cWF} + K_{dicFeO} C_{cFeO} + K_{dicGW} C_{cGW}) C_i] \\
 &\pm Q_{idp} - (\rho_b \bar{s}_{CP} + \theta_w C_{cFeO} \bar{s}_{cFeO}) k_{if} C_i + \rho_b \bar{s}_{CP} k_{ir} \hat{C}_{iCP} - \theta_w \lambda_i^{embed} C_i \\
 &+ \theta_w [\lambda_i^p r_{Mi}^p R_{fi}^p C_i^p - \lambda_i R_{fi} C_i], \\
 \frac{\partial}{\partial t} [\theta_w R_{fi} C_i] &= \nabla \cdot (\theta_w D_i \nabla C_i) \\
 &+ \nabla \cdot \{ \theta_w D_c \nabla [(K_{dicWF} C_{cWF} + K_{dicFeO} C_{cFeO} + K_{dicGW} C_{cGW}) C_i] \} \\
 &- \nabla \cdot [\mathbf{q}_w (1 + K_{dicWF} C_{cWF} + K_{dicFeO} C_{cFeO} + K_{dicGW} C_{cGW}) C_i] \quad \text{(Eq. 6.5.1.2-39)} \\
 &\pm Q_{idp} - (\rho_b \bar{s}_{CP} + \theta_w C_{cFeO} \bar{s}_{cFeO}) k_{if} C_i + \rho_b \bar{s}_{CP} k_{irs} \hat{C}_{iCP} \\
 &+ \theta_w C_{cFeO} \bar{s}_{cFeO} k_{irecm} \hat{C}_{iFeO} - \theta_w \lambda_i^{embed} C_i + \theta_w [\lambda_i^p r_{Mi}^p R_{fi}^p C_i^p - \lambda_i R_{fi} C_i],
 \end{aligned}$$

where the retardation factor for species i is defined by:

$$R_{fi} = 1 + \frac{\rho_b K_{dis}}{\theta_w} + K_{dicWF} C_{cWF} + K_{dicCP} C_{cFeO} + K_{dicGW} C_{cGW}, \quad \text{(Eq. 6.5.1.2-40)}$$

and R_{fi}^p is the corresponding retardation factor for the parent of radionuclide species i :

$$R_{fi}^p = 1 + \frac{\rho_b K_{dis}^p}{\theta_w} + K_{dicWF}^p C_{cWF} + K_{dicCP}^p C_{cFeO} + K_{dicGW}^p C_{cGW}. \quad \text{(Eq. 6.5.1.2-41)}$$

In Equation 6.5.1.2-39, the left side of the equation represents the accumulation of dissolved and reversibly sorbed radionuclide species i . The term in brackets is the mass of species i present in a unit bulk volume of EBS material, so the equation units are mass of species i per unit bulk volume of EBS per time. The first term on the right side represents the rate of diffusion of dissolved species i in the aqueous phase. The second term accounts for diffusion of mobile colloids on which species i is sorbed. The third term is the rate at which species i dissolved mass and mass reversibly sorbed to mobile colloids is transported by advection. The fourth term represents the net rate of dissolution or precipitation of species i . The fifth term is the conversion rate due to kinetic sorption on both iron oxyhydroxide stationary corrosion products and mobile colloids. The sixth and seventh terms are the conversion rate due to desorption from the iron oxyhydroxide corrosion products and iron oxyhydroxide colloids (in the corrosion products domain). The eighthseventh term is the rate of capture of species i by embedding in waste form colloids. The last (nintheighth) term accounts for ingrowth, or production of species i by decay of the parent of i , and decay of species i , as dissolved species and as sorbed onto colloids.

Inserting the source terms into Equation 6.5.1.2-30, the mass balance for kinetically sorbed radionuclides on iron oxyhydroxide corrosion product colloids becomes:

$$\frac{\partial(\theta_w \hat{C}_{icFeO})}{\partial t} = \nabla \cdot (\theta_w D_c \nabla \hat{C}_{icFeO}) - \nabla \cdot (\mathbf{q}_w \hat{C}_{icFeO}) + \theta_w C_{cFeO} \bar{s}_{cFeO} k_{if} C_i + \theta_w (\lambda_i^p r_{Mi}^p \hat{C}_{icFeO}^p - \lambda_i \hat{C}_{icFeO}).$$

$$\frac{\partial(\theta_w \hat{C}_{icFeO})}{\partial t} = \nabla \cdot (\theta_w D_c \nabla \hat{C}_{icFeO}) - \nabla \cdot (\mathbf{q}_w \hat{C}_{icFeO}) + \theta_w C_{cFeO} \bar{s}_{cFeO} k_{if} C_i - \theta_w C_{cFeO} \bar{s}_{cFeO} k_{ircm} \hat{C}_{icFeO} + \theta_w (\lambda_i^p r_{Mi}^p \hat{C}_{icFeO}^p - \lambda_i \hat{C}_{icFeO}). \quad (\text{Eq. 6.5.1.2-42})$$

The terms $\theta_w C_{cFeO} \bar{s}_{cFeO} k_{if} C_i$ and $\theta_w C_{cFeO} \bar{s}_{cFeO} k_{ircm} \hat{C}_{icFeO}$ in Equation 6.5.1.2-42 couples this equation to Equation 6.5.1.2-39.

The mass balance for kinetically sorbed radionuclides onto stationary iron oxyhydroxide corrosion products, Equation 6.5.1.2-32, accounts for sorption/desorption reactions and decay and is given by:

$$\frac{\partial(\theta_w \hat{C}_{iCP})}{\partial t} = \rho_b \bar{s}_{CP} k_{if} C_i - \rho_b \bar{s}_{CP} k_{irs} \hat{C}_{iCP} + \theta_w (\lambda_i^p r_{Mi}^p \hat{C}_{iCP}^p - \lambda_i \hat{C}_{iCP}). \quad (\text{Eq. 6.5.1.2-43})$$

The ~~source~~ terms $\rho_b \bar{s}_{CP} k_{if} C_i$ and $\rho_b \bar{s}_{CP} k_{irs} \hat{C}_{iCP}$ in Equation 6.5.1.2-43, ~~$\rho_b \bar{s}_{CP} k_{if} C_i$~~ , couples this equation to Equation 6.5.1.2-39.

For a single continuum medium with no colloids or corrosion products present, Equation 6.5.1.2-39 reduces to the conventional advection/diffusion transport equation (with source and sink terms):

$$\frac{\partial(\theta_w R_{fi} C_i)}{\partial t} = \nabla \cdot (\theta_w D_i \nabla C_i) - \nabla \cdot (\mathbf{q}_w C_i) \pm Q_{idp} + \theta_w (\lambda_i^p r_{Mi}^p C_i R_{fi}^p - \lambda_i C_i R_{fi}). \quad (\text{Eq. 6.5.1.2-44})$$

with the conventional retardation factors for radionuclide species i and parent of species i , respectively:

$$R_{fi} = 1 + \frac{\rho_b K_{dis}}{\theta_w} \quad (\text{Eq. 6.5.1.2-45})$$

and

$$R_{fi}^p = 1 + \frac{\rho_b K_{dis}^p}{\theta_w}. \quad (\text{Eq. 6.5.1.2-46})$$

Equations 6.5.1.2-39 (mass balance for dissolved and reversibly sorbed radionuclide species i), 6.5.1.2-42 (mass balance for radionuclide species i kinetically sorbed onto iron oxyhydroxide colloids) and 6.5.1.2-43 (mass balance radionuclide species i kinetically sorbed onto stationary

iron oxyhydroxide corrosion products) are solved simultaneously for all radionuclides to obtain the dependent variables, C_i , \hat{C}_{iCP} , and \hat{C}_{iFeO} , the concentration of dissolved radionuclide species i , the concentration of species i kinetically sorbed onto iron oxyhydroxide colloids, and species i kinetically sorbed onto stationary iron oxyhydroxide corrosion products, respectively. The solution is a finite difference approximation to the continuum equations with discretization of time and space (Section 6.5.2.5).

The initial conditions are $C_i = \hat{C}_{iCP} = \hat{C}_{iFeO} = 0$ for all species i . Upstream of the waste form domain, all radionuclide concentrations are zero. Consequently, the upstream boundary maintains a zero flux condition. Radionuclide concentrations will remain zero until a waste package failure occurs. A treatment of the zero downstream concentration boundaries within the UZ is provided in Section 6.5.2.6. The radionuclides are released or mobilized within the waste form domain. Flow is expected to be predominately downward. Then the resulting transport will be in a downward direction from the waste form to the corrosion products, which will accumulate in the bottom of the waste container. From the corrosion products, the radionuclides will migrate down to the invert, and from there they will enter the UZ. The representation for the radionuclide transport is consequently a one-dimensional mass balance equation for radionuclide species. For the one-dimensional EBS radionuclide transport model, the positive z -direction is oriented downward. The specific discharge (Darcy velocity) vector, \mathbf{q}_w , is always in the downward positive z -direction and is denoted by $\mathbf{q}_w = q_{wz}\mathbf{i}$, where \mathbf{i} is a unit vector in the positive z -direction, and q_{wz} is the scalar specific discharge in the z -direction (zero in the other two directions). In one dimension, the mass balance equations can be written as scalar equations and are summarized as follows.

The one-dimensional mass balance equation describing transport of dissolved, ~~and~~ reversibly sorbed, and kinetically sorbed radionuclide species i (Equation 6.5.1.2-39) is:

$$\begin{aligned}
 \frac{\partial}{\partial t} [\theta_w R_{fi} C_i] &= \frac{\partial}{\partial z} \left(\theta_w D_i \frac{\partial C_i}{\partial z} \right) \\
 &+ \frac{\partial}{\partial z} \left(\theta_w D_c \frac{\partial}{\partial z} [(K_{dicWF} C_{cWF} + K_{dicFeO} C_{cFeO} + K_{dicGW} C_{cGW}) C_i] \right) \\
 &- \frac{\partial}{\partial z} [q_{wz} (1 + K_{dicWF} C_{cWF} + K_{dicFeO} C_{cFeO} + K_{dicGW} C_{cGW}) C_i] \\
 &\pm Q_{idp} - (\rho_b \bar{s}_{CP} + \theta_w C_{cFeO} \bar{s}_c) k_{if} C_i + \rho_b \bar{s}_{CP} k_{ir} \hat{C}_{iCP} \\
 &- \lambda_i^{embed} C_i + \theta_w [\lambda_i^p r_{Mi}^p R_{fi}^p C_i^p - \lambda_i R_{fi} C_i]. \\
 \frac{\partial}{\partial t} [\theta_w R_{fi} C_i] &= \frac{\partial}{\partial z} \left(\theta_w D_i \frac{\partial C_i}{\partial z} \right) \\
 &+ \frac{\partial}{\partial z} \left(\theta_w D_c \frac{\partial}{\partial z} [(K_{dicWF} C_{cWF} + K_{dicFeO} C_{cFeO} + K_{dicGW} C_{cGW}) C_i] \right) \\
 &- \frac{\partial}{\partial z} [q_{wz} (1 + K_{dicWF} C_{cWF} + K_{dicFeO} C_{cFeO} + K_{dicGW} C_{cGW}) C_i] \\
 &\pm Q_{idp} - (\rho_b \bar{s}_{CP} + \theta_w C_{cFeO} \bar{s}_c) k_{if} C_i + \rho_b \bar{s}_{CP} k_{ir} \hat{C}_{iCP} + \theta_w C_{cFeO} \bar{s}_{cFeO} k_{ircm} \hat{C}_{iFeO} \\
 &- \lambda_i^{embed} C_i + \theta_w [\lambda_i^p r_{Mi}^p R_{fi}^p C_i^p - \lambda_i R_{fi} C_i].
 \end{aligned} \tag{Eq. 6.5.1.2-47}$$

Within the corrosion products domain, the concentrations will remain below the solubility limit, and the term $Q_{idp} = 0$ in Equation 6.5.1.2-47. Also, within the corrosion products domain there is no source term for the waste form colloids, and $\lambda_i^{embed} = 0$. Within the waste form domain, there are no groundwater or iron oxyhydroxide colloids and no immobile corrosion product material, which imply the terms in Equation 6.5.1.2-47 associated with these processes will be zero.

Similarly, the one-dimensional mass balance equation for kinetically sorbed radionuclide species i on mobile iron oxyhydroxide colloids (Equation 6.5.1.2-42) is:

$$\begin{aligned}
 \frac{\partial (\theta_w \hat{C}_{iFeO})}{\partial t} &= \frac{\partial}{\partial z} \left(\theta_w D_c \frac{\partial \hat{C}_{iFeO}}{\partial z} \right) - \frac{\partial}{\partial z} (q_{wz} \hat{C}_{iFeO}) \\
 &+ \theta_w C_{cFeO} \bar{s}_{cCP} k_{if} C_i + \theta_w (\lambda_i^p r_{Mi}^p \hat{C}_{iFeO}^p - \lambda_i \hat{C}_{iFeO}). \\
 \frac{\partial (\theta_w \hat{C}_{iFeO})}{\partial t} &= \frac{\partial}{\partial z} \left(\theta_w D_c \frac{\partial \hat{C}_{iFeO}}{\partial z} \right) - \frac{\partial}{\partial z} (q_{wz} \hat{C}_{iFeO}) \\
 &+ \theta_w C_{cFeO} \bar{s}_{cCP} k_{if} C_i - \theta_w C_{cFeO} \bar{s}_{cFeO} k_{ircm} \hat{C}_{iFeO} \\
 &+ \theta_w (\lambda_i^p r_{Mi}^p \hat{C}_{iFeO}^p - \lambda_i \hat{C}_{iFeO}).
 \end{aligned} \tag{Eq. 6.5.1.2-48}$$

This equation is not required within the waste form domain.

The one-dimensional mass balance equation for kinetically sorbed radionuclide species i on stationary iron oxyhydroxide corrosion products is the same as Equation 6.5.1.2-43, since there is no advection or diffusion of corrosion products:

$$\frac{\partial(\theta_w \hat{C}_{iCP})}{\partial t} = \rho_b \bar{s}_{CP} k_{if} C_i - \rho_b \bar{s}_{CP} k_{ir} \hat{C}_{iCP} + \theta_w (\lambda_i^p r_{M_i}^p \hat{C}_{iCP}^p - \lambda_i \hat{C}_{iCP}). \quad (\text{Eq. 6.5.1.2-49})$$

This equation only applies to the corrosion product domain.

In one dimension, the mass balance equation for waste form colloid transport (Equation 6.5.1.2-37) is:

$$\frac{\partial(\theta_w C_{cWF})}{\partial t} = \frac{\partial}{\partial z} \left(\theta_w D_c \frac{\partial C_{cWF}}{\partial z} \right) - \frac{\partial}{\partial z} (\mathbf{q}_w C_{cWF}) + Q_{cWFs}. \quad (\text{Eq. 6.5.1.2-50})$$

Within the waste package, the media supporting transport are represented as single continua. In the UZ, however, the bulk medium is conceptualized as a dual continuum, characterized by two sets of local-scale properties unique to each continuum. Transport in the dual continuum media is represented by a mass balance equation for each continuum. The single invert continuum interfaces a dual continuum (fracture/matrix) UZ medium. Advective transport from the invert enters both the UZ fracture and matrix continua.

The diffusive transport between the single invert continuum and the dual UZ continua is determined from the continuity of mass transport across the interface. This requirement states that the diffusive rate exiting or entering the invert domain is equal to the sum of the diffusive rates fluxes entering or exiting the two UZ continua. The diffusive rate split at the interface will depend on the diffusive properties in the invert domain and both UZ continua together with the concentration gradients across the interface.

For discussion of the diffusive transport treatment at the invert/UZ interface, consider a diffusive rate term, either aqueous or colloid, within the transport mass balance equation. Let $z_{interface}$ denote the spatial location of the invert/UZ interface. Then for $z < z_{interface}$, the diffusive rate for radionuclide species i at a location within the invert domain is:

$$\theta_{wI} A_I D_{iI} \frac{\partial C_{iI}}{\partial z}, \quad (\text{Eq. 6.5.1.2-51})$$

where subscript I denotes the single-continuum invert domain.

For $z > z_{interface}$, the diffusive rates within the UZ matrix and UZ fracture continua are, respectively,

$$\theta_{wm} A_{mf} D_{im} \frac{\partial C_{im}}{\partial z}, \quad (\text{Eq. 6.5.1.2-52})$$

$$\theta_{wf} A_{mf} D_{if} \frac{\partial C_{if}}{\partial z}. \quad (\text{Eq. 6.5.1.2-53})$$

where A_{mf} denotes the area normal to transport in the matrix/fracture domain.

The mass transport rate via diffusion across this interface is modeled as continuous at the interface:

$$\theta_{wl} A_l D_{il} \frac{\partial C_{il}}{\partial z^-} = \theta_{wm} A_{mf} D_{im} \frac{\partial C_{im}}{\partial z^+} + \theta_{wf} A_{mf} D_{if} \frac{\partial C_{if}}{\partial z^+}, \quad (\text{Eq. 6.5.1.2-54})$$

where

$$\frac{\partial}{\partial z^-} \quad \text{and} \quad \frac{\partial}{\partial z^+}$$

are the derivative from the left (backward) and the derivative from the right (forward), respectively, at the interface. The spatial direction from the invert to the UZ domain is in the positive z -direction.

The waste form colloids are generated in the waste form domain and are transported in accordance with an advective/diffusive mass balance. The waste form colloid concentration is subject to stability constraints based on the local domain chemistry. The waste form colloids transport both reversibly sorbed radionuclide mass and embedded radionuclide mass. The iron oxyhydroxide colloids exist in the corrosion products and invert domains, and the colloid concentrations are dependent on the local domain chemistry. The iron oxyhydroxide colloids transport both reversibly sorbed and kinetically sorbed radionuclide mass. The kinetically sorbed radionuclides are sorbed onto the surface of these colloids, rather than being embedded within the colloid matrix, as are the radionuclides associated with the waste form colloids.

[Kinetic desorption of radionuclides from the iron oxyhydroxide colloids is modeled in the corrosion products domain as a way to implement the sorbed mass in proportions predicted by the competitive sorption model discussed in Sections 6.5.2.4 and 6.5.2.7. Once the iron oxyhydroxide colloids leave the corrosion products domain, the kinetically sorbed mass is treated as irreversibly sorbed in the downstream transport domains.](#)

The groundwater colloids exist in the corrosion products and invert domains, and their concentrations are dependent on the local domain chemistry. The groundwater colloids transport only reversibly sorbed radionuclide mass. The iron oxyhydroxide corrosion products are immobile and found only in the corrosion products domain. These corrosion products support both reversibly sorbed and kinetically sorbed radionuclide mass with the kinetic sorbed mass desorbing to solution.

All of the features of the EBS radionuclide transport abstraction are accounted for in Equations 6.5.1.2-39, 6.5.1.2-37, 6.5.1.2-42, and 6.5.1.2-43 (or the one-dimensional versions of these equations, Equations 6.5.1.2-47, 6.5.1.2-50, 6.5.1.2-48, and 6.5.1.2-49, respectively), including invert diffusion, retardation in the waste package, in-package diffusion, and transport facilitated by reversible and irreversible colloids. Implementation of these equations into TSPA involves additional simplifications and restrictions that are discussed in Section 6.5.2.

6.5.2 Summary of Computational Model

The object of the EBS radionuclide transport abstraction is to determine the rate of radionuclide releases from the EBS to the UZ. In the EBS transport model, the EBS is spatially partitioned into the following domains: (1) waste form, consisting of, for example, fuel rods, HLW glass, and DSNF; (2) waste package corrosion products; and (3) invert. In addition, the UZ immediately underlying the invert is conceptualized as a dual continuum consisting of (4) UZ matrix continuum and (5) UZ fracture continuum. The inclusion of a portion of the UZ is needed for an accurate calculation of the invert-to-UZ interface fluxes by providing a diffusive path length that is sufficiently long such that the concentration at the outlet of the UZ can realistically be assigned a value of zero.

In the waste form domain, degradation processes occur, including breaching and axial splitting of fuel rods, dissolution of SNF and HLW glass, and formation of waste form colloids wherever applicable. Dissolved species are transported by advection and/or diffusion to the waste package corrosion products domain. The primary interactions in the corrosion products domain involving radionuclide species are competitive reversible and kinetic sorption onto stationary corrosion products ~~and, reversible and kinetic sorption of dissolved species onto~~ iron oxyhydroxide colloids, and reversible sorption onto groundwater colloids and waste form colloids (when present). In the invert domain, radionuclides released from the corrosion products domain are transported by advection and diffusion, and interact with the crushed tuff by adsorption processes. The properties of each domain, including the volume, porosity, water saturation, diffusion cross-sectional area, and diffusive path length, affect the rate of advective and diffusive transport of radionuclides through the domain. The invert domain interfaces with both continua of the UZ. The properties of the domains are defined in the following sections.

6.5.2.4 Sorption onto Iron Oxyhydroxide Colloids and Stationary Corrosion Products

As stated earlier (Section 6.3.4.2.3), the sorption processes in transport calculations are applied to the isotopes of uranium, neptunium, plutonium, americium, and thorium. Transport of nickel is not considered in the TSPA even though it is included in the surface complexation based model in order to account for competition among various elements for sorption on a finite number of sites. The equilibrium sorption is modeled for uranium, neptunium, and thorium, while kinetic sorption/desorption on the stationary corrosion products and iron oxyhydroxide colloids is modeled for plutonium and americium. Once the iron oxyhydroxide colloids leave the corrosion products domain, the kinetically sorbed mass of plutonium and americium is treated as, because they also get transported while irreversibly sorbed onto iron oxyhydroxide colloids for transport through the downstream domains.

6.5.2.4.1 Sampling Methodology

In order to perform calculations based on surface complexation, the input concentrations of various elements expected in the TSPA over the course of simulated timescale, need to be determined. This is difficult to predict because waste form degradation rates, transport processes, water volumes, chemical conditions, decay and in-growth rates, etc., vary with time and space. There are virtually an infinite number of combinations for the set of concentrations of various elements that could be considered in the sorption calculations. Each combination of concentration could lead to different sorption amounts.

Even though the concentrations for various elements considered, cannot be determined *a priori*, the range over which they could vary can be estimated. The maximum value cannot be greater than the solubility of the controlling mineral phase, and the minimum value could be nearly zero. Once the maximum and minimum values for each element are determined, the concentration space can be sampled randomly using the Latin Hypercube Sampling methodology. This provides various combinations of elemental concentrations for which the surface complexation calculations can be performed to determine sorbed mass.

The maximum value or the dissolved concentration limit for the controlling mineral phase for a given pH and P_{CO_2} is determined by *Dissolved Concentration Limits of Elements with Radioactive Isotopes* (SNL 2007 [DIRS 177418]). The methodology outlined in DTN: MO0702PADISCON.001 [DIRS 179358] is to compute the mean value of the solubility controlling mineral phase for a given pH and P_{CO_2} to which two uncertainties are added as shown below:

$$\text{Solubility}[\text{Pu, Np, U, Am, \&Th}] = 10^S 10^{\varepsilon_1} + \varepsilon_2 N, \quad (\text{Eq. 6.5.2.4.1-1})$$

where 10^S is the mean actinide solubility provided in a series of 2-D look up tables provided in DTN: MO0702PADISCON.001 [DIRS 179358], ε_1 is the uncertainty term associated with uncertainty in $\log K$ (\log of the solubility product) values described by a normal distribution truncated at 2σ , and ε_2 is the uncertainty term associated with variations in fluoride concentration that varies by the type of waste package being considered and by the pH. The fluoride uncertainty for the various actinides is perfectly correlated during sampling and is defined by a right-sided triangular distribution. N is the factor by which the maximum fluoride uncertainty (ε_2) is normalized for pH.

Due to the complexity involved in calculating the range of solubility for various combinations of pH and P_{CO_2} and incorporating the uncertainties, the methodology was simplified by determining the maximum possible value of solubility. This approach is reasonable and sufficient, because ultimately the dissolved concentration space will have to be sampled between the maximum and minimum values. The minimum value is arbitrarily chosen to be 10^{-8} times the maximum value, to cover the range of expected concentrations in the TSPA Model. The maximum solubility of an element at a given pH and P_{CO_2} is calculated by placing the maximum of ε_1 (from DTN: MO0702PADISCON.001 [DIRS 179358]) and the maximum of ε_2 (from DTN: MO0702PAFLUORI.000 [DIRS 181219]) values in Equation 6.5.2.4.1-1 for that element (see Table 6.5-10):

$$\text{Solubility}^{\max} = 10^S 10^{\varepsilon_1^{\max}} + \varepsilon_2^{\max} N. \quad (\text{Eq. 6.5.2.4.1-2})$$

Since the surface complexation based calculations have been done using PHREEQC (V. 2.11 2006 [DIRS 175698]), the pre-sampled combination of dissolved concentrations would have to be first generated in PHREEQC. This can be achieved by simply adjusting the saturation index of the solubility controlling phase in PHREEQC such that the adjusted amount is either an additive or subtractive term in the log space, which translates into a multiplicative ratio in the linear space whose value varies from greater than one to less than one. The multiplicative ratio is equal to the ratio of the dissolved concentration to the mean solubility, and thus the log of the ratio is equivalent to the adjusted saturation index of the controlling phase—a value that can be

directly used as input in the PHREEQC simulations. The maximum value of the ratio, R^{\max} , is calculated by dividing the maximum solubility (that includes the two uncertainty terms; Equation 6.5.2.4.1-2) by the mean solubility as shown below:

$$R^{\max} = 10^{\epsilon_1^{\max}} + \epsilon_2^{\max} (N/10^S)^{\max}. \quad (\text{Eq. 6.5.2.4.1-3})$$

The maximum value of this ratio is shown in Table 6.5-10 for the actinides of interest. For Ni, the maximum value of the ratio is set to 1.0, indicating that there is no uncertainty in the solubility.

The maximum ratio value for a given element is then multiplied by an uncertainty distribution that varies log-uniformly from 1 to 10^{-8} in order to sample the range of concentrations expected in TSPA. The uncertainty distribution for each element is defined by a separate stochastic that is sampled using the Latin Hypercube Sampling methodology using GoldSim V. 8.02.500 (2005 [DIRS 174650]) (file: *Sampling_Surface_Complexation_Calc_v8.02.500*, output DTN: SN0703PAEBSRTA.002). A total of 100 realizations are generated, where each realization represents a unique combination of concentrations of actinides (via the adjustment of the saturation index of the solubility controlling phase). In addition, the log of the drift P_{CO_2} is also sampled uniformly, over 100 realizations, from $\log_{10}(10^{-2} \text{ bar})$ to $\log_{10}(10^{-4} \text{ bar})$, since it affects the pH and aqueous speciation. The sampled values are listed in output DTN: SN0703PAEBSRTA.002 (file: *Final_Calc_Results_Surf_Complx_Data_1.xls*).

Besides the varying dissolved concentrations of the competing species, the surface properties would also vary in the EBS transport model implemented in the TSPA. The available surface area for sorption per unit water volume varies as a function of water saturation, corrosion rate, sampled specific surface area, and site density. The relative abundance of goethite and HFO is also uncertain and affects the sorption sites per unit water volume for both the stationary corrosion products and iron oxyhydroxide colloids. The number of sites available for sorption, in units of moles per liter of water, is calculated from the uncertain surface properties, considering the stationary corrosion products concentration to vary uniformly from 1 kg L^{-1} to 50 kg L^{-1} and iron oxyhydroxide colloid concentrations to vary log-uniformly from 0.001 mg L^{-1} to 30 mg L^{-1} . The uncertainty distributions are sampled using the Latin Hypercube Sampling methodology using GoldSim V. 8.02.500 (2005 [DIRS 174650]) (file: *Sampling_Surface_Complexation_Calc_v8.02.500*, output DTN: SN0703PAEBSRTA.002). A total of 50 realizations are generated to compute the total available sites for sorption per liter of water (output DTN: SN0703PAEBSRTA.002, file: *Final_Calc_Results_Surf_Complx_Data_1.xls*). The number of realizations chosen was deemed adequate since larger number of realizations did not change the shape of the output distribution appreciably.

For each realization of the surface property, 100 realizations of the dissolved concentrations and P_{CO_2} are considered in the SCM. In effect, the surface property realizations represents the outer loop while the dissolved concentration realizations represents the inner loop over which the SCM is exercised. A total of $50 \times 100 = 5,000$ combinations of surface property and dissolved concentrations are analyzed using the SCM.

Table 6.5-10. Data Used For Calculating Maximum Solubility Ratio

Element	ϵ_1^{\max}	$10^{\epsilon_1^{\max}}$	ϵ_2^{\max}	$\epsilon_2^{\max} (N/10^S)^{\max}$	Max Ratio
U	1.2	15.8	5385	216.6	232.4
Np	1.7	50.1	853	0.87	51
Pu	1.52	33.1	5460	0.249	33.3
Th	1.52	33.1	23723	3542	3575
Am	2.08	120.2	688.6	6.88	127

Output DTN: SN0703PAEBSRTA.002

6.5.2.4.2 Surface Complexation Modeling

A two-step modeling approach is adopted in PHREEQC. In the first step, equilibrium chemical modeling is performed to generate the dissolved concentrations for all six elements corresponding to the sampled saturation indices (sampled ratios) and P_{CO_2} for the 100 realizations. This step encompasses equilibrium speciation of the J-13 water composition (DTN: MO0006J13WTRCM.000 [DIRS 151029]) with dissolved actinides at concentrations calculated as a function of the saturation index of their solubility controlling phase. The J-13 composition was chosen to be consistent with *Dissolved Concentration Limits of Elements with Radioactive Isotopes* (SNL 2007 [DIRS 177418]).

In the second step, surface complexation reactions are modeled for the given surface property of stationary corrosion products and iron oxyhydroxide colloids (out of 50 realizations) by equilibrating the solution from the first step with both stationary corrosion products and iron oxyhydroxide colloid surfaces. In this step the dissolved concentrations are held at the values generated in the first step.

The first step contains additional sub-steps to account for the adjusted Eh model used for plutonium. The output of the surface complexation modeling includes the total aqueous concentration and the total sorbed concentration for each of the six elements, as well as the equilibrium pH.

The solubility controlling phases were the same as those used in *Dissolved Concentration Limits of Elements with Radioactive Isotopes* (SNL 2007 [DIRS 177418]). The actinides and their solubility controlling phases are listed in Table 6.5-11.

Table 6.5-11. Solubility Controlling Phase

Element	Solubility Controlling Phase
Uranium	Schoepite
Plutonium	PuO ₂ (hyd,aged)
Neptunium	NpO ₂
Americium	AmOHCO ₃
Thorium	ThO ₂ (am)

Output DTN: SN0703PAEBSRTA.002

The ~~thermodynamic~~ database “*phreeqcDATA025bdotCr3az.dat*” (DTN: MO0609SPAINOUT.002 [DIRS 179645]) was used in both steps of the PHREEQC modeling, with the surface complexation reactions and log K values entered directly in each input file. This is the most up to date thermo-chemical database available for PHREEQC; as such, its use in these calculations is justified.

The 100 realizations of the multiplication ratios generated are analogous to the ratio of dissolved concentration to the mean saturated concentration at a given P_{CO_2} . Thus, the log of the ratio yields the saturation index of the solubility controlling phase for any particular actinide element for a given P_{CO_2} . The nickel concentration is sampled directly, from 3×10^{-8} mg L⁻¹ to 3 mg L⁻¹. This range was chosen based on possible variability in the steel corrosion rates. In PHREEQC, it is possible to specify the concentration of an element in terms of the degree of saturation of a mineral phase containing that element, thus making it possible to combine elemental concentrations, i.e., the J-13 composition, with the sampled actinide solubility ratios and P_{CO_2} , while allowing PHREEQC to calculate the equilibrium actinide concentrations and pH of the solution.

The solution pH and aqueous solution concentration for all of the actinides, with the exception of plutonium, were calculated first where the P_{CO_2} , actinide phase saturation, J-13 composition, and P_{O_2} were specified. In *Dissolved Concentration Limits of Elements with Radioactive Isotopes* (SNL 2007 [DIRS 177418]), the Eh is calculated as a function of oxygen fugacity, where the fugacity is set to the atmospheric partial pressure of oxygen ($10^{-0.7}$ bar). Likewise, this same redox constraint was used in the present model for all of the actinides with the exception of plutonium.

Plutonium was excluded from the initial solution calculation because its solubility is redox sensitive, and the modified Eh relationship from *Dissolved Concentration Limits of Elements with Radioactive Isotopes* (SNL 2007 [DIRS 177418]) was implemented. This relationship calculates an Eh value based on the solutions pH via

$$Eh = 1.10 - 0.0592 \text{ pH.} \quad (\text{Eq. 6.5.2.4.2-1})$$

Thus, the solution pH from initial PHREEQC calculation was used to calculate the Eh condition under which PuO₂ (phase hyd,aged) would dissolve. The output concentrations (J-13 water plus actinide) from the initial PHREEQC run were used as input for the Pu calculation step.

Of the 100 realizations for the fluid composition, 96 converged in PHREEQC. Four realizations did not converge due to very high values of schoepite saturation (>100×), or high values of schoepite saturation combined with high saturation of another controlling phase. In these extreme circumstances, the PHREEQC convergence criteria could not be met, and the realization had to be dropped from further consideration. The non-convergence of four realizations (out of 100) is simply an artifact of pre-sampling the uncertainty in the solubility for various elements and P_{CO_2} independently of each other for input into PHREEQC. It is manifested by adjusting the saturation indices of the mineral phases. Because the uncertainties are pre-sampled randomly, some of the inputs to PHREEQC become non-physical in that the saturation indices for schoepite and other mineral phases had to be set to extreme values.

The results of the solution calculation Step 1, which were passed to the corrosion product equilibration Step 2, included the J-13 composition with the sampled P_{CO_2} , and the PHREEQC calculated pH and actinide concentration values. In Step 2, each of the 96 aqueous solutions from Step 1 was equilibrated with the 50 sets of corrosion product and colloid surface properties while the P_{CO_2} , P_{O_2} , and actinide solubility controlling phases were maintained at their Step 1 values. The actinide phase solubility control was maintained for the purpose of loading the adsorption sites on the iron corrosion products and colloids such that surface loading could be accounted for in the K_d abstractions.

The surface complexation reactions and their accompanying log K values used in the analyses are listed in Table 6.5-12. These reactions and log K values were entered directly in each of the PHREEQC input files (*stat_col_ZPC.pqi*) included in output DTN: SN0703PAEBSRTA.002 and were not contained in the thermodynamic database "*phreeqcDATA025bdotCr3az.dat*". The surface complexes in Table 6.5-12 were identified and chosen for inclusion in the model because they represented the most comprehensive and best available internally consistent set of single-site complexes for the actinides of interest (a literature search and selection details for surface complexation reactions and their accompanying log K values are described in Appendix J). The output of Step 2 included the sorbed actinide concentrations for the corrosion products and colloids, the aqueous actinide concentrations, and the pH. These output data were reduced in Excel using the surface properties of the corrosion products and colloids to yield the distribution coefficients for each of the actinide elements. Uncertainty in the surface complexation constants (Table 6.5-12) was not considered at this stage; instead, uncertainty in the mineral and aqueous species thermochemical data was propagated through the SCM.

Table 6.5-12. Surface Complexation Reactions and log K Values

Surface Complexation Reaction*	Log K
HfssOH + H+ = HfssOH2+	7.35
HfssOH = HfssO- + H+	-9.17
HfssOH + UO2+2 + 2CO3-2 + H+ = HfssOH2UO2(CO3)2-	29.15
HfssOH + UO2+2 + 3CO3-2 + H+ = HfssOH2UO2(CO3)3-3	36.28
HfssOH + 2UO2+2 + CO3-2 + 3H2O = HfssOH2(UO2)2CO3(OH)3 + 2H+	12.62
HfssOH + PuO2+ = HfssOPuO2+	5.14
HfssOH + PuO2+ = HfssOPuO2 + H+	-2.95
HfssOH + PuO2+ + H2O = HfssOPuO2OH- + 2H+	-11.35
HfssOH + Pu+4 = HfssOPu+3 + H+	14.33
HfssOH + Pu+4 + H2O = HfssOPuOH+2 + 2H+	8.79
HfssOH + Pu+4 + 3H2O = HfssOPu(OH)3 + 4H+	-3.92
HfssOH + PuO2+2 = HfssOPuO2+ + H+	3.0
HfssOH + NpO2+ = HfssOHNpO2+	6.03
HfssOH + NpO2+ + H2O = HfssONpO2OH- + 2H+	-12.0
HfssOH + Am+3 + H2O = HfssOAmOH+ + 2H+	-6.27
HfssOH + Th+4 = HfssOHTh+4	18.7

Table 6.5-12. Surface Complexation Reactions and log K Values (Continued)

Surface Complexation Reaction*	Log K
HfssOH + Th+4 + 2H2O= HfssOTh(OH)2+ + 3H+	-2.0
HfssOH + Th+4 + 4H2O= HfssOTh(OH)4- + 5H+	-16.7
HfssOH + Ni+2 = HfssONi+ + H+	-2.5
HfssOH + CO3-2 = HfssOHCO3-2	4.78
HfssOH + CO3-2 + 2H+ = HfssHCO3 + H2O	20.3

*Hfss represents the iron oxy-hydroxide surface.

Output DTN: SN0703PAEBSRTA.002

6.5.2.4.3 Abstraction and Multiple Linear Regression

The output of the surface complexation based competitive sorption modeling included a total of 4,800 simulated realizations (= 50 surface property × 96 dissolved concentration combinations) of sorbed masses. These results are abstracted in order to develop a response surface to predict the sorbed amounts for each of the elements for implementation in the TSPA Model.

Since the total available sites for sorption (spl), in mole per liter of water, are computed from the specific surface area (ssa), in $\text{m}^2 \text{g}^{-1}$, and the concentrations, in $\text{g L}^{-1} \text{H}_2\text{O}$, of corrosion products (mass) and iron oxyhydroxide colloids, these two parameters were also considered in computing the response surface. It was noted that the sorbed masses on the stationary corrosion products and iron oxyhydroxide colloids, when normalized (per [sorbate-sorbent](#) mass), gave the same values. Thus, the response surface for sorption need not be computed separately for the corrosion products and iron oxyhydroxide colloids, but rather the response surface developed for sorption on the corrosion products could be directly applied to the iron oxyhydroxide colloids.

For computing the response surface of the sorbed masses, the three corrosion product properties, $\text{pCO}_2 = -\log_{10}(P_{\text{CO}_2})$, and the dissolved concentration of the six elements were considered as predictors. This made a total of ten possible variables to be considered as predictors for the six regression models (one each for the element of interest). In addition, a regression model is developed for predicting the pH, since it is also an output of the SCM. Table 6.5-13 shows the predictors, response variables and their corresponding abbreviations as used in this section.

Table 6.5-13. List of Predictor and Response Variables

Predictor Variables	Abbreviation
$-\log_{10}(P_{\text{CO}_2})$	pCO2
Corrosion product sites per volume of water	spl
Corrosion product specific surface area	ssa
Corrosion product mass concentration	mass
U dissolved concentration	U
Pu dissolved concentration	Pu
Np dissolved concentration	Np
Am dissolved concentration	Am
Th dissolved concentration	Th

Ni dissolved concentration	Ni
$\log_{10}(X)$, where X is the nuclide concentration abbreviation	$\log X$
Response Variables	Abbreviation
pH	pH
U sorbed concentration	sU.CP
Pu sorbed concentration	sPu.CP
Np sorbed concentration	sNp.CP
Am sorbed concentration	sAm.CP
Th sorbed concentration	sTh.CP
Ni sorbed concentration	sNi.CP
$\log_{10}(X)$, where X is the nuclide concentration abbreviation	$\log X$

The most important criterion in abstracting the results from the competitive sorption modeling was that the regression model had to provide good predictive capability over the anticipated parameter space. In this section, the term “model” is used to refer to the abstracted (regression) model. Another important consideration was that the model had to be implemented for prediction in GoldSim, so a simple closed-form analytical expression was desirable.

Several regression approaches were considered in developing the model using the statistical software S-PLUS. The simplest approach would be multiple regressions with a linear model. Other forms of the linear model could involve transformations of the parameters or polynomial terms. Nonparametric regression approaches were also considered, such as alternating conditional expectations and projection pursuit regression, which includes predictor interactions. Because these nonparametric approaches did not yield results that were substantially better than the simpler linear models, and since the nonparametric approaches could be more difficult to implement as predictive models in GoldSim, the preference was given to a form of multiple regression.

6.5.2.4.4 Analysis

In any regression analysis, a prudent first step is examining scatter plot matrices of the predictor and response variables, to see if any obvious correlations exist among the variables. Figure 6.5-10 shows an example of a scatter plot matrix for pCO_2 , and the corrosion product properties, along with the response variable, pH. Concentrations for both the predictor (and response variables, not shown in this plot) are log-transformed, since they range over many orders of magnitude. Scatter plot matrices are useful in showing both predictor-predictor relationships and predictor-response relationships. For example, Figure 6.5-10 shows the strong correlation between pH and pCO_2 , with little correlation with any of the other predictors. Figure 6.5-11 shows the dissolved nuclide concentration predictors plotted with the same response variable, pH. There is no strong, monotonic trend between pH and any of these predictors. However, for some ranges of pH, there is a trend. For example, for high values of pH, $\log Am$ has a good positive correlation with pH. Thus, some of these predictors may appear in the pH regression model, but will not be the dominant predictors. Plots such as these give an early indication of what variables may be important in the regression models.

The initial multiple regression models explored log transformations of the corrosion product predictors. It was determined, through trial and error, that log transformation of spl improved the

regression fit. It was also determined that adding second order polynomial terms improved the regression models. Therefore, the initial model was a model with all 10 predictors and corresponding second order terms for the 10 predictors.

To increase the simplicity and robustness of the models, the first and second order terms were evaluated by stepwise regression. In stepwise regression, each term is added or removed from the model to judge its effect on a particular model selection criteria. In this case, the model selection criterion is the Akaike Information Criteria, or AIC (Venables and Ripley 2001 [DIRS 159088]). The AIC is calculated as follows:

$$\text{AIC} = 2k - 2 \log_{10}(L). \quad (\text{Eq. 6.5.2.4.4-1})$$

Here, k is the number of model parameters, and L is the likelihood function. The AIC is a measure of the goodness of fit of the model balanced against the complexity of the model.

The stepwise regression started with a full model, with all predictors as second order polynomials. The stepwise regression process then drops terms, refits the model, and evaluates the AIC to see whether the model is better without a particular term. A penalty parameter (penalizing model complexity) can be adjusted by the analyst to force the stepwise regression to produce a simpler model, with fewer terms. Figure 6.5-12 shows an example of the coefficient of variation (R^2) increase with increasing number of predictors, for the logsU.CP model. The figure shows that the fit does not improve significantly after the inclusion of about five predictors.

6.5.2.4.5 Results

The stepwise regression for all of the response variables was performed. The primary predictors for all of the sorbed concentration models followed a similar trend. First, spl and pCO₂ were included. In addition, the dissolved concentration of the nuclide corresponding to the response variable and the dissolved concentration of U were included. Table 6.5-14, below, shows the coefficients for each of the predictors, for each of the response variables.

Table 6.5-14. Coefficients for the Final Regression Models

	pH	logsU.CP	logsPu.CP	logsNp.CP	logsAm.CP	logsTh.CP	logsNi.CP
(Intercept)	4.5342	0.9727	-2.0371	0.1561	-3.2250	-0.3107	-5.0808
pCO ₂	0.6132		0.6036		1.0190		0.8026
pCO ₂ ²		-0.0837				0.0838	
log(spl)		1.0027	0.9972	0.9789	0.9754	1.0151	0.9144
log(U)	-0.3805	-0.3489	-0.9172	-1.1643	-1.4669	-0.7201	-1.6646
log(U) ²	-0.0254	-0.0922	-0.0516	-0.0671	-0.0887	-0.0379	-0.1019
logPu			0.9500				
logNp				0.9784			
logAm					0.9423		
logTh						0.8942	
logNi							0.9478
R^2	0.6281	0.9509	0.9460	0.9539	0.9606	0.9574	0.9584

Output DTNs: SN0703PAEBSRTA.001, SN0703PAEBSRTA.002

Also shown in Table 6.5-14 is the coefficient of variation (R^2) for each model. For the sorbed concentration responses, the coefficient of variation is close to unity in each case, indicating a good model fit. For pH, the R^2 value is 0.63, which still indicates a decent predictive capability for the model, however, with some unexplained variance. This unexplained variance can be accounted by adding an error term to the regression model. The error term is computed by considering the plot of the residuals (Figure 6.5-13), which indicates that the residuals (unexplained variance) follow a normal distribution with mean of zero and standard deviation of 0.32. As a result, the error term is defined by the same distribution but truncated at ± 2 standard deviations.

Figure 6.5-13 shows the diagnostic plots for the regression model of pH. The plot in the upper left shows the observed versus predicted points in the data set. Although the general trend of the points follows the 1:1 line, there is some scatter, which is expected given the R^2 value of 0.63. This is contrasted with the logsU.CP diagnostics in Figure 6.5-14, where the observed versus predicted plot shows points more tightly clustered around the 1:1 line, with the higher R^2 value of 0.95. In Figure 6.5-13, the plot in the upper right shows fitted versus residuals. Most of the residuals are evenly distributed around zero over the data range, which indicates minimal bias in the model. Most of the residuals lie between -0.5 and 0.5 pH unit. Finally, the plot in the lower left shows the normal q-q diagnostic plot. The points fall on the line from approximately -2 to 2, indicating a close-to-normal distribution of residuals from -2 to +2 standard deviations. This normal distribution of residuals helps confirm the lack of bias in the model.

Figures 6.5-14 through 6.5-19 show the diagnostic plots for the sorbed concentration regression models. These are mostly unremarkable; that is, the fitted versus response plots show tight clustering around the 1:1 line, and the residual versus fitted plots show most of the points clustered around the origin, with the occasional small group of outliers. There is some indication of non-normality for the quantiles < -1.0 , for some of the models.

6.5.2.4.6 Model Implementation

Based on the results presented in Table 6.5-14, the sorbed mass on stationary corrosion products and iron oxyhydroxide colloids for a given element is computed in terms of sorbed moles per liter of water. This amount is then converted to an effective K_d value by dividing first by the mass concentration of stationary corrosion products (kg L^{-1}) and then dividing it by the dissolved concentration that is computed at the beginning of the time step. The effective K_d calculated for the stationary corrosion products is the same as that for the iron oxyhydroxide colloids. Although the model calculations are performed by varying the P_{CO_2} over two orders of magnitude (ranging from 10^{-2} to 10^{-4} bars) and by varying the stationary corrosion products concentrations over an order of magnitude (ranging from 1.0 to 50 kg L^{-1}), the regression results can be extrapolated with a reasonable degree of confidence over a broader range of P_{CO_2} ranging from less than 10^{-4} bars to 2×10^{-2} bars. Extrapolating the regression equation over this range is reasonable as the extrapolated values would fall within the uncertainty band of the dataset reflected in the coefficient of variation of the regression model. Furthermore the in-drift P_{CO_2} values less than 10^{-4} bars and greater than 10^{-2} bars are expected to be possible only during the early phase of the thermal cooling down period and to last for only a short time period compared to the simulation time.

The computed effective K_d value is directly applicable in the transport equation for U, Np, and Th that are modeled to undergo equilibrium sorption. The transport for these elements is described by Equation 6.5.1.2-47. For plutonium and americium, that undergo kinetic sorption-desorption reactions, Equations 6.5.1.2-48 and 6.5.1.2-49 are applied. A kinetic approach is taken for Pu and Am plutonium and americium because information suggests that desorption from iron oxyhydroxide colloids is much slower than the sorption processes (Lu et al. 1998 [DIRS 174714], Lu et al. 2000 [DIRS 166315]) and thus best modeled with a non-equilibrium (kinetic) based approach. The forward reaction rate is calculated by Equations 6.5.1.2-14 and 6.5.1.2-20, while the reverse (desorption) rate is calculated from Equation 6.5.1.2-15 and 6.5.1.2-20a. The forward rate constant is a sampled parameter that is an output from DTN: MO0701PAIRONCO.000 [DIRS 180440]. It ranges from 0.002 to 0.05 $\text{m}^3 \text{m}^{-2} \text{yr}^{-1}$ with a log-uniform distribution. The same forward rate constant value is applied to both ~~Pu and Am~~ plutonium and americium. The reverse rate constant is computed by dividing the forward rate constant by the K_d value derived from surface complexation based modeling. Separate reverse reaction rates (on a bulk volume basis) are calculated for the stationary corrosion products and iron oxyhydroxide colloids due to their different bulk surface areas. ~~A kinetic approach is taken for plutonium and Am as there is information that suggests the desorption from iron oxyhydroxide colloids is much slower than the sorption processes (Lu et al. 1998 [DIRS 174714], Lu et al. 2000 [DIRS 166315]) and thus best modeled with a non-equilibrium (kinetic) based approach.~~

Results from experiments performed to study sorption of plutonium and americium on colloidal hematite and montmorillonite (Lu et al. 2000 [DIRS 166315]) indicate that almost all of the plutonium and americium mass is strongly sorbed on the colloids and negligibly small fraction remains in dissolved state or desorbs over the observation timeframes. Thus, it can be considered that plutonium and americium are so strongly bound to colloids that they are considered practically irreversibly sorbed during the residence time of the colloids in the EBS. Observations in nature, such as the transport of plutonium from the Benham test site (Kersting et al. 1999 [DIRS 103282]) indicate that >99 percent of the total plutonium mass being transported is on the colloids. In an attempt to match the field and experimental observations, a target flux out ratio (Ω) is set, which is described as the target ratio of radionuclide flux exiting the corrosion product domain that is transported by colloids (both reversibly and irreversibly sorbed) to the total radionuclide flux exiting the corrosion product domain carrying plutonium and americium in both dissolved state and sorbed onto colloids):

$$\Omega = \frac{\text{colloid mass flux out}}{\text{total mass flux out}} \quad (\text{Eq. 6.5.2.4.6-1})$$

The target flux out ratio rather than being set as a fixed number is given a range of 0.9 to 0.99 (uniform distribution) (BSC 2005 [DIRS 177423], Section 6.3.3.2) to indicate epistemic uncertainty in this value. The mass of radionuclides in the fluid exiting the corrosion products domain is expected to be proportioned such that the mass of radionuclide species i both reversibly and irreversibly sorbed onto all colloids is some fraction of the total mass of radionuclide species i exiting the system in all forms—aqueous, reversibly sorbed, and irreversibly sorbed.

The concept of target flux out ratio is purely theoretical based on the observations and expert judgment used in predicting the general transport behavior of plutonium and americium such that

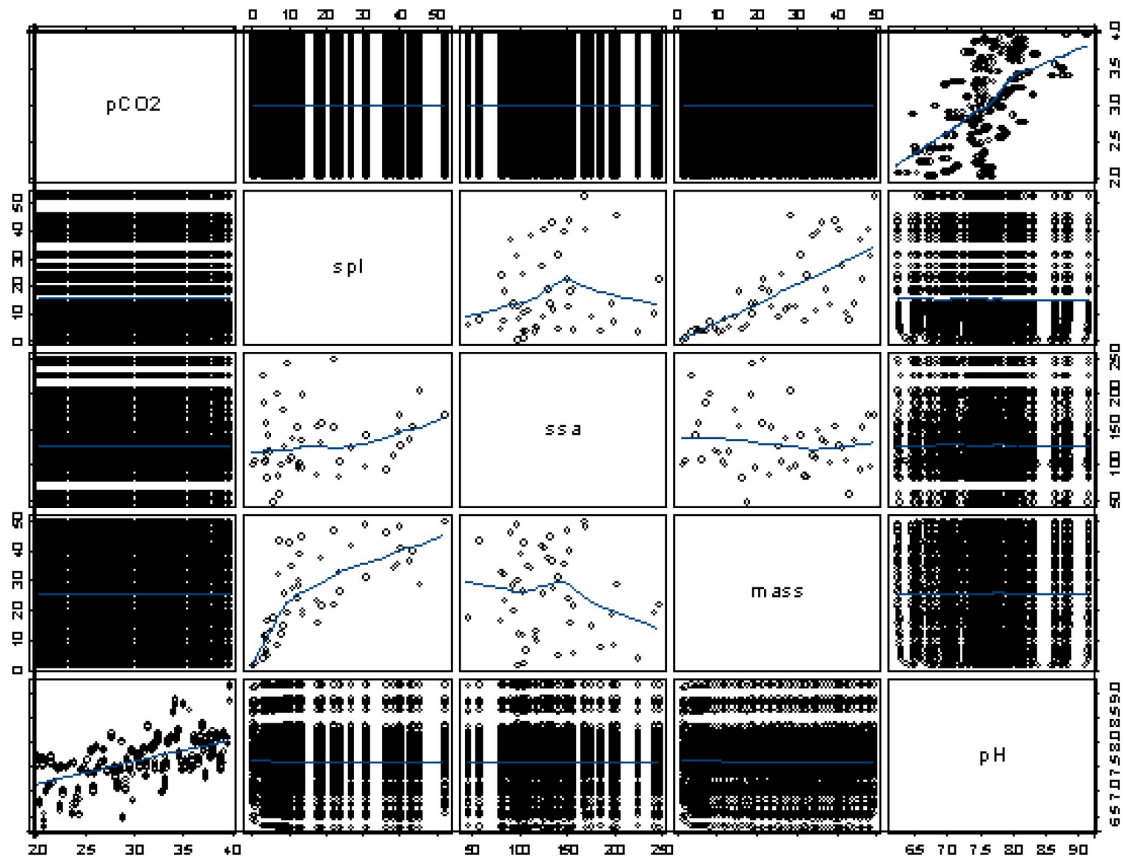
most of the mass is transported on colloids as compared to the dissolved state. Thus an attempt is made to reach the target flux out ratio whenever possible during the transport calculations but if this is not attainable under given physical-chemical-thermal conditions or by remaining within the valid range of transport parameters then the target flux out ratio is not honored. In other words, there is no attempt made to force the transport parameters such as forward rate constant or dissolved concentrations or colloid concentrations to go outside their valid range in order to meet the target flux out ratio. The methodology used (an inverse analytical solution) in computing the forward rate constant to match the target flux out ratio is described in detail in Appendix B. The application of the inverse solution has limitations in that it is not practical to apply when the colloids are unstable or when there is no advective transport due to long times needed to reach steady-state concentrations compared to the simulation time. The computed forward rate constant (from inverse solution) is further checked by comparing it to the physically acceptable range. If the value is outside the physical range then it is set to maximum (or minimum) value of the range.

The pH for the corrosion products domain (Cell 2) is computed by applying the following equation:

$$\text{pH} = 4.5342 + 0.6132(\text{pCO}_2) - 0.3805 \log_{10}[U] - 0.0254(\log_{10}[U])^2 + E, (\text{Eq. 6.5.2.4.6-2})$$

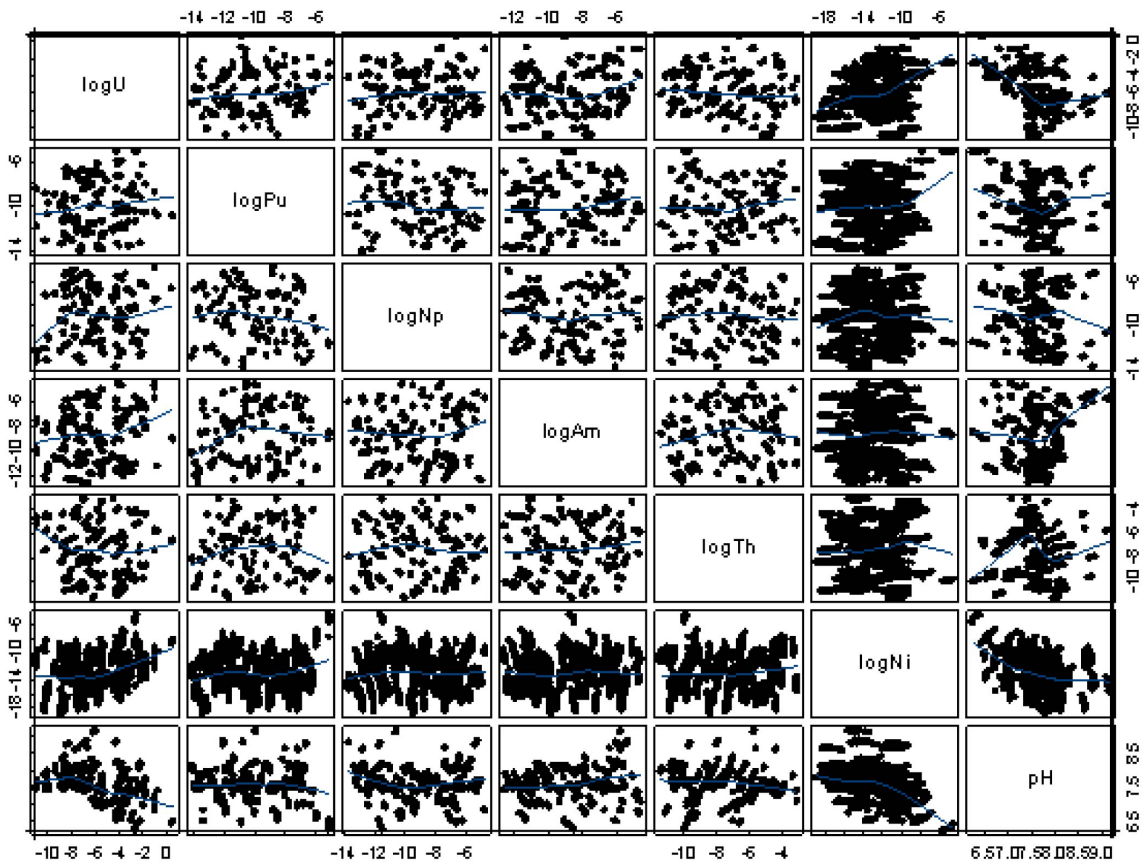
where, pCO_2 is the negative log of the in-drift CO_2 partial pressure (bars), $[U]$ is the dissolved concentration of U in mol L^{-1} , and E is the error term ($\text{pH_Cell_2_Regression_Error}$) defined by a normal distribution with mean of zero and standard deviation of 0.32 truncated at ± 2 standard deviations.

The ionic strength for the corrosion products domain is assumed to be the same as that computed for the upstream domain by the in-package chemistry model.



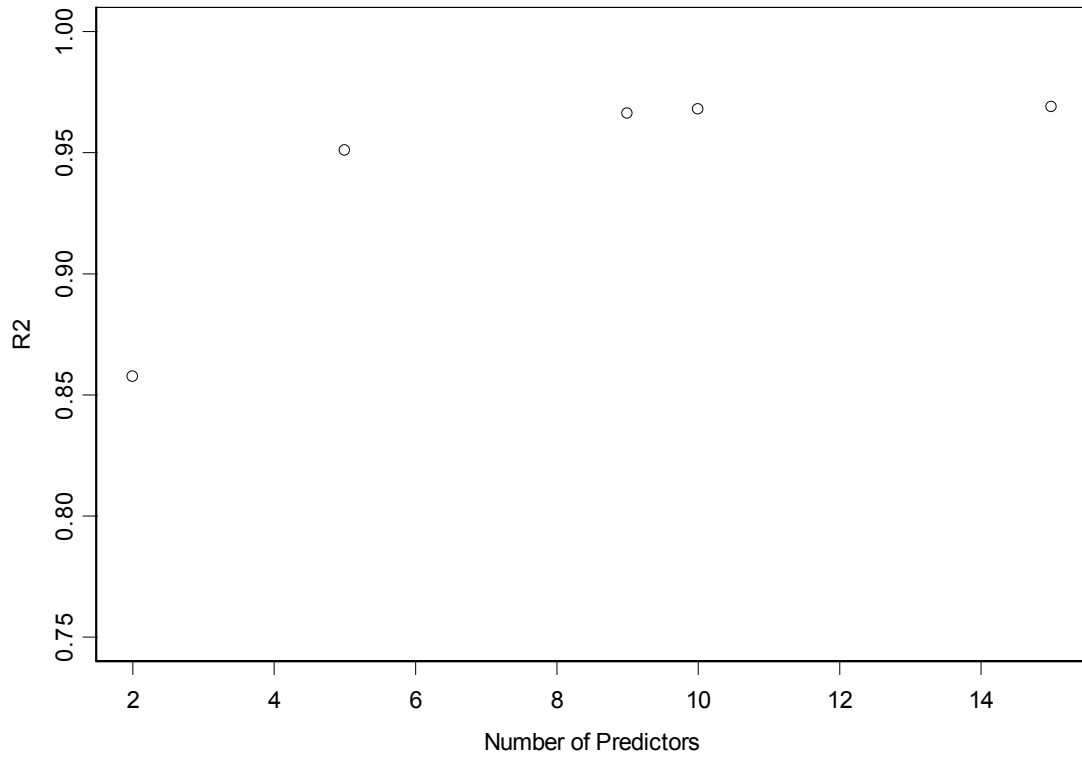
S-PLUS plot of data in output DTN: SN0703PAEBSRTA.002

Figure 6.5-10. Scatter Plot Matrix of First 5 Predictors Versus the pH Response



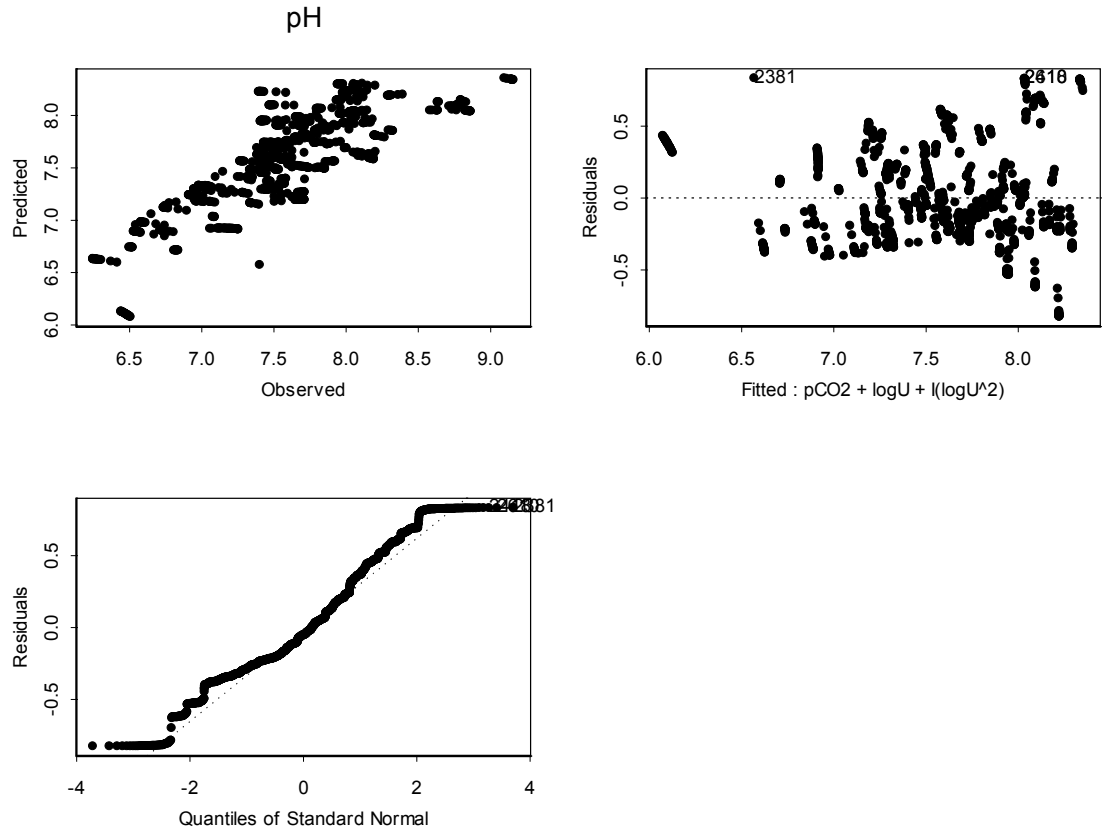
S-PLUS plot of data in output DTN: SN0703PAEBSRTA.002

Figure 6.5-11. Scatter Plot Matrix of 6 Dissolved Concentration Predictors Versus the pH Response



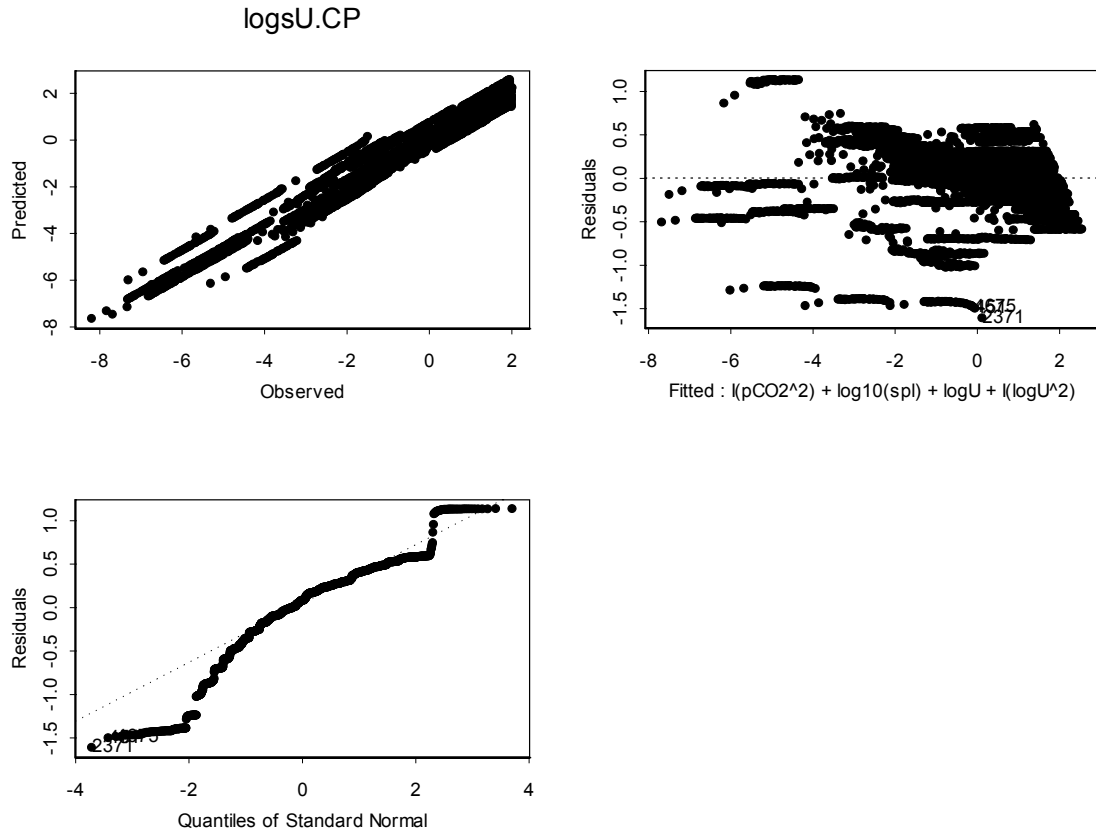
S-PLUS plot of data in output DTN: SN0703PAEBSRTA.002

Figure 6.5-12. Plot of R^2 Versus the Number of Model Terms for the logsU.CP Model



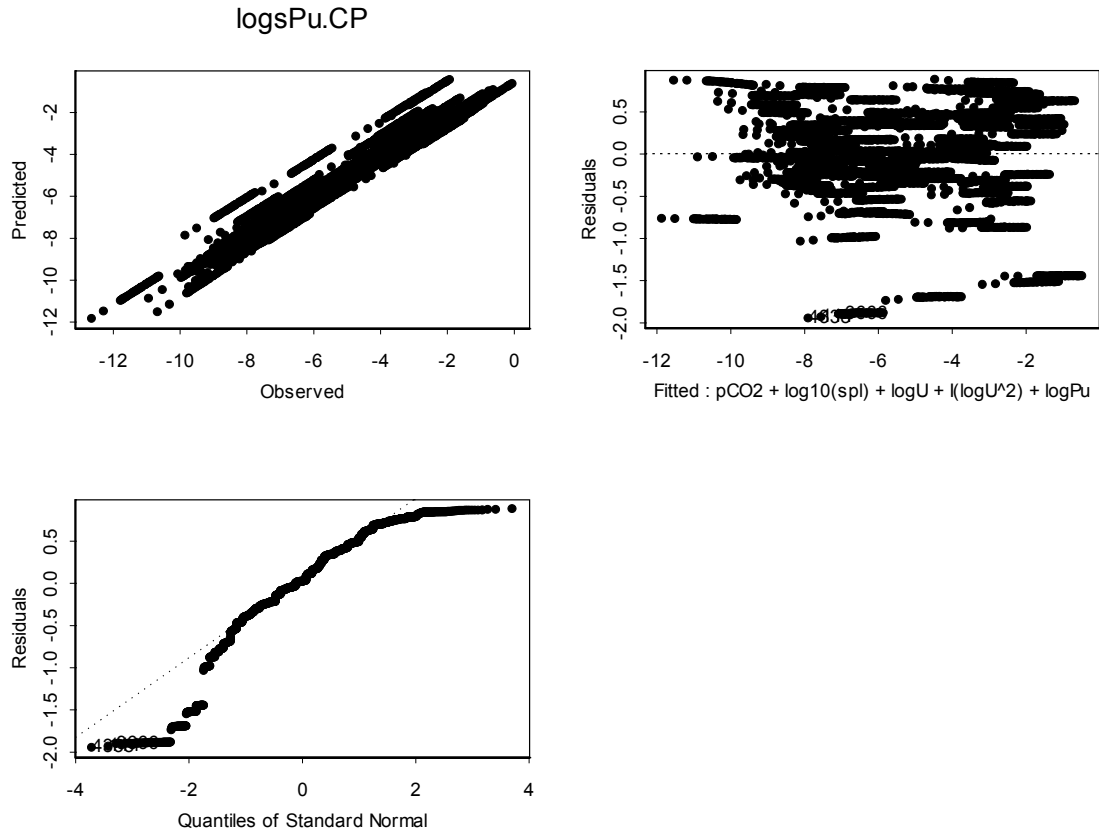
S-PLUS plot of data in output DTN: SN0703PAEBSRTA.002

Figure 6.5-13. Diagnostic Plots for Regression Model of Response Variable pH



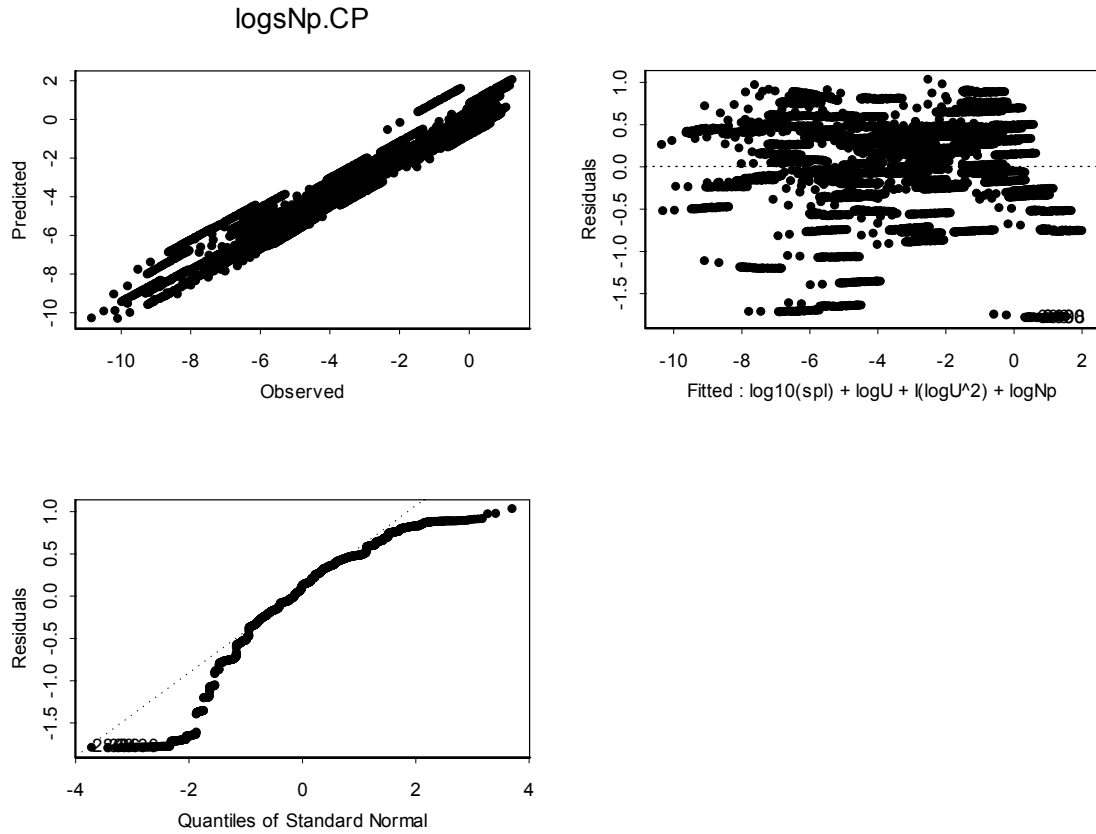
S-PLUS plot of data in output DTN: SN0703PAEBSRTA.002

Figure 6.5-14. Diagnostic Plots for Regression Model of Response Variable logsU.CP



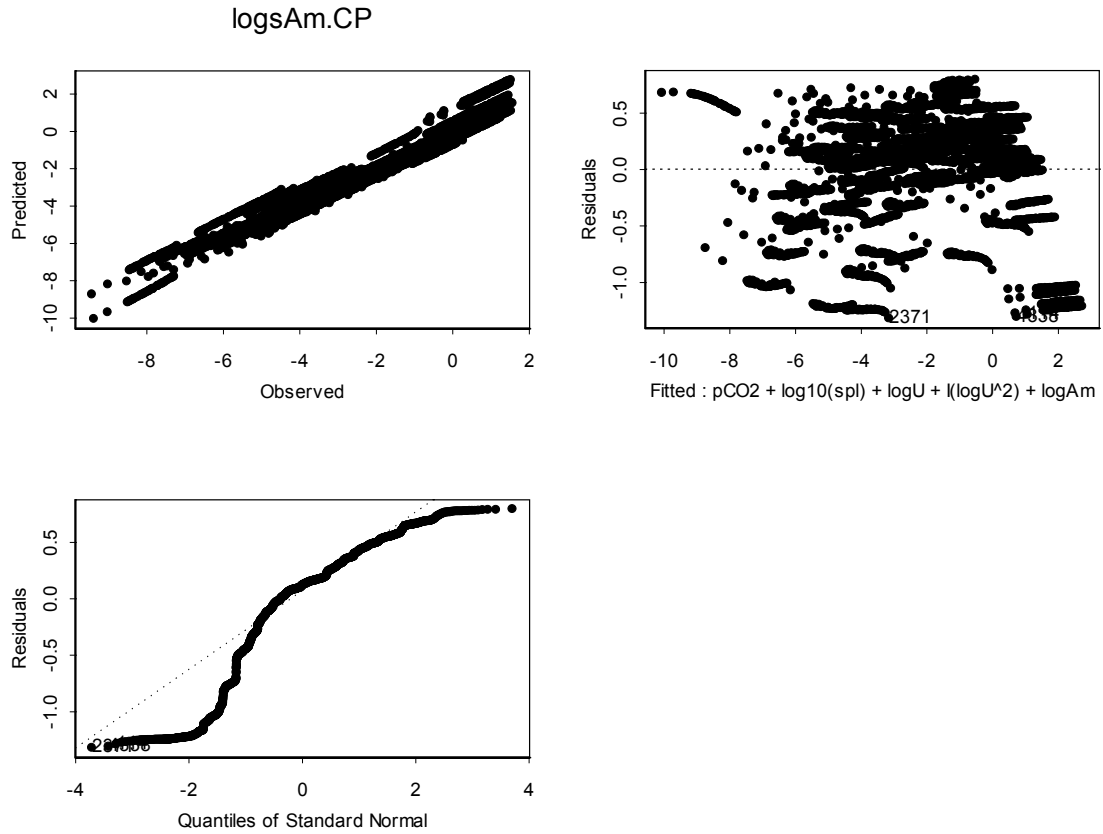
S-PLUS plot of data in output DTN: SN0703PAEBSRTA.002

Figure 6.5-15. Diagnostic Plots for Regression Model of Response Variable $\log_{10}(\text{Pu.CP})$



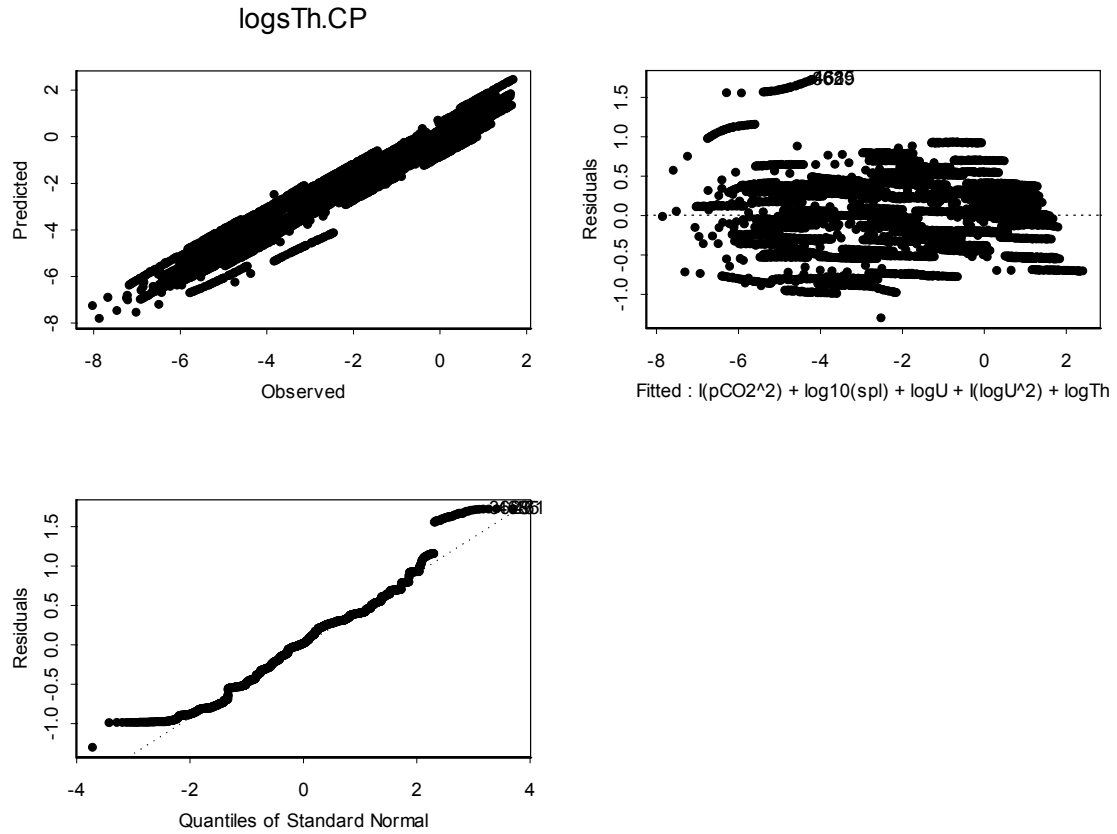
S-PLUS plot of data in output DTN: SN0703PAEBSRTA.002

Figure 6.5-16. Diagnostic Plots for Regression Model of Response Variable $\log N_p.CP$



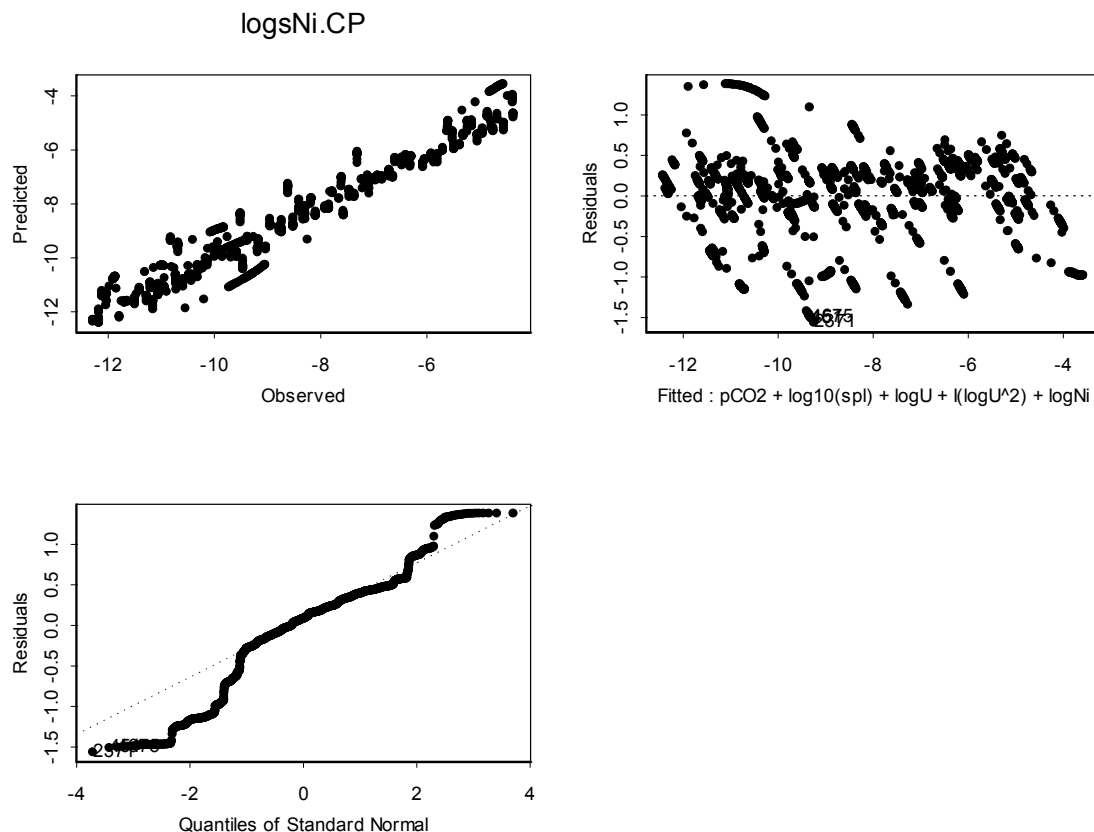
S-PLUS plot of data in output DTN: SN0703PAEBSRTA.002

Figure 6.5-17. Diagnostic Plots for Regression Model of Response Variable logsAm.CP



S-PLUS plot of data in output DTN: SN0703PAEBSRTA.002

Figure 6.5-18. Diagnostic Plots for Regression Model of Response Variable logsTh.CP



S-PLUS plot of data in output DTN: SN0703PAEBSRTA.002

Figure 6.5-19. Diagnostic Plots for Regression Model of Response Variable logsNi.CP

6.5.2.5 Discretization and Development of Computational Model for the TSPA

The continuum mass balance equations for EBS transport model are described and developed in Section 6.5.1.2. The one-dimensional mass balance equation describing transport of dissolved and reversibly sorbed radionuclide species i is provided by Equation 6.5.1.2-48. The one-dimensional mass balance equations for kinetically sorbed radionuclide species i on iron oxyhydroxide colloids and corrosion products are given by Equations 6.5.1.2-49 and 6.5.1.2-50, respectively. The solution of these continuum-form mass balance equations is approximated for the purpose of numerical modeling by the solution of discrete forms of these equations using a finite-difference approach. This requires the discretization of the time derivative (or mass accumulation term) and the advective and diffusive terms for both dissolved and colloidal transport. All other source terms and decay terms do not require discretization in either time or space.

Numerical modeling of the EBS radionuclide transport is performed using the GoldSim software (GoldSim Technology Group 2007 [DIRS 181727]) cell pathway capability, available in the GoldSim Contaminant Transport Module. The cell pathway acts as a batch reactor, where radionuclide mass is assumed to be instantaneously and completely mixed and partitioned among all media (fluid or solid) within the cell. Both advective and diffusive transport mechanisms can be explicitly represented using the cell pathways. When multiple cells are linked together via

advective and diffusive mechanisms, the behavior of the cell network is mathematically described using a coupled system of differential equations, and is mathematically equivalent to a finite difference network. GoldSim numerically solves the coupled system of equations to compute the radionuclide mass present in each cell and the mass fluxes between cells as a function of time. Both initial and boundary conditions for a cell can be defined explicitly, and systems of varying geometry can be modeled.

Within a computational cell network, each cell is allowed to communicate by advection and/or diffusion with any other cell. This concept is crucial in implementing the bifurcation of diffusive fluxes across an interface between a single continuum domain and a dual continuum domain, such as at the interface between the invert domain and the UZ. Each computational cell is provided with parameters describing water volumes, diffusive properties, and advective and diffusive flux links to other cells. Between any two cells, the diffusive flux can be bidirectional, depending on the concentration gradient, while the advective flux is unidirectional. The output of a cell is given in terms of the advective and diffusive mass fluxes for radionuclide species i and its concentration at the cell center.

The number of cells in the finite-difference network and the discretization of the cells is chosen in such a way as to capture the unique physical and chemical properties of the EBS components with respect to radionuclide transport. The abstractions are in the form of logic statements and stochastic distributions that provide a method for linking various cells in the network. Implementation of the EBS flow and transport model for the TSPA uses the output of the drift seepage model (SNL 2007 [DIRS 181244]), the models for drip shield and waste package degradation (SNL 2007 [DIRS 178871]), the EBS physical and chemical environment model (SNL 2007 [DIRS 177412]), the thermal-hydrologic environment model (SNL 2007 [DIRS 181383]), and the waste form degradation and mobilization model (BSC 2004 [DIRS 172453]); *Defense HLW Glass Degradation Model* (BSC 2004 [DIRS 169988]); and *CSNF Waste Form Degradation: Summary Abstraction* (BSC 2004 [DIRS 169987]). The flow through various cells is based on the continuity equations and conservation of mass, as discussed in Section 6.3. An overview of the computational model for TSPA, as implemented using GoldSim, is provided below.

Radionuclide transport through the waste package is modeled by spatially discretizing the waste package into two domains: an upstream waste form domain and a downstream corrosion products domain. This discretization although simplistic is reasonable and adequate for the spatial and temporal resolution at which the flow and transport processes are understood and modeled. When the degradation of the waste-form starts, the waste package internals (the basket material and the inner vessel), will also start to corrode due to the presence of water vapor and oxygen. The exact geometry and transport pathway inside the waste package cannot be predicted *a priori*, but it is reasonable and realistic to assume that some corrosion products will be present along the transport pathway since the radionuclide mass would have to eventually pass through the corroding inner vessel and some basket material in order to get out of the waste package. The transport domains are illustrated in Figure 6.5-20 by the EBS portion of the cell network – waste form cell, corrosion products cell, and invert cell. More specifically,

the waste form and corrosion products computational domains contain mass from the degradation of following components:

CSNF Waste Package:

- CSNF Waste Form Domain — Waste form (CSNF rods), basket tubes (Stainless Steel Type 316), absorber plates (Borated Stainless Steel Type 304B4)
- Corrosion Products Domain — Transportation, aging and disposal (TAD) canister (Stainless Steel Type 316), guide assembly (Stainless Steel Type 316), inner vessel (Stainless Steel Type 316)

CDSP Waste Package:

- HLWG Waste Form Subdomain — HLW glass, HLWG canisters (Stainless Steel Type 316)
- DSNF Waste Form Subdomain — DSNF (SNF and Stainless Steel Type 304), DSNF canister (Carbon Steel Type A 516, Borated Stainless Steel Type 304, and Stainless Steel Type 316)
- Corrosion Products Domain — Divider plate (Carbon Steel Type A 516), inner brackets (Carbon Steel Type A 516), outer brackets (Carbon Steel Type A 516), support tube (Carbon Steel Type A 516), inner vessel (Stainless Steel Type 316)

In order to model transport through each domain on a macro scale, consistent with the in-package chemistry model and waste form and waste package degradation models, the transport pathways are predominantly based on geometry of the intact waste package. As such the waste form domains include some steel degradation products besides the waste form while corrosion products domain contain remaining steel degradation products that are not included in the waste form domain. The cylindrical geometry of the waste package is approximated using Cartesian grid geometry. The suitability of this representation for radial diffusive transport is discussed in Appendix L.

The waste form cell receives mass from a specialized GoldSim “Source” cell, which models the waste package failure, degradation of the waste form, and release of the inventory for possible transport through the EBS. The “Source” cell provides the specified flux boundary condition for solving the mass transport equations. Both advective and diffusive transport can occur from the waste form cell to the corrosion products cell. Both equilibrium and kinetic sorption of radionuclides to the corrosion products along with colloid facilitated transport of radionuclides is modeled. Three types of colloids, namely, waste form colloids, iron oxyhydroxide colloids, and groundwater colloids, are considered that can facilitate the transport of radionuclides by reversible and/or kinetic sorption. The waste form colloids are generated in the waste form cell (from degradation of CSNF, HLW, and DSNF), the iron oxyhydroxide colloids are modeled in the corrosion products cell (even though they could also be potentially generated in the waste form cell), and groundwater colloids are modeled in both waste form cell and the corrosion products cell. All three types of colloids can be transported to the downstream cells by diffusion and advection.

The discretization of the invert domain, using GoldSim, consists of one cell. Both advective and diffusive flux communication exist between the corrosion product and invert cells. Advective flux due to imbibition from the host rock to the invert may enter the invert cell.

Below the invert, part of the near-field UZ is modeled by an array of cells. The inclusion of the UZ portion in the model serves to establish a far field zero-concentration boundary and an accurate representation of the radionuclide flux at the invert-to-UZ interface. The EBS-UZ interface model is described in more detail in Section 6.5.2.6. The dual continuum approach for modeling the UZ is achieved by creating UZ matrix and fracture cells. The invert cell communicates with the UZ matrix and fracture cells directly below it in the UZ cell array (see Section 6.5.2.6).

The following description focuses on discretization of the mass balance equation for the dissolved and reversibly sorbed mass (Equation 6.5.1.2-4847). Similar treatments apply to the mass balance transport equations for the irreversibly sorbed radionuclide species. In order to describe the time discretization, let the superscript n represent a solution at the n^{th} time. The n^{th} time step assumes the radionuclide concentrations are known at time step n , and the solution provides the concentrations at time step $n+1$. Over this time step, the accumulation term uses a first order backward-in-time discretization:

$$\frac{\partial}{\partial t} [\theta_w R_{fi} C_i] \approx \frac{\theta_w R_{fi}^n (C_i^{n+1} - C_i^n)}{\Delta t}, \quad (\text{Eq. 6.5.2.5-1})$$

where the adsorption retardation factor,

$$R_{fi} = 1 + \frac{\rho_b K_{dis}}{\theta_w} + \bar{K}_{dic} \quad R_{fi} = 1 + \frac{\rho_b K_{dis}}{\theta_w} + \sum \bar{K}_{dic}, \quad (\text{Eq. 6.5.2.5-2})$$

and the cell water content are evaluated at the beginning of the time step, and Δt is the time step size from the n^{th} to the $(n+1)^{\text{th}}$ time. $\sum \bar{K}_{dic}$ is the sum over all the colloids present in the domain of the ratios of reversibly sorbed radionuclide mass on colloids to the dissolved mass (kg kg^{-1}), on a unit water volume basis. For each colloid type, \bar{K}_{dic} is calculated as $\bar{K}_{dic} = C_c K_{dic}$ is the dimensionless distribution coefficient for equilibrium sorption onto colloids, where with C_c is the concentration of species i in the colloidal state colloids ($\text{kg } i \text{ m}^{-3}$), and K_{dic} is the distribution coefficient for equilibrium sorption of radionuclide species i onto colloids ($\text{m}^3 \text{ kg}^{-1}$).

The advective transport is discretized with a first order backward (with respect to the flow direction) difference approximation. If the mass balance is applied to cell B , and the advective flux is from cell A to cell B with magnitude q_{wz} ($\text{m}^3 \text{ water m}^{-2} \text{ yr}^{-1}$), then

$$\frac{\partial}{\partial z} [q_{wz} (1 + \sum \bar{K}_{dic}) C_i] \approx [Q_{wz}^n (1 + \sum \bar{K}_{dic})^n C_i^{n+1}]_A - [Q_{wz}^n (1 + \sum \bar{K}_{dic})^n C_i^{n+1}]_B,$$

$$\frac{\partial}{\partial z} [q_{wz} (1 + \bar{K}_{dic}) C_i] \approx [Q_{wz}^n (1 + \bar{K}_{dic})^n C_i^{n+1}]_A - [Q_{wz}^n (1 + \bar{K}_{dic})^n C_i^{n+1}]_B, \quad (\text{Eq. 6.5.2.5-3})$$

where Q_{wz} ($\text{m}^3 \text{ water m}^{-3} \text{ cell B yr}^{-1}$) is the advective water volumetric flow rate per unit bulk volume. The advective volumetric flow rate and colloid concentrations are evaluated at the beginning of the time step. The concentration of radionuclide species i is evaluated at the end of time step. The first term in the difference approximation is the advective mass flow rate entering cell B from cell A . The second term is the advective mass flow rate exiting cell B .

Consider the accumulation of solute mass in cell B due to diffusion. Suppose there are diffusive flux links from cell A to cell B and from cell B to cell C . The dissolved mass diffusive flux accumulation in cell B is approximated by:

$$\frac{\partial}{\partial x} \left(\theta_w D_i \frac{\partial C_i}{\partial x} \right) \approx \frac{F_{A/B} - F_{B/C}}{V_B}, \quad (\text{Eq. 6.5.2.5-4})$$

where $F_{A/B}$ is the diffusion rate (mass/time) across the cell A and B interface. Similarly, $F_{B/C}$ is the diffusion rate (mass/time) across the cell B and C interface.

Consider the discretization of the diffusive flux at the A/B interface. A similar representation occurs at the B/C interface. Apply Fick's First Law and continuity of flux at the interface. Then the flux entering the A/B interface from cell A must equal the flux exiting the A/B interface to cell B . This interface flux continuity condition is expressed as:

$$\begin{aligned} F_{A/B} &= \left(\frac{\theta_w D_i A}{L} \right)_A \left([C_i^{n+1}]_A - [C_i^{n+1}]_{A/B} \right) \\ &= \left(\frac{\theta_w D_i A}{L} \right)_B \left([C_i^{n+1}]_{A/B} - [C_i^{n+1}]_B \right), \end{aligned} \quad (\text{Eq. 6.5.2.5-5})$$

where $[C_i^{n+1}]_{A/B}$ is the concentration at time step $n+1$ at the interface, as indicated by the subscript A/B , and D_i , A , and L are the cell effective diffusion coefficient, diffusive area, and diffusive length, respectively. If the A/B interface diffusion rate is expressed as an interface diffusive conductance times the concentration difference between cells A and B :

$$F_{A/B} = D_{ic_A/B} (C_{iA} - C_{iB}), \quad (\text{Eq. 6.5.2.5-6})$$

then the flux continuity condition provided by Equation 6.5.2.5-5 gives the interface diffusive conductance as:

$$D_{ic_A/B} = \frac{1}{\left(\frac{L}{\theta_w D_i A} \right)_A + \left(\frac{L}{\theta_w D_i A} \right)_B}. \quad (\text{Eq. 6.5.2.5-7})$$

The diffusive conductance is the harmonic average of $\frac{\theta_w D_i A}{2L}$ between the two cells. At the B/C interface a similar expression gives:

$$D_{ic_B/C} = \frac{1}{\left(\frac{L}{\theta_w D_i A}\right)_B + \left(\frac{L}{\theta_w D_i A}\right)_C}. \quad (\text{Eq. 6.5.2.5-8})$$

The discretization of the accumulation of solute mass in cell B due to diffusive transport is:

$$\frac{\partial}{\partial x} \left(\theta_w D_i \frac{\partial c}{\partial x} \right) \approx \frac{D_{ic_B/C} \left([C_i^{n+1}]_C - [C_i^{n+1}]_B \right) - D_{ic_A/B} \left([C_i^{n+1}]_B - [C_i^{n+1}]_A \right)}{V_B}. \quad (\text{Eq. 6.5.2.5-9})$$

The mass balance equations are discretized with the dependent concentration variable for the spatially dependent terms evaluated at the end of time step, C_i^{n+1} . This is stated explicitly in the discretization of the advective/diffusive terms. For other source terms, such as radionuclide decay, kinetic sorption reaction onto iron oxyhydroxide material and so forth, the concentration is also evaluated at the end of the time step. In this sense, the mass balance equations are fully implicit and the discretization provides numerical stability. However, coefficient terms such as the moisture content are evaluated at the beginning of the time step. This formulation results in a linear system of equations that is solved for concentrations. If the coefficients depending on concentration were evaluated at the end of time step, then the resulting discretized algebraic equations would be nonlinear. The nonlinear system would require much more computational effort. Furthermore, the computational modeling tool (GoldSim) only solves linear systems. For this reason, all concentration-dependent coefficient terms are evaluated explicitly at time step n .

Within the waste form domain, some part of the dissolved mass of plutonium and americium made available from the degradation of HLW glass and CSNF is converted to “embedded” mass on the waste form colloids. This conversion is required to satisfy the condition that some mass of plutonium and americium is “embedded” as an intrinsic part of the colloid and is not in equilibrium with the aqueous system, when generated from the degradation of HLW glass and CSNF. This mass is thus transported separately as a distinct species [*Waste Form and In-Drift Colloids-Associated Radionuclide Concentrations: Abstraction and Summary* (BSC 2005 [DIRS 177423], Sections 6.3.1 & 6.3.3.3)]. The mass rate of conversion per unit volume of water is modeled as a first order reaction given by $\lambda_i^{embed} C_i$, where λ_i^{embed} is the linear rate constant, and concentration C_i is the dissolved concentration of plutonium and americium species in the waste form domain. The conversion rate λ_i^{embed} is calculated at each time step in the waste form domain. Its calculation is discussed below.

The concentration of the embedded radionuclide mass with respect to the water volume in the waste form domain, C_i^{embed} , and the concentration of waste form colloids, C_{cWF} , are determined at each time step based on the logic given in the *Waste Form and In-Drift Colloids-Associated Radionuclide Concentrations: Abstraction and Summary* (BSC 2005 [DIRS 177423], Section 6.5.1.1). Taking the ratio of embedded radionuclide concentration to the waste form

colloid concentration, $\frac{C_i^{embed}}{C_{cWF}}$, gives the embedded radionuclide mass per unit mass of the waste form colloid.

Suppose that the solution for embedded radionuclide concentration $(C_i^{embed})^n$ and colloid concentration $(C_{cWF})^n$ has been determined at time step n and the solution at current time step $n+1$ is required. Furthermore, suppose that the total mass flux (combined advective and diffusive mass flux) of waste form colloids per unit bulk volume, $(Q_{adv/diff}^{wfc})^n$, is available from the solution at time step n from the waste form colloid mass balance equation (Eq. 6.5.1.2-38). Then the quantity, $\left(Q_{adv/diff}^{wfc} \frac{C_i^{embed}}{C_{cWF}}\right)^n$, represents the mass flux at time level n of embedded radionuclide species i from the waste form subdomain containing the HLW or CSNF glass logs to the downstream domain. A continuum mass balance for embedded radionuclide mass within the waste form domain is:

$$\frac{\partial(\theta_w C_i^{embed})}{\partial t} = -Q_{adv/diff}^{wfc} \frac{C_i^{embed}}{C_{cWF}} + \lambda_i^{embed} \theta_w C_i. \quad (\text{Eq. 6.5.2.5-10})$$

Discretization of this equation gives:

$$\frac{(\theta_w C_i^{embed})^{n+1} - (\theta_w C_i^{embed})^n}{t^{n+1} - t^n} = -\left(Q_{adv/diff}^{wfc} \frac{C_i^{embed}}{C_{cWF}}\right)^n + \lambda_i^{embed} (\theta_w C_i)^n. \quad (\text{Eq. 6.5.2.5-11})$$

This equation is solved for the conversion rate:

$$\lambda_i^{embed} = \frac{\frac{(\theta_w C_i^{embed})^{n+1} - (\theta_w C_i^{embed})^n}{\Delta t} + \left(Q_{adv/diff}^{wfc} \frac{C_i^{embed}}{C_{cWF}}\right)^n}{(\theta_w C_i)^n}. \quad (\text{Eq. 6.5.2.5-12})$$

$(C_i^{embed})^{n+1}$ is calculated from the logic provided in the *Waste Form and In-Drift Colloids-Associated Radionuclide Concentrations: Abstraction and Summary* (BSC 2005 [DIRS 177423], Section 6.5.1.1). The concentration $(C_i^{embed})^{n+1}$ in the waste form domain is a function of the ionic strength and pH. This waste form domain conversion rate is applied to the i species mass balance equation for the solution mass, Eq. 6.5.1.2-39, and for the embedded mass, Eq. 6.5.1.2-38.

The above diffusive flux discussion considers the diffusive flux communication from cells within a single continuum. For transport from the invert domain (single continuum) to the UZ (dual continuum), the flux continuity condition at the interface provides the diffusive flux bifurcation between the single continuum and the dual continuum.

The diffusive fluxes of radionuclide species i within the invert cell, the UZ fracture cell, and the UZ matrix cell are, respectively,

$$\begin{aligned} F_{il} &= \frac{\theta_w D_{il} A_{I/UZ}}{L_I} (C_{il} - C_{il/UZ}) \\ &= \hat{D}_{il} (C_{il} - C_{il/UZ}), \end{aligned} \quad (\text{Eq. 6.5.2.5-13})$$

$$\begin{aligned} F_{if} &= \frac{\theta_w D_{if} A_{I/UZ}}{L_f} (C_{il/UZ} - C_{if}) \\ &= \hat{D}_{if} (C_{il/UZ} - C_{if}), \end{aligned} \quad (\text{Eq. 6.5.2.5-14})$$

$$\begin{aligned} F_{im} &= \frac{\theta_w D_{im} A_{I/UZ}}{L_m} (C_{il/UZ} - C_{im}) \\ &= \hat{D}_{im} (C_{il/UZ} - C_{im}), \end{aligned} \quad (\text{Eq. 6.5.2.5-15})$$

where

- D_{il} = effective diffusion coefficient within the invert cell ($\text{m}^2 \text{s}^{-1}$),
- D_{if} = effective diffusion coefficient within the UZ fracture cell ($\text{m}^2 \text{s}^{-1}$),
- D_{im} = effective diffusion coefficient within the UZ matrix cell ($\text{m}^2 \text{s}^{-1}$),
- $A_{I/UZ}$ = diffusive area between the invert and UZ cells (m^2),
- L_I = diffusive length within the invert cell (m),
- L_f = diffusive length within the UZ fracture cell (m),
- L_m = diffusive length within the UZ matrix cell (m) = L_f ,
- C_{il} = concentration of radionuclide species i in the invert cell ($\text{kg } i \text{ m}^{-3}$),
- C_{if} = concentration of radionuclide species i in the UZ fracture cell ($\text{kg } i \text{ m}^{-3}$),
- C_{im} = concentration of radionuclide species i in the UZ matrix cell ($\text{kg } i \text{ m}^{-3}$),
- $C_{il/UZ}$ = concentration of radionuclide species i at the interface between the invert and UZ cells ($\text{kg } i \text{ m}^{-3}$),

and the $\hat{D}_i = \frac{\theta_w D_i A}{L}$ are respective diffusive conductances ($\text{m}^3 \text{s}^{-1}$) of radionuclide species i .

The flux continuity at the interface requires:

$$F_{il} = F_{if} + F_{im}. \quad (\text{Eq. 6.5.2.5-16})$$

From the flux continuity, the interface concentration of radionuclide species i is determined as a function of the diffusive parameters and the cell concentrations as:

$$C_{il/uz} = \frac{\hat{D}_{il}C_{il} + \hat{D}_{if}C_{if} + \hat{D}_{im}C_{im}}{\hat{D}_{il} + \hat{D}_{if} + \hat{D}_{im}}. \quad (\text{Eq. 6.5.2.5-17})$$

This provides the diffusive fluxes of radionuclide species i in UZ fracture and matrix cells, respectively, as:

$$F_{if} = \frac{\hat{D}_{il}\hat{D}_{if}}{\hat{D}_{il} + \hat{D}_{if} + \hat{D}_{im}}(C_{il} - C_{if}) + \frac{\hat{D}_{if}\hat{D}_{im}}{\hat{D}_{il} + \hat{D}_{if} + \hat{D}_{im}}(C_{im} - C_{if}) \quad (\text{Eq. 6.5.2.5-18})$$

$$F_{im} = \frac{\hat{D}_{il}\hat{D}_{im}}{\hat{D}_{il} + \hat{D}_{if} + \hat{D}_{im}}(C_{il} - C_{im}) + \frac{\hat{D}_{if}\hat{D}_{im}}{\hat{D}_{il} + \hat{D}_{if} + \hat{D}_{im}}(C_{im} - C_{if}). \quad (\text{Eq. 6.5.2.5-19})$$

The expression for the diffusive flux of radionuclide species i from the invert cell to the UZ fracture cell can be expressed as a diffusive conductance multiplied by a concentration difference of radionuclide species i between the invert cell and the UZ fracture cell plus a corrective flux between the UZ fracture and matrix cells. Similarly, the expression for the diffusive flux from the invert to the UZ matrix cell is expressed as a diffusive flux between the invert and the UZ matrix cell minus the same corrective flux between the UZ cells. The corrective flux term accounts for coupling among the invert cell, UZ fracture and matrix cells, as the following explains. The flux to both UZ cells should depend on the diffusive properties in the invert cell and the two UZ cells, together with the concentrations in these three cells. Therefore, the flux to the UZ fracture cell cannot be expressed only in terms of the concentration drawdown between the invert cell and the UZ fracture cell. The corrective term includes the dependence of the UZ fracture flux on the concentration of radionuclide species i in the UZ matrix cell due to the requirement that the sum of the two UZ continua receive exactly the flux leaving the invert. The corrective flux term is not a true flux expression between the two UZ cells, since the diffusive conductance coefficient is dependent on the diffusive area between the invert and the UZ, and the diffusive lengths are the lengths with respect to flow from the invert cell to the UZ cells. The model also explicitly includes diffusion between the UZ fracture and matrix continua, as shown in Figure 6.5-20.

The UZ fluxes result in defining three diffusive conductances from the flux expressions:

$$\hat{D}_{ilf}(C_{il} - C_{if}) = \frac{\hat{D}_{il}\hat{D}_{if}}{\hat{D}_{il} + \hat{D}_{if} + \hat{D}_{im}}(C_{il} - C_{if}), \quad (\text{Eq. 6.5.2.5-20})$$

$$\hat{D}_{ilm}(C_{il} - C_{im}) = \frac{\hat{D}_{il}\hat{D}_{im}}{\hat{D}_{il} + \hat{D}_{if} + \hat{D}_{im}}(C_{il} - C_{im}), \quad (\text{Eq. 6.5.2.5-21})$$

$$\hat{D}_{imf}(C_{im} - C_{if}) = \frac{\hat{D}_{im}\hat{D}_{if}}{\hat{D}_{il} + \hat{D}_{if} + \hat{D}_{im}}(C_{im} - C_{if}), \quad (\text{Eq. 6.5.2.5-22})$$

where

\hat{D}_{if} = effective diffusive conductance between invert cell and UZ fracture cell
($\text{m}^3 \text{s}^{-1}$);

\hat{D}_{ilm} = effective diffusive conductance between invert cell and UZ matrix cell
($\text{m}^3 \text{s}^{-1}$);

\hat{D}_{imf} = effective diffusive conductance between UZ fracture and matrix cells
($\text{m}^3 \text{s}^{-1}$).

In order to accommodate the GoldSim representation of diffusive conductance as a two-term expression, the diffusive conductances of radionuclide species i are written as:

$$\hat{D}_{if} = \frac{1}{\frac{L_f}{(\theta_w D_i A)_f} + \frac{L_I}{(\theta_w D_i A)_I \left[\frac{(\theta_w D_i)_f}{(\theta_w D_i)_f + (\theta_w D_i)_m} \right]}}, \quad (\text{Eq. 6.5.2.5-23})$$

$$\hat{D}_{ilm} = \frac{1}{\frac{L_m}{(\theta_w D_i A)_m} + \frac{L_I}{(\theta_w D_i A)_I \left[\frac{(\theta_w D_i)_m}{(\theta_w D_i)_f + (\theta_w D_i)_m} \right]}}, \quad (\text{Eq. 6.5.2.5-24})$$

$$\hat{D}_{imf} = \frac{1}{\frac{L_m}{(\theta_w D_i A)_m} + \frac{L_f}{(\theta_w D_i A)_f \left[\frac{L_I (\theta_w D_i)_m}{L_I (\theta_w D_i)_m + L_m (\theta_w D_i)_I} \right]}}. \quad (\text{Eq. 6.5.2.5-25})$$

Although the above approach is rigorous, it is complex and difficult to implement in the TSPA Model. A second approach that is easier to understand and simpler to implement, while providing the same results as the above approach, is presented here and is implemented in TSPA. This approach requires introduction of an interface cell, located between the invert cell and the UZ cells. This interface cell provides an approximate interface concentration and the resulting flux split at the invert-to-UZ cell interface. The interface cell is conceptualized as a very thin slice of the invert cell. This implies the interface cell takes on the invert diffusive properties, with the exception of diffusive length. Let the diffusive length within the interface cell be some small fraction (a scale factor) of the invert diffusive length, say, $\text{Interface_Scale_Factor} = 10^{-6}$:

$$L_{I-int} = 10^{-6} L_I. \quad (\text{Eq. 6.5.2.5-26})$$

As in Equation 6.5.2.5-7, the diffusive conductance between the invert cell and the invert interface cell is calculated as the harmonic average:

$$\hat{D}_{il/I-int} = \frac{1}{\frac{L_I}{(\theta_w D_i A)_I} + \frac{L_{I-int}}{(\theta_w D_i A)_{I-int}}}. \quad (\text{Eq. 6.5.2.5-27})$$

For diffusion between the interface cell and the UZ fracture and matrix cells, the diffusive conductances of radionuclide species i are, respectively,

$$\hat{D}_{il-int/f} = \frac{1}{\frac{L_{I-int}}{(\theta_w D_i A)_{I-int}} + \frac{L_{UZ}}{(\theta_w D_i A)_f}}, \quad (\text{Eq. 6.5.2.5-28})$$

$$\hat{D}_{il-int/m} = \frac{1}{\frac{L_{I-int}}{(\theta_w D_i A)_{I-int}} + \frac{L_{UZ}}{(\theta_w D_i A)_m}}. \quad (\text{Eq. 6.5.2.5-29})$$

The interface cell concentration of radionuclide species i is computed as part of the cell network solution. Because the transport mass balance equations conserve mass, the mass flux leaving the interface cell must equal the sum of the mass fluxes entering the two UZ cells. The solution provides the flux continuity across the interface between the invert interface cell and UZ cells. This formulation expects the flux exiting the invert cell (or entering the interface cell) is approximately equal to the flux exiting the interface cell. This approximation is dependent on the diffusive length within the interface cell. The error in this approximate solution approaches zero as the diffusive length of the interface cell approaches zero.

6.5.2.7 Stoichiometry for Conversion of Radionuclide Mass to Kinetically Sorbed Mass onto Iron Oxyhydroxide Colloids, Stationary Corrosion Products, and Waste Form Colloids

6.5.2.7.1 Conceptual Model

The EBS Transport Submodel is implemented using the cell pathway capability of GoldSim (GoldSim Technology Group 2007 [DIRS 181727]). The cell pathways act as a batch reactor, where radionuclide mass is modeled as instantaneously and completely mixed, and partitioned among all media, fluid or solid, within the cell. The following five reactions for converting radionuclide mass to other species mass are considered at each time step:

- Simple radioactive decay reaction of a parent species to a daughter species for the entire mass in the cell pathway in all domains
- Reaction of dissolved mass to form radionuclide species embedded in waste form colloids within the waste form domain
- Reaction of dissolved mass to form kinetic sorption species to the iron oxyhydroxide colloids within the corrosion products domain

- Reaction of dissolved mass to form kinetic sorption species to the iron oxyhydroxide corrosion products within the corrosion products domain
- Reverse kinetic reaction of sorption species from the iron oxyhydroxide corrosion products [and iron oxyhydroxide colloids](#) to dissolved mass within the corrosion products domain.

Within GoldSim, the total of all appropriate reactions is modeled by combining the individual reaction rate constants into a single effective reaction rate constant. After the reaction is completed, the relative masses formed from each reaction are determined by applying appropriate stoichiometry to the effective daughter products. Because all reaction rate constants are of first order, they can be summed together into an effective reaction rate constant. The mass of a given species in the cell pathway is thus converted into the different daughter species and tracked separately in GoldSim. The radionuclides that are specifically modeled for kinetic sorption are the plutonium and americium isotopes that are mobilized inside the waste package after the waste form has degraded. Americium and plutonium species that undergo these reactions will form embedded mass on the waste form colloids and kinetically sorbed mass on the iron oxyhydroxide colloids and corrosion products in addition to true radioactive decay and equilibrium sorption to waste form and groundwater colloids. Further, a reverse kinetic sorption reaction accounts for a slow desorption from the corrosion products sorbed mass to solution mass. [Reverse kinetic sorption reaction is also modeled for the iron oxyhydroxide colloids in the corrosion products domain, consistent with the prediction of the surface complexation based competitive sorption model. Once the iron oxyhydroxide colloids leave the corrosion products domain, the kinetically sorbed mass of plutonium and americium is treated as being irreversibly sorbed.](#) For other radionuclide species with only true radioactive decay, stoichiometry for the daughter species is set to unity. Radiolysis is not considered here. Instead the impacts of radiolysis on in-package chemistry and transport are shown to be limited in FEP Number 2.1.13.01A (DTN: MO0706SPAFEPLA.001 [DIRS 181613]).

6.5.2.7.2 Stoichiometry Calculations

The discussion regarding the stoichiometry associated with all reactions is presented with respect to ^{243}Am , though similar treatment holds for other americium and plutonium species. The ^{243}Am species will experience radioactive decay to ^{239}Pu for both dissolved mass, [precipitated mass](#), and the mass in equilibrium sorption with the waste form and groundwater colloids. The ^{243}Am species will require conversion to embedded mass on the waste form colloids within the waste form domain, and will require conversion to kinetically sorbed mass on the iron oxyhydroxide colloids and corrosion products within the corrosion products domain. In order to account for these four conversion processes, ^{243}Am is assigned four daughters:

- ^{239}Pu : radioactive daughter of [total \$^{243}\text{Am}\$ present in the domain](#)
- $Ic^{243}\text{Am}$: ^{243}Am species embedded on waste form colloids
- $If^{243}\text{Am}$: ^{243}Am species kinetically sorbed to iron oxyhydroxide colloids
- $Ifcp^{243}\text{Am}$: ^{243}Am species kinetically sorbed to iron oxyhydroxide corrosion products.

~~Also, a reverse (desorption) kinetic reaction converts $I_{fcp}^{243}Am$ mass to solution mass, ^{243}Am , and to $I_{fcp}^{243}Am$ radioactive daughter $I_{fcp}^{239}Pu$ (^{239}Pu kinetically sorbed to corrosion products).~~

In the subsequent discussion, the above reactions as applied to ^{243}Am within the corrosion product domain are considered first, followed by the application of the above reactions to ^{243}Am species within the waste form cell. Finally, the stoichiometry for the kinetically sorbed species $I_{fcp}^{243}Am$ is considered within the corrosion product cell. In the present implementation, the radioactive decay of $I_{fcp}^{243}Am$ leads to radioactive daughter $I_{fcp}^{239}Pu$ (^{239}Pu kinetically sorbed to corrosion products), while the radioactive decay of $I_f^{243}Am$ leads to radioactive daughter $I_f^{239}Pu$ (^{239}Pu kinetically sorbed to iron oxyhydroxide colloids).

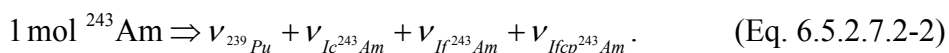
The ^{243}Am conversion rates (yr^{-1}) for each of the above four reaction processes are denoted respectively:

- ~~$\lambda_{243}Am$~~ $\lambda_{243}Am^{Total}$
- $\lambda_{243}Am^{embed}$
- R_{fc}
- R_{fcp} .

However, within the waste form domain, the forward conversion rates for kinetic sorption to iron oxyhydroxide colloids (R_{fc}) and stationary corrosion products materials, ~~R_{fc} and (R_{fcp});~~ will be zero as there ~~is~~ are no sorption considered on steel corrosion products. Similarly, within the corrosion products domain, the conversion rate to embedded waste form colloids, $\lambda_{243}Am^{embed}$, is zero as the waste form is not present. With this understanding of the domain dependence of the reactions, the general form for the total or effective ^{243}Am conversion rate is written as:

$$\rho_{243}Am \equiv \lambda_{243}Am + \lambda_{243}Am^{embed} + R_{fc} + R_{fcp} \rho_{243}Am = \lambda_{243}Am^{Total} + \lambda_{243}Am^{embed} + R_{fc} + R_{fcp}. \quad (\text{Eq. 6.5.2.7.2-1})$$

The following stoichiometric coefficients for species i , ν_i , illustrate how a unit mole of ^{243}Am is partitioned among the four daughters:



This states that one mole of ^{243}Am converts to ν_{239Pu} (mol) of ^{239}Pu , $\nu_{Ic^{243}Am}$ (mol) of $Ic^{243}Am$, $\nu_{I_f^{243}Am}$ (mol) of $I_f^{243}Am$, and $\nu_{I_{fcp}^{243}Am}$ (mol) of $I_{fcp}^{243}Am$. Specification of the total effective conversion rate (Equation 6.5.2.7.2-1), the daughter species formed from the reaction, and the stoichiometric coefficients of each daughter species (Equation 6.5.2.7.2-2) completely describes all reactions.

The effective conversion rate within the corrosion products domain will include a total of three reactions, the two forward kinetic reactions of the ^{243}Am onto iron oxyhydroxide colloids and

corrosion products, respectively, and the radioactive decay of ^{243}Am . There is no conversion to embedded waste form colloids in the corrosion product domain. The total effective forward conversion rate (based on the formulation of Equation 6.5.1.2-39) ~~which accounts for both the dissolved mass and the equilibrium sorbed mass~~ can be written as:

$$\Lambda_{^{243}\text{Am}} = R_{fc} + R_{fcp} + \lambda_{^{243}\text{Am}} \left(1 + \bar{K}_{dcWF} + \bar{K}_{dcGW} + M_{^{243}\text{Am}}^{ppt} \right), \quad (\text{Eq. 6.5.2.7.2-3})$$

or

$$\Lambda_{^{243}\text{Am}} = R_{fc} + R_{fcp} + \lambda_{^{243}\text{Am}} \left(1 + \sum \bar{K}_d \right), \quad \Lambda_{^{243}\text{Am}} = R_{fc} + R_{fcp} + \lambda_{^{243}\text{Am}} \left(1 + \sum \bar{K}_{dic} + M_{^{243}\text{Am}}^{ppt} \right), \quad (\text{Eq. 6.5.2.7.2-4})$$

where the radioactive decay of the entire ^{243}Am ($\lambda_{^{243}\text{Am}}^{\text{Total}}$) mass present in the domain is divided into individual components: the dissolved mass, the equilibrium sorbed mass on the waste form and groundwater colloids, and the precipitated mass.

$M_{^{243}\text{Am}}^{ppt}$ is the ratio of the precipitated mass in the domain to the dissolved mass, and $\sum \bar{K}_{dic}$ is the sum over all the colloids present in the domain of the ratios of combined equilibrium sorbed mass onto the waste form and ground water colloids to the dissolved mass are included. Note that \bar{K}_{dcWF} and \bar{K}_{dcGW} are the dimensionless distribution coefficients for equilibrium sorption onto waste form colloids and ground water colloids, respectively, and represent the ratios of mass sorbed on colloids to dissolved mass, on a per unit water volume basis. For a given colloid type, $\bar{K}_{dic} = C_c K_{dic}$, where C_c is the concentration of colloids (kg m^{-3}), and K_{dic} is the distribution coefficient for equilibrium sorption of radionuclide species i onto colloids ($\text{m}^3 \text{kg}^{-1}$).

The stoichiometric coefficient for the radioactive decay to species ^{239}Pu is the ratio of the radioactive conversion rate of ^{243}Am to the total effective conversion rate. This is given by:

$$v_{^{239}\text{Pu}} = \frac{\lambda_{^{243}\text{Am}} \left(1 + \sum \bar{K}_d \right)}{R_{fc} + R_{fcp} + \lambda_{^{243}\text{Am}} \left(1 + \sum \bar{K}_d \right)}, \quad v_{^{239}\text{Pu}} = \frac{\lambda_{^{243}\text{Am}} \left(1 + \sum \bar{K}_{dic} + M_{^{243}\text{Am}}^{ppt} \right)}{R_{fc} + R_{fcp} + \lambda_{^{243}\text{Am}} \left(1 + \sum \bar{K}_{dic} + M_{^{243}\text{Am}}^{ppt} \right)}, \quad (\text{Eq. 6.5.2.7.2-5})$$

Similarly, the stoichiometric coefficient for the conversion of ^{243}Am to daughter $I_f^{243}\text{Am}$ is:

$$v_{I_f^{243}\text{Am}} = \frac{R_{fc}}{R_{fc} + R_{fcp} + \lambda_{^{243}\text{Am}} \left(1 + \sum \bar{K}_d \right)}, \quad v_{I_f^{243}\text{Am}} = \frac{R_{fc}}{R_{fc} + R_{fcp} + \lambda_{^{243}\text{Am}} \left(1 + \sum \bar{K}_{dic} + M_{^{243}\text{Am}}^{ppt} \right)}, \quad (\text{Eq. 6.5.2.7.2-6})$$

and the stoichiometric coefficient for the conversion of ^{243}Am to daughter $\text{Ifcp}^{243}\text{Am}$ is:

$$v_{\text{Ifcp}^{243}\text{Am}} = \frac{R_{\text{fcp}}}{R_{\text{fc}} + R_{\text{fcp}} + \lambda_{^{243}\text{Am}} \left(1 + \sum \bar{K}_d\right)} v_{\text{Ifcp}^{243}\text{Am}} = \frac{R_{\text{fcp}}}{R_{\text{fc}} + R_{\text{fcp}} + \lambda_{^{243}\text{Am}} \left(1 + \sum \bar{K}_{\text{dic}} + M_{^{243}\text{Am}}^{\text{ppt}}\right)} \quad (\text{Eq. 6.5.2.7.2-7})$$

As noted above, within the corrosion products domain, the stoichiometric coefficient for the embedded waste form colloids is zero:

$$v_{\text{Ifcp}^{243}\text{Am}} = 0. \quad (\text{Eq. 6.5.2.7.2-8})$$

In order to implement the above stoichiometric coefficients in GoldSim, a modification is needed because Equation 6.5.2.7.2-1 is formulated with respect to dissolved concentrations while the material balance equations in GoldSim are formulated with respect to the total mass in the cell pathway (dissolved mass plus equilibrium sorbed mass). As a result, the radioactive decay rate constant that is applied in GoldSim is just λ_i (or $\lambda_{^{243}\text{Am}}$ in this example) without the term $\left(1 + \sum \bar{K}_{\text{dic}}\right)$. In other words, the conversion of $\left(1 + \sum \bar{K}_{\text{dic}}\right)$ is not needed in GoldSim because the radioactive decay is applied to the entire mass in the cell pathway and not just to the dissolved mass. However, the forward kinetic reaction rate constants, R_{fc} and R_{fcp} , require modification in GoldSim, as these reactions only apply to the dissolved mass rather than to the entire mass in the cell pathway (Equation 6.5.2.7-1). Thus, these rate constants must be multiplied by a conversion factor, which is equivalent to the ratio of mass in solution to mass in pathway. The conversion factor for americium species, f_{Am} , as applied in GoldSim for the current time step (n+1), is given as:

$$f_{\text{Am}} = \frac{V_w}{V_w + m_{\text{cWF}} K_{\text{dc,Am,WF}} + m_{\text{cGW}} K_{\text{dc,Am,GW}}} \quad f_{\text{Am}} = \frac{M_{\text{Am}_{\text{diss}}}^n}{M_{\text{Am}_{\text{total}}}^n} \quad (\text{Eq. 6.5.2.7.2-9})$$

where

$$\begin{aligned} \frac{M_{\text{Am}_{\text{diss}}}^n}{M_{\text{Am}_{\text{total}}}^n} &= \text{volume dissolved mass of americium [(kg)] water in the corrosion products cell [m}^3\text{] at the end of previous time step } n \\ \frac{M_{\text{Am}_{\text{total}}}^n}{m_{\text{cWF}}} &= \text{total mass of waste form colloids americium [(kg)] in the corrosion products cell at the end of previous time step } n. \text{ It includes the dissolved mass, sorbed mass, and precipitated mass of americium in the corrosion products cell pathway. [kg]} \\ \frac{m_{\text{cWF}}}{m_{\text{cGW}}} &= \text{mass of ground water colloids in the corrosion products [kg]} \\ \frac{K_{\text{dc,Am,WF}}}{K_{\text{dc,Am,GW}}} &= \text{americium distribution coefficient for waste form colloids [m}^3\text{ kg}^{-1}\text{]} \\ \frac{K_{\text{dc,Am,GW}}}{K_{\text{dc,Am,GW}}} &= \text{americium distribution coefficient for ground water colloids [m}^3\text{ kg}^{-1}\text{]} \end{aligned}$$

A one-time-step delay is necessary because this calculation is done in an explicit manner, following the completion of the transport solution for the time step.

Then the total or effective rate in a given domain (Equation 6.5.2.7.2-1) for ^{243}Am , as applied in GoldSim, can be written as:

$$\Lambda_{^{243}\text{Am},GS} = \lambda_{^{243}\text{Am}} + \lambda_{^{243}\text{Am}}^{embed} + f_{Am} (R_{fc} + R_{fcp}). \quad (\text{Eq. 6.5.2.7.2-10})$$

Note that the second term in the above equation is zero in the corrosion products domain, while the third term is zero in the waste form domain.

The total kinetic forward reaction rate in the corrosion products domain, or kinetic conversion rate is:

$$\lambda_{T,Am} = f_{Am} (R_{fc} + R_{fcp}). \quad (\text{Eq. 6.5.2.7.2-11})$$

For implementation in GoldSim, the term R_{fcp} is defined as, $C_{CP} \bar{s}_{CP} k_{if}$, while R_{fc} is defined as $C_{cFeO} \bar{s}_{CP} k_{if}$, where C_{CP} is the concentration of stationary corrosion products (kg stationary corrosion products per m^3 water), C_{cFeO} is the concentration of iron oxyhydroxide colloids (kg iron oxyhydroxide colloids per m^3 water), \bar{s}_{CP} is the specific surface area of iron corrosion products (m^2 iron corrosion products per kg iron corrosion products), and k_{if} is the kinetic forward rate constant for species i (m^3 water per m^2 iron corrosion products per year). Because specific surface area and kinetic forward rate constants are normalized to unit mass and unit area, respectively, the same value of these two parameters is used in the calculation of reaction rate for stationary corrosion products and iron oxyhydroxide colloids.

Denote:

$$f_c = \frac{R_{fc}}{R_{fc} + R_{fcp}}. \quad (\text{Eq. 6.5.2.7.2-12})$$

Then stoichiometric coefficient in the corrosion products domain, as applied in GoldSim, for kinetic sorption to the corrosion products colloids (forward reaction rate) is calculated as:

$$v_{If^{243}\text{Am}} = \frac{f_c \lambda_{T,Am}}{\lambda_{T,Am} + \lambda_{^{243}\text{Am}}} V_{If^{243}\text{Am}} = \frac{f_c \lambda_{T,Am}}{\lambda_{T,Am} + \lambda_{^{243}\text{Am}}} = \frac{f_{Am} \cdot R_{fc}}{f_{Am} (R_{fc} + R_{fcp}) + \lambda_{^{243}\text{Am}}}, \quad (\text{Eq. 6.5.2.7.2-13})$$

and the stoichiometric coefficient for corrosion products (forward reaction rate) is calculated as:

$$v_{Ifcp^{243}\text{Am}} = \frac{(1 - f_c) \lambda_{T,Am}}{\lambda_{T,Am} + \lambda_{^{243}\text{Am}}} V_{Ifcp^{243}\text{Am}} = \frac{(1 - f_c) \lambda_{T,Am}}{\lambda_{T,Am} + \lambda_{^{243}\text{Am}}} = \frac{f_{Am} \cdot R_{fcp}}{f_{Am} (R_{fc} + R_{fcp}) + \lambda_{^{243}\text{Am}}}. \quad (\text{Eq. 6.5.2.7.2-14})$$

It can be shown that Equations 6.5.2.7-13 and 6.5.2.7-14, as implemented in GoldSim, are equivalent to Equations 6.5.2.7-6 and 6.5.2.7-7.

If both the numerator and denominator of Equation 6.5.2.7.2-9 are divided by $\frac{M^n_{Am,diss}}{V_w}$, the dissolved mass, the conversion factor for americium species can be written as:

$$f_{Am} = \frac{1}{1 + \bar{K}_{dc,Am,WF} + \bar{K}_{dc,Am,GW}} \quad f_{Am} = \frac{1}{1 + \bar{K}_{dc,Am,WF} + \bar{K}_{dc,Am,GW} + M_{243Am}^{ppt}} \quad (\text{Eq. 6.5.2.7.2-15})$$

$$= \frac{1}{1 + \sum \bar{K}_d} \quad = \frac{1}{1 + \sum \bar{K}_{dic} + M_{243Am}^{ppt}}$$

As a result, Equation 6.5.2.7.2-11 can be expressed as:

$$\lambda_{T,Am} = \frac{R_{fc} + R_{fcp}}{1 + \sum \bar{K}_d} \quad \lambda_{T,Am} = \frac{R_{fc} + R_{fcp}}{1 + \sum \bar{K}_{dic} + M_{243Am}^{ppt}}, \quad (\text{Eq. 6.5.2.7.2-16})$$

Substitution of Equations 6.5.2.7.2-12 and 6.5.2.7.2-16 into Equations 6.5.2.7.2-13 and 6.5.2.7.2-14 yields:

$$v_{If^{243}Am} = \frac{\left(\frac{R_{fc}}{R_{fc} + R_{fcp}} \right) \left(\frac{R_{fc} + R_{fcp}}{1 + \sum \bar{K}_d} \right)}{\left(\frac{R_{fc} + R_{fcp}}{1 + \sum \bar{K}_d} \right) + \lambda_{243Am}} \quad v_{If^{243}Am} = \frac{\left(\frac{R_{fc}}{1 + \sum \bar{K}_{dic} + M_{243Am}^{ppt}} \right)}{\left(\frac{R_{fc} + R_{fcp}}{1 + \sum \bar{K}_{dic} + M_{243Am}^{ppt}} \right) + \lambda_{243Am}}, \quad (\text{Eq. 6.5.2.7.2-17})$$

$$v_{Ifcp^{243}Am} = \frac{\left(1 - \frac{R_{fc}}{R_{fc} + R_{fcp}} \right) \left(\frac{R_{fc} + R_{fcp}}{1 + \sum \bar{K}_d} \right)}{\left(\frac{R_{fc} + R_{fcp}}{1 + \sum \bar{K}_d} \right) + \lambda_{243Am}} \quad v_{Ifcp^{243}Am} = \frac{\left(\frac{R_{fcp}}{1 + \sum \bar{K}_{dic} + M_{243Am}^{ppt}} \right)}{\left(\frac{R_{fc} + R_{fcp}}{1 + \sum \bar{K}_{dic} + M_{243Am}^{ppt}} \right) + \lambda_{243Am}}, \quad (\text{Eq. 6.5.2.7.2-18})$$

The above expressions simplify to:

$$v_{If^{243}Am} = \frac{R_{fc}}{R_{fc} + R_{fcp} + \lambda_{243Am} (1 + \sum \bar{K}_d)} \quad v_{If^{243}Am} = \frac{R_{fc}}{R_{fc} + R_{fcp} + \lambda_{243Am} (1 + \sum \bar{K}_{dic} + M_{243Am}^{ppt})}, \quad (\text{Eq. 6.5.2.7.2-19})$$

$$v_{Ifcp^{243}Am} = \frac{R_{fcp}}{R_{fc} + R_{fcp} + \lambda_{243Am} (1 + \sum \bar{K}_d)} \quad v_{Ifcp^{243}Am} = \frac{R_{fcp}}{R_{fc} + R_{fcp} + \lambda_{243Am} (1 + \sum \bar{K}_{dic} + M_{243Am}^{ppt})}, \quad (\text{Eq. 6.5.2.7.2-20})$$

which is the expression for these stoichiometric coefficients given in Equations 6.5.2.7.2-6 and 6.5.2.7.2-7.

The stoichiometric coefficient for the radioactive decay to species ^{239}Pu in GoldSim is computed as:

$$v_{239Pu} = \frac{\lambda_{243Am}}{\lambda_{T,Am} + \lambda_{243Am}}. \quad (\text{Eq. 6.5.2.7.2-21})$$

Substituting Equation 6.5.2.7.2-16 in the above equation gives:

$$\begin{aligned}
 v_{^{239}\text{Pu}} &= \frac{\lambda_{^{243}\text{Am}}}{\left(\frac{R_{fc} + R_{fcp}}{1 + \sum \bar{K}_d} \right) + \lambda_{^{243}\text{Am}}} \\
 &= \frac{\lambda_{^{243}\text{Am}} (1 + \sum \bar{K}_d)}{R_{fc} + R_{fcp} + \lambda_{^{243}\text{Am}} (1 + \sum \bar{K}_d)} \\
 v_{^{239}\text{Pu}} &= \frac{\lambda_{^{243}\text{Am}}}{\left(\frac{R_{fc} + R_{fcp}}{1 + \sum \bar{K}_{dic} + M_{^{243}\text{Am}}^{ppt}} \right) + \lambda_{^{243}\text{Am}}} \\
 &= \frac{\lambda_{^{243}\text{Am}} (1 + \sum \bar{K}_{dic} + M_{^{243}\text{Am}}^{ppt})}{R_{fc} + R_{fcp} + \lambda_{^{243}\text{Am}} (1 + \sum \bar{K}_{dic} + M_{^{243}\text{Am}}^{ppt})}
 \end{aligned}
 \tag{Eq. 6.5.2.7.2-22}$$

which is the same as Equation 6.5.2.7.2-5.

The reaction rate constant for conversion of embedded mass on the waste form colloids, $\lambda_{^{243}\text{Am}}^{embed}$, as shown in Equation 6.5.2.7.2-1, remains unchanged in GoldSim, as the conversion is applied to the entire mass in the waste form cell pathway (solution and reversibly sorbed mass). The two nonzero stoichiometric coefficients within the waste form domain are:

$$v_{^{239}\text{Pu}} = \frac{\lambda_{^{243}\text{Am}}}{\lambda_{^{243}\text{Am}}^{embed} + \lambda_{^{243}\text{Am}}} \tag{Eq. 6.5.2.7.2-23}$$

$$v_{Ic^{243}\text{Am}} = \frac{\lambda_{^{243}\text{Am}}^{embed}}{\lambda_{^{243}\text{Am}}^{embed} + \lambda_{^{243}\text{Am}}} \tag{Eq. 6.5.2.7.2-24}$$

Within the corrosion product domain the mass species $I_{fcp}^{243}\text{Am}$, kinetically sorbed mass to the corrosion products, experiences reactions from radioactive decay and kinetic desorption. Since the radioactive daughter of ^{243}Am is ^{239}Pu , the radioactive daughter of $I_{fcp}^{243}\text{Am}$ is $I_{fcp}^{239}\text{Pu}$. This implies that any ^{243}Am mass kinetically sorbed to the corrosion products decays to ^{239}Pu kinetically sorbed to the corrosion products. The effective conversion rate [for the reverse reaction](#) for the $I_{fcp}^{243}\text{Am}$ species is:

$$\rho_{I_{fcp}^{243}\text{Am}} = \lambda_{^{243}\text{Am}} + R_{rcp}, \tag{Eq. 6.5.2.7.2-25}$$

where R_{rcp} is the reverse (desorption) rate for the $I_{fcp}^{243}\text{Am}$ species [that desorbs \$^{243}\text{Am}\$ mass from stationary corrosion products to the solution](#). For the $I_{fcp}^{243}\text{Am}$ species, the effective conversion rate is applied to the entire mass in the corrosion product cell pathway [that is sorbed to the stationary corrosion products](#). That is to say, there is no equilibrium sorption of the $I_{fcp}^{243}\text{Am}$ species. Therefore, the stoichiometric coefficients are:

$$v_{I_{fcp}^{239}\text{Pu}} = \frac{\lambda_{^{243}\text{Am}}}{\lambda_{^{243}\text{Am}} + R_{rcp}} \tag{Eq. 6.5.2.7.2-26}$$

$$v_{^{239}\text{Pu}} = \frac{R_{rcp}}{\lambda_{^{243}\text{Am}} + R_{rcp}} v_{I_{fcp}^{243}\text{Am}} = \frac{R_{rcp}}{\lambda_{^{243}\text{Am}} + R_{rcp}} \tag{Eq. 6.5.2.7.2-27}$$

A similar methodology is applied for kinetic desorption from iron oxyhydroxide colloids while the colloids are in the corrosion products domain. A separate reverse (desorption) rate, denoted as R_{rcFeO} , is calculated for the $I_f^{243}Am$ species that desorbs ^{243}Am mass from iron oxyhydroxide colloids to the solution. The stoichiometric coefficients defining the desorption reaction from the iron oxyhydroxide colloids that are implemented are similar to Equations 6.5.2.7.2-26 and 6.5.2.7.2-26.

The reverse reaction rates are computed as:

$$R_{rcp} = \frac{R_{fcp}}{K_d^{Am} C_{CP}} \quad (\text{Eq. 6.5.2.7.2-28})$$

$$R_{rcFeO} = \frac{R_f}{K_d^{Am} C_{cFeO}} \quad (\text{Eq. 6.5.2.7.2-29})$$

where K_d^{Am} is the K_d for americium calculated from the surface complexation based modeling described in Section 6.5.2.4.